



**Restoring tissue-like functionality in circulating CD8 T-cells: mechanistic studies and application in immunomonitoring of cancer patients**

**Wiederherstellen einer gewebeartigen Funktionalität in humanen CD8 T-Zellen des Blutes: mechanistische Studien und Anwendung beim Immunomonitoring von Krebspatienten**

Thesis for a doctoral degree  
at the Graduate School of Life Sciences,  
Julius-Maximilians-University Würzburg,  
Section Infection and Immunity

submitted by  
**Julia Wegner**  
from  
Schweinfurt

Würzburg, 2015



Submitted on: .....

Office stamp

Members of the *Promotionskomitee*:

Chairperson: Prof. Dr. Manfred Gessler

Primary Supervisor: Prof. Dr. Thomas Hünig

Supervisor (Second): PD Dr. Götz Ulrich Grigoleit

Supervisor (Third): Prof. Dr. Stefan Stevanović

Date of Public Defence: .....

Date of Receipt of Certificates: .....

## Affidavit

I hereby confirm that my thesis entitled “Restoring tissue-like functionality in circulating CD8 T-cells: mechanistic studies and application in immunomonitoring of cancer patients“ is the result of my own work. I did not receive any help except as noted or support from commercial consultants. All sources and / or materials applied are listed and specified in the thesis.

Furthermore, I confirm that this thesis has not yet been submitted as part of another examination process neither in identical nor in similar form.

---

Place, date

---

Signature

# Acknowledgements

I would like to take this opportunity to thank Prof. Dr. Thomas Hünig for his excellent supervision and competent advice as a mentor and immunologist. Thank you for giving me the chance to continue a research project in the field of human immunology and for accepting me in your laboratory as your 'last PhD student'.

I wish to thank my thesis committee members PD Dr. Götz Ulrich Grigoleit and Prof. Dr. Stefan Stevanović, Prof. Dr. Manfred Gessler, chairperson of my committee as well as the co-authors of our paper for their help, critical comments and continuous support. Thank you for the efficient collaboration between clinics and research.

My gratitude goes to my lab co-workers at the Institute for Virology and Immunobiology in Würzburg as well as to my colleagues and friends of the Immunomodulation Graduate Program for their kindness, helpfulness and fruitful discussions.

I wish to thank the Graduate School of Life Sciences of the University of Würzburg, especially Dr. Gabriele Blum-Oehler and Jennifer Heilig for support and funding throughout my time as a PhD student.

I am sincerely grateful to those people who encouraged me to pursue my dreams, especially my husband, parents and sisters.

# Table of contents

<b>Affidavit</b> .....	<b>3</b>
<b>Acknowledgements</b> .....	<b>4</b>
<b>Summary</b> .....	<b>8</b>
<b>Zusammenfassung</b> .....	<b>9</b>
<b>1 Introduction</b> .....	<b>11</b>
1.1 Human T-cells – key players of the adaptive immune system.....	11
1.1.1 Innate and adaptive immunity.....	11
1.1.2 Cellular interactions between T-cells and antigen presenting cells .....	11
1.1.3 T-cells in blood and tissues.....	12
1.2 T-cell receptor (TCR)-mediated activation .....	13
1.2.1 TCR signaling and stimulation via MHC/foreign-antigen recognition.....	13
1.2.2 Tonic TCR signaling via MHC/self-peptide recognition in tissues.....	14
1.2.3 Enhanced foreign-antigen sensitivity of murine T-cell responses through tonic TCR signaling .....	15
1.3 Restoring transiently lost TGN1412 reactivity of circulating CD4 memory T-cells.....	16
1.3.1 HD preculture of PBMCs allows <i>in-vitro</i> responses of human CD4 T-cells to soluble TGN1412 .....	17
1.3.2 HD preculture of PBMCs induces tonic TCR signaling for amplification by TGN1412.....	18
1.4 The RESTORE protocol – a tool for reliable monitoring of T-cell responses directed to viral and tumor antigens?.....	18
1.4.1 Monitoring of human T-cell responses specific for viral and tumor antigens .....	18
1.4.2 Aims of this study .....	19
1.5 Introductory statement on contributions and previous publication.....	19
<b>2 Material</b> .....	<b>21</b>
2.1 Equipment and supplies.....	21
2.2 Software .....	22
2.3 Chemicals and reagents .....	22
2.4 Buffers, media and solutions .....	24
2.5 Commercial kits.....	28
2.6 Anti-human antibodies .....	28
2.7 Cell stimulation reagents .....	29
2.8 Human material.....	30
<b>3 Methods</b> .....	<b>31</b>
3.1 Cellular methods.....	31
3.1.1 Isolation of human lymphoid cells from blood and tissue.....	31
3.1.1.1 From blood .....	31
3.1.1.2 From lamina propria of the small intestine.....	31
3.1.1.3 From tonsils .....	32

3.1.1.4	Study approval .....	32
3.1.2	Freezing and thawing of mononuclear cells .....	32
3.1.3	Isolation and depletion of subpopulations .....	32
3.1.3.1	Isolation of CD8 T-cells and monocytes .....	32
3.1.3.2	Depletion of regulatory T-cells .....	33
3.1.4	Cell culture and stimulation assays .....	33
3.1.4.1	Standard PBMC cultures and T-cell stimulation.....	33
3.1.4.2	RESTORE protocol for human PBMCs .....	33
3.1.4.3	<i>In-vitro</i> expansion assay .....	34
3.2	Immunological methods .....	34
3.2.1	Flow cytometry (phenotyping).....	34
3.2.2	Quantification of IFN- $\gamma$ releasing cells.....	34
3.2.2.1	Intracellular IFN- $\gamma$ staining .....	34
3.2.2.2	IFN- $\gamma$ ELISPOT assay.....	35
3.2.2.3	IFN- $\gamma$ secretion assay .....	35
3.3	Molecular methods .....	35
3.3.1	Western blotting.....	35
3.3.1.1	Sample preparation .....	35
3.3.1.2	SDS-polyacrylamide gel electrophoresis.....	36
3.3.1.3	Transfer of proteins and staining.....	36
3.3.2	Microarray analysis.....	36
3.3.2.1	Total RNA isolation and ethanol precipitation of nucleic acids.....	36
3.3.2.2	Gene Array.....	36
3.4	Statistical analysis.....	37
<b>4</b>	<b>Results.....</b>	<b>38</b>
4.1	HD preculture of PBMCs enhances anti-viral IFN- $\gamma$ responses in human CD8 memory T-cells	38
4.2	Determination of optimal preculture conditions for increasing the sensitivity of CD8 T-cell responses .....	39
4.3	Mechanistic studies on restored virus-specific CD8 T-cell responses.....	40
4.3.1	Functional maturation of human CD8 T-cells and monocytes contribute to the HD preculture effect.....	40
4.3.2	RESTORE effect is not due to a reduction in Treg activity.....	42
4.3.3	HD preculture prepares T-cells to better respond to antigen, but does not increase the frequency of antigen-specific cells.....	43
4.4	HD preculture of PBMCs boosts antigen sensitivity of virus-specific CD8 T-cells.....	44
4.5	Comparison of T-cell responses in blood and tissue .....	48
4.5.1	Phenotyping of CD4 and CD8 T-cells from LPMCs and HD precultured PBMCs .....	48
4.5.2	Loss of T-cell sensitivity to TAB08 in dispersed LPMC cultures .....	49
4.5.3	Phenotyping of CD4 and CD8 T-cells from TMCs and HD precultured PBMCs.....	51
4.5.4	Loss of anti-viral CD8 T-cell sensitivity in dispersed TMC cultures .....	52
4.6	Facilitation of CD8 T-cell responses to the tumor-associated antigen WT1 by HD preculture of PBMCs from leukemia patients after allogeneic HSCT.....	53
4.7	HD preculture allows the generation of CD8 T-cell lines with an improved representation of clones responding to low antigen concentrations.....	56
4.8	Phosphorylation of proximal TCR signaling components upon HD preculture of PBMCs.....	59

---

4.9	Gene expression analysis of CD8 memory T-cells from HD precultured PBMCs and tonsils compared to fresh PBMCs .....	61
4.10	HD preculture of PBMCs affects integrin expression .....	66
<b>5</b>	<b>Discussion.....</b>	<b>69</b>
5.1	Increased antigen sensitivity of CD8 memory T-cells upon HD preculture of PBMCs.....	69
5.2	Enhanced T-cell sensitivity depends on cellular interactions.....	71
5.3	Maturation of monocytes and sub-threshold activation of CD8 T-cells contribute to the enhanced T-cell functionality .....	72
5.4	Few genes displaying concordant expression changes between CD8 memory T-cells from tonsils and HD precultures of PBMCs.....	75
5.5	The RESTORE protocol as a promising, cost-effective and reliable diagnostic and research tool.....	76
	<b>List of figures.....</b>	<b>77</b>
	<b>List of abbreviations and acronyms .....</b>	<b>84</b>
	<b>References .....</b>	<b>88</b>
	<b>Curriculum vitae.....</b>	<b>95</b>

## Summary

Peripheral blood mononuclear cells (PBMCs) are the only source of human lymphoid cells routinely available for immunologic research and for immunomonitoring of T-cell responses to microbial and tumor-associated antigens. However the large majority of human T-cells resides in tissues, especially in lymphatic organs, while only 1 % of the body's T-cells circulate in the blood stream. Previous work in mice and humans had indicated that CD4 T-cells transiently lose antigen sensitivity when cellular contacts are lost, *e.g.* by leaving lymphoid organs such as lymph nodes (LNs) and entering the circulation. In this study, these findings were extended to CD8 T-cells. Thus, CD8 T-cell responses of the human tonsil show a significant drop in sensitivity to viral antigens if tissue-exit was simulated by keeping cells in dispersed culture at body temperature for two hours.

Conversely, tissue-like functionality in blood-derived CD8 T-cells was restored by applying the simple and robust RESTORE protocol. Indeed, application of the RESTORE protocol, *i.e.* pre-culturing PBMCs for two days at a high cell density before initiation of antigenic stimulation, demonstrated that CD8 T-cell responses to a broad range of viral and to tumor-associated antigens are greatly underestimated, and sometimes even remain undetected if conventional, unprocessed PBMC cultures are used. The latter finding is particularly striking with regard to the appearance of Wilms tumor 1 (WT1)-specific CD8 T-cell responses in leukemia patients after allogeneic bone marrow transplantation. My studies on the mechanism of the RESTORE protocol show that HD preculture of PBMCs does not involve antigen-or cytokine-driven clonal expansion of T-cells. Moreover, the gain in antigen sensitivity cannot be explained by a decreased activity of regulatory T-cells during the preculture step. The increased antigen sensitivity of CD8 T-cells from HD precultures of PBMCs is associated with tonic T-cell receptor signaling as indicated by enhanced tyrosine phosphorylation of the CD3  $\zeta$  chains and the tyrosine kinase Lck, thereby preparing T-cells for full responses. The upregulation of genes involved in aerobic glycolysis in "restored" CD8 memory T-cells relative to fresh cells might be an essential requirement for increased T-cell functionality including the regulation of IFN- $\gamma$  production. Taken together, the RESTORE protocol, which was initially described for the CD4 T-cell response to the antibody TGN1412 permits a more meaningful monitoring of CD8 T-cell responses to viral infections and tumors. Furthermore, when generating T-cell lines for adoptive T-cell therapy, the RESTORE protocol allows the generation of CD8 T-cell lines with an improved representation of clones responding to low antigen concentrations.



## Zusammenfassung

Mononukleäre Zellen des peripheren Blutes (PBMCs: peripheral blood mononuclear cells) stellen die einzige routinemäßig zugängliche Quelle für humane Lymphozyten dar, welche für die immunologische Forschung und das „Immunomonitoring“ von T-Zellantworten gegen mikrobielle und Tumor-assoziierte Antigene verwendet werden. Jedoch befindet sich der Großteil der T-Zellen des Menschen in Geweben, insbesondere den lymphatischen Organen, wohingegen sich nur 1 % der T-Zellen im Blut aufhalten. Frühere Studien, die sowohl mit murinen als auch mit humanen Zellen durchgeführt wurden, zeigten, dass CD4 T-Zellen ihre Sensitivität gegenüber Antigenen zeitweise verlieren sobald zelluläre Kontakte unterbrochen werden. Dies erfolgt beispielsweise beim Verlassen der T-Zellen von Geweben und dem Eintreten in die Blutzirkulation. In dieser Arbeit wurden diese Beobachtungen auf CD8 T-Zellen ausgeweitet. So weisen humane tonsilläre CD8 T-Zellen eine signifikant niedrigere Sensitivität gegenüber viralen Antigenen auf, wenn diese in Dispersion bei Körpertemperatur für zwei Stunden gehalten werden, um das Verlassen von Geweben und somit den Verlust von zellulären Kontakten zu simulieren.

Im Gegenzug konnte eine gewebeähnliche T-Zellfunktionalität bei Blutzellen durch Anwendung des RESTORE Protokolls wiederhergestellt werden. In der Tat zeigte die Anwendung des RESTORE Protokolls, welches eine Vorkultur von PBMCs für zwei Tage bei hoher Zelldichte vor antigenspezifischer T-Zellstimulation einschließt, dass CD8 T-Zellantworten gegen eine Vielzahl viraler und Tumor-assoziiierter Antigene deutlich unterschätzt werden, wenn herkömmliche Stimulationsansätze verwendet werden. Teilweise können diese so gemessenen T-Zellantworten bei Verwendung herkömmliche Stimulationsansätze auch gar nicht nachgewiesen werden. Dieser Effekt war bei der Detektion von Wilms Tumor 1 (WT1)-spezifischen CD8 T-Zellantworten bei Leukämiepatienten nach allogener Stammzelltransplantation besonders deutlich zu beobachten. Meine mechanistischen Studien zeigten, dass die Vorkultur von PBMCs bei hoher Zelldichte selbst nicht zu einer Antigen- oder Zytokin-getriebenen T-Zell Expansion führt. Des Weiteren wurde gezeigt, dass der RESTORE Effekt durch den Zugewinn an CD8 T-Zellsensitivität erklärt werden kann und nicht auf eine verringerte CD8 T-Zellsuppression durch regulatorische T-Zellen während der Vorkultur zurückzuführen ist. Die erhöhte Antigensensitivität von vorkultivierten CD8 T-Zellen steht im Zusammenhang mit tonischer T-Zell Signalweiterleitung, welche anhand von erhöhter Tyrosin Phosphorylierung der CD3  $\zeta$  Ketten des T-Zell-Rezeptors und der Tyrosinkinase Lck nachgewiesen werden kann. Diese tonischen T-Zellsignale bereiten CD8 T-Zellen darauf vor, bereits auf kleine Mengen Antigen effektiv zu reagieren. Auch die Hochregulierung von Genen, welche der aeroben Glykolyse zuzuordnen sind in vorkultivierten CD8 Gedächtniszellen im Vergleich zu CD8 Gedächtniszellen, welche direkt aus dem Blut isoliert wurden, trägt zu einer erhöhten T-Zellfunktionalität bei, welche die Regulation der IFN- $\gamma$  Produktion einschließt. Zusammenfassend lässt sich sagen, dass die Anwendung des RESTORE Protokolls, welches ursprünglich zum Nachweis von

CD4 T-Zellantworten gegen den Antikörper TGN1412 entwickelt wurde, eine verlässliche Methode zum Nachweis von CD8 T-Zellantworten gegen virale Infektionen und Tumore darstellt. Des Weiteren kann das RESTORE Protokoll zur Generierung von T-Zelllinien in der adoptive T-Zelltherapie eingesetzt werden. Die Anwendung des Protokolls erlaubt das Generieren von Zelllinien, welche auch T-Zellklone beinhalten, die durch Immunantworten auf geringe Antigenkonzentrationen entstanden sind.

# 1 Introduction

## 1.1 Human T-cells – key players of the adaptive immune system

### 1.1.1 Innate and adaptive immunity

The human immune system mediates the body's defense against pathogenic microbes, such as viruses, and against transformed body cells. It can be classified into the innate and the adaptive immune system. Innate immunity constitutes the first line of host defense during infection and therefore plays a crucial role in the early recognition and subsequent triggering of a proinflammatory response to invading pathogens. It consists of (a) cellular and chemical barriers such as skin, mucosal epithelia and antimicrobial molecules, (b) blood proteins such as complement, and (c) cells such as phagocytes and natural killer cells. The mechanisms of innate immunity rely on a large family of pattern recognition receptors (PRRs), which detect distinct evolutionarily conserved structures on pathogens, termed pathogen-associated molecular patterns (PAMPs) (Reviewed by (Mogensen 2009)).

The adaptive immune system, on the other hand, is responsible for the elimination of pathogens in the late phase of infection. It is characterized by its highly specific receptors, which are generated by clonal gene rearrangements and form a broad repertoire of antigen-specific receptors on bone marrow- (B) or thymus- (T) derived lymphocytes (Reviewed by (Litman, Rast *et al.* 2010)). Antigens are any structural substances which serve as a target for the antigen receptor of lymphocytes regardless of whether they do or do not stimulate immune responses (Lindenmann 1984). They may originate from within the body (known as “self”) or from the external environment (known as “foreign”). In healthy individuals the immune system is under homeostatic conditions non-reactive against self-antigens due to several mechanisms, such as the elimination of self-reactive lymphocytes during their development (Reviewed by (Starr, Jameson *et al.* 2003)) or the inactivation or the suppression of these cells by regulatory T-cells (Tregs) (Reviewed by (Sakaguchi 2004)). Adaptive immune responses can be subdivided into the humoral immunity and cell-mediated immunity. The humoral immunity is mediated by antibodies (Abs) secreted by B-lymphocytes (also called B-cells) and their fully differentiated progeny, the plasma cells. Abs recognize foreign antigens, such as antigens from microbes, then neutralize the infectivity of these microbes and lastly target these microbes for elimination through various effector mechanisms.

### 1.1.2 Cellular interactions between T-cells and antigen presenting cells

Cell-mediated immunity is mediated by T-lymphocytes, which either activate phagocytic macrophages to kill microbes or transformed body cells (known as helper T-cells) or destroy infected or transformed cells through their cytotoxic granules, which contain perforin and granzymes (known as cytotoxic T-lymphocytes (CTL)) and ligation of the death receptor cluster of differentiation (CD) 95 (Reviewed by

(McNeela and Mills 2001)). Whereas helper T-cells express the co-receptor CD4, CTL express the co-receptor CD8 and are of major interest in this thesis. T-cells respond to antigens processed and presented by professional antigen presenting cells (APCs) such as B-cells, macrophages and dendritic cells (DCs) through distinct mechanisms (Reviewed by (Neefjes, Jongma *et al.* 2011)). Human CD4 T-cells recognize exogenous antigens which are captured and processed by APCs to peptides of 12-15 residues or more and are finally bound to the peptide-binding cleft of major histocompatibility complex (MHC) class II molecules. MHC class II molecules consist of an  $\alpha$  and  $\beta$  polypeptide chain. CD8 T-cells recognize endogenous antigens, *e.g.* from viral infection, that are processed to peptides of only 8-11 residues in association with MHC class I molecules (Wang and Reinherz 2002). MHC class I molecules are composed of a polymorphic  $\alpha$  chain that is non-covalently attached to the non-polymorphic  $\beta_2$ -microglobulin. In humans, MHC is also referred to as human leukocyte antigens (HLA). Whereas MHC class I corresponds to HLA-ABC, MHC class II corresponds to HLA-DR, DP, DQ (Bodmer, Marsh *et al.* 1994).

### 1.1.3 T-cells in blood and tissues

Upon maturation, T-cells leave the thymus via the blood stream to populate the secondary lymphoid organs, such as lymph nodes (LNs), tonsils, the spleen or Payer's patches. In secondary lymphoid organs the immune responses are initiated by T-cell-APC interactions and T-cells migrate as activated T-cells to multiple tissue sites where they exert immune surveillance by scanning for microbial infections or transformed cells (Reviewed by (Germain and Stefanova 1999)). Although most activated effector T-cells die after a brief life-span, a subset of primed T-cells develops into long-lived memory T-cells that persist as heterogeneous populations in the human body and accumulate with age (Reviewed by (Farber, Yudanin *et al.* 2014)). Approximately 1% of the body's T-cells found in the blood stream are in transit while the rest of the T-lymphocytes are searching for antigens in the tissue, where the initiation and execution of effector functions occurs (Sathaliyawala, Kubota *et al.* 2013).

Human T-cell subsets in blood and tissue can be phenotypically characterized by the expression of the common leukocyte antigen CD45 isoforms (CD45RA or CD45R0) and/or the homing receptor L-selectin (CD62L) (Tough 2002). Whereas naive T-cells express the isoform CD45RA, memory T-cells express the isoform CD45R0. Memory T-cells are further subdivided into central memory (CD45R0<sup>+</sup>CD62L<sup>+</sup>) and effector memory (CD45R0<sup>+</sup>CD62L<sup>-</sup>) T-cells. The expression of CD62L allows homing of the T-cells to secondary lymphoid organs via high endothelial venules, while the absence of CD62L expression leads to an accumulation of T-cells in peripheral tissue.

Sathaliyawala *et al.* performed a multi-dimensional analysis of T-cells throughout the human body from 24 different donors aged 15–60 years, revealing distinct compartmentalization of naive, effector and memory CD4 and CD8 T-cell subsets intrinsic to the tissue site that is remarkably consistent in diverse individuals. Effector memory CD4 T-cells predominate in mucosal tissue and accumulate as central memory subsets in lymphoid tissue, whereas CD8 T-cells are maintained as naive subsets in lymphoid tissue and effector memory CD8 T-cells in mucosal sites (Sathaliyawala, Kubota *et al.* 2013). Sathaliyawala *et al.* concluded that tissue-resident T-cells exhibit distinct phenotypic and

functional properties and differ from circulating T-cell subsets to a greater or lesser extent, depending on the tissue-type (Sathaliyawala, Kubota *et al.* 2013). Nevertheless, due to the lack of healthy human tissue-material, both basic immunological research and immune monitoring of T-cell responses are almost exclusively performed on blood-derived T-cells.

## 1.2 T-cell receptor (TCR)-mediated activation

### 1.2.1 TCR signaling and stimulation via MHC/foreign-antigen recognition

T-cells are characterized by the expression of antigen receptor complexes, also known as T-cell receptors (TCRs). TCRs are heterodimers consisting of two covalently linked transmembrane polypeptide chains, designated TCR  $\alpha$  and  $\beta$ , and a non-covalently associated monomorphic CD3 signaling component (Wang, Lim *et al.* 1998). Each chain ( $\alpha$  and  $\beta$ ) consists of one immunoglobulin (Ig)-like N-terminal variable domain for specific recognition of MHC/peptide complexes, one Ig-like constant domain, a hydrophobic transmembrane region and a short cytoplasmic region. The CD3 signaling component consists of a series of dimers, including the heterodimer  $\gamma\epsilon$ , the heterodimer  $\delta\epsilon$  and the homodimer  $\zeta\zeta$ . These TCR-associated dimers are essential for intracellular signal transduction through the phosphorylation of their intracellular immunoreceptor-tyrosine-based activation motifs (ITAMs) (Cambier 1995).

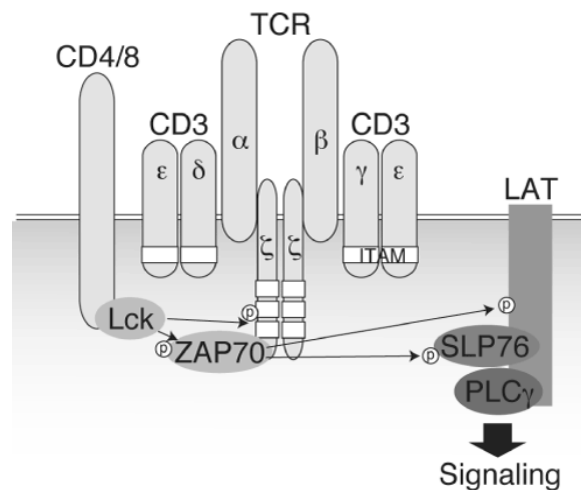


Figure 1.1: **TCR/CD3-mediated proximal signaling.** Upon TCR complex engagement a phosphorylation cascade is induced (Watanabe 2012). © Journal of Clinical & Cellular Immunology

T-cells are instructed to initiate their developmental and effector programs through stimulation of their TCR complex (signal 1) and co-stimulatory molecules (signal 2), such as CD28, which are presented by professional APCs (Reviewed by (Sharpe 2009)). Lack of co-stimulatory molecules combined with high-affinity TCR complex engagement leads naive T-cells to an anergic state in which they are refractory to activation. If both signals are present, protein clustering on the T-cell and the APC is initiated. Active reorganization via cytoskeleton-directed movements give rise to the immunological

synapse (Kumari, Curado *et al.* 2014), which is also referred to as a supra-molecular activation cluster (SMAC) (Delon and Germain 2000). The SMAC consist of a central region (cSMAC), which consists of TCR-MHC/peptide complexes, the co-receptors CD4 or CD8, co-stimulation receptor complexes (*e.g.* CD28-CD80/-CD86), enzymes and adaptor proteins. The peripheral zone (pSMAC) stabilizes the cell interaction by adhesion molecules and integrins *e.g.* the interaction between leukocyte function-associated antigen-1 (LFA-1) and intracellular adhesion molecule-1 (ICAM-1). CD45 molecules stay outside the pSMAC in an area termed the distal SMAC (dSMAC) (Grakoui, Bromley *et al.* 1999, Delon and Germain 2000). During signal transduction, the co-receptors CD4 or CD8 recruit the Src family kinases Fyn and Lck (lymphocyte-specific protein tyrosine kinase) close to the TCR complex. Additionally, some ITAMs of the heterodimer  $\delta\epsilon$  and the homodimer  $\zeta\zeta$  are phosphorylated as an early, prerequisite step for TCR-directed T-cell activation. Conformational changes of partially phosphorylated CD3 $\epsilon$  and CD3 $\zeta$  make ITAMs even more accessible for phosphorylation and are required for full T-cell activation. Subsequently, ZAP-70 ( $\zeta$ -chain associated protein kinase 70 kDa) is recruited and binds to the transmembrane adaptor protein LAT (linker for the activation of T-cells) and the cytosolic adaptor protein SLP-76 (Src homology 2 domain-containing leukocyte phosphoprotein of 76 kDa). A cascade of phosphorylation events is initiated which concludes with the activation of the transcription factors NF- $\kappa$ B (nuclear factor  $\kappa$ B), NFAT (nuclear factor of activated T-cells) and AP-1 (activation protein-1), which regulate T-cell gene expression related to cytokine production (Cham and Gajewski 2005), clonal expansion, metabolism and/or differentiation into effector or memory T-cell subsets (Reviewed by (Fox, Hammerman *et al.* 2005, Smith-Garvin, Koretzky *et al.* 2009, Wahl, Byersdorfer *et al.* 2012)).

### 1.2.2 Tonic TCR signaling via MHC/self-peptide recognition in tissues

In order to be able to detect antigens during the priming or the effector phase, T-cells actively search for MHC/peptide complexes displayed on the surfaces of other cells, which can either be professional APCs, mainly DCs in LNs during the priming phase or almost any other cell type of the body during immune surveillance (Garbi, Hammerling *et al.* 2010, Garbi and Kreutzberg 2012, Sathaliyawala, Kubota *et al.* 2013). This search for antigens is performed by a highly-dynamic crawling process in which T-cells crawl in the tissue context along collagen fibrils with an average speed of 10  $\mu$ m per minute (Wolf, Muller *et al.* 2003, Skokos, Shakhbar *et al.* 2007). The amoeboid migration of the T-cells is interrupted by contact periods lasting between 3 and 5 minutes which allow TCRs to recognize MHC molecules on the surface of other cells (Friedl and Weigelin 2008). During this scanning process, most of the binding interface of the TCRs involves contact between the complementarity-determining regions 1 and 2 (CDR1, 2) and the conserved parts of the MHC helices. Thus, TCRs identify MHC molecules independent of class or allele (Wu, Tuot *et al.* 2002, Garcia, Adams *et al.* 2009). During crawling, integrin-mediated cell adhesion and cytoskeletal rearrangements are essential processes that support the slow-down of T-cell migration and the polarization of T-cells (Revy, Sospedra *et al.* 2001, Randriamampita, Boulla *et al.* 2003, Fischer, Jacovetty *et al.* 2007, Friedl and Weigelin 2008, Conche, Boulla *et al.* 2009). Integrin-mediated cell contacts as well as low- or intermediate-affinity contacts

between TCRs and MHC molecules that are frequently loaded with self-peptides in the tissue context pre-sensitize the signaling machinery of T-cells through their induction of tonic TCR signals. Tonic TCR signals, which are also referred to as basal TCR signals (Garbi and Kreutzberg 2012) are low phosphorylation levels of proximal TCR signaling molecules presented in Figure 1.1 that increase T-cell sensitivity towards foreign antigens, meaning that lower amounts of MHC/peptide recognition is required to trigger full T-cell activation via the additional interaction of CDR3s and antigenic peptide residues (Figure 1.2) (Stefanova, Dorfman *et al.* 2002, Randriamampita, Boulla *et al.* 2003, Garbi, Hammerling *et al.* 2010). When T-cells interrupt their search for antigens in the tissue context to travel to a different body site via the circulation, they transiently live as dispersed cells without cellular contacts and, consequently, lose their pre-activated status and stop being prepared for immediate activation (Stefanova, Dorfman *et al.* 2002, Garbi, Hammerling *et al.* 2010, Hochweller, Wabnitz *et al.* 2010, Romer, Berr *et al.* 2011).

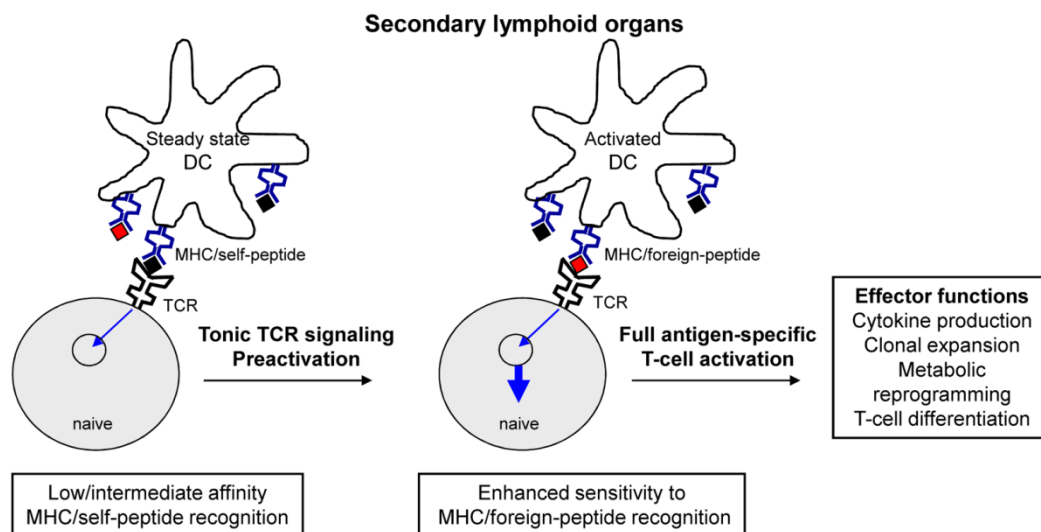


Figure 1.2: **Model: MHC/(self-peptide) recognition enhances sensitivity of T-cells to foreign antigens.** In secondary lymphoid organs low- or intermediate affinity MHC/(self-peptide) recognition of naive T-cells on steady state DCs results in tonic TCR signaling and a pre-activated T-cell status that makes cells sensitive to MHC/foreign-peptide recognition on DCs activated by inflammatory stimuli. Modified from (Garbi, Hammerling *et al.* 2010)

### 1.2.3 Enhanced foreign-antigen sensitivity of murine T-cell responses through tonic TCR signaling

Mouse models have demonstrated extensively that tonic TCR signaling maintains the sensitivity of murine CD4 T-cells towards subsequent foreign antigens in the tissue environment (Stefanova, Dorfman *et al.* 2002, Hochweller, Wabnitz *et al.* 2010, Garbi and Kreutzberg 2012). Stefanová *et al.* have shown that post-thymic recognition of self-peptide loaded MHC molecules facilitates the antigen reactivity of mature CD4 T-cells (Stefanova, Dorfman *et al.* 2002). Tonic TCR signaling was measured by the phosphorylation level of the ZAP-70 associated TCR  $\zeta$  chains. Freshly prepared, blood-derived TCR transgenic CD4 T-cells had nearly undetectable levels of partially phosphorylated TCR  $\zeta$  chains

and displayed a 10-fold lower sensitivity to their cognate antigen, a 17-mer peptide fragment of pigeon cytochrome c (PCC 88-104), compared with LN cells from the same animals. Moreover, interruption of tonic TCR signals led to a rapid decline in sensitivity to the tested antigen (Stefanova, Dorfman *et al.* 2002). Loss of murine CD4 T-cell responsiveness to PCC 88-104 was observed within 15-30 minutes from LN-derived T-cells that had been placed in dispersed cultures. The requirement for basal activation of murine T-cells for high responsiveness to foreign antigens was also reported by Hochweller and colleagues. By using a diphtheria toxin (DT)-based murine model for DC depletion, it was shown that DCs support the responsiveness of TCR transgenic CD4 T-cells to titrated amounts of the myelin oligodendrocyte glycoprotein (MOG 33-35) peptide, and the responsiveness of TCR transgenic CD8 T-cells to the ovalbumin (OVA) agonist peptide SIINFEKL. The role of TCR signaling has been further investigated in regard to the polyclonal reactivity of murine T-cells to a bacterial superantigen. A dramatically enhanced proliferation of murine T-cells to titrated amounts of staphylococcal enterotoxin A (SEA) was observed when T-cells obtained tonic TCR signals by contacting DCs before superantigen stimulation (Hochweller, Wabnitz *et al.* 2010). DC depletion led to a 50 % decline in ZAP-70-associated basal TCR  $\zeta$  phosphorylation in T-cells compared with T-cells from DC-sufficient mice, indicating that MHC-expressing DCs sustain tonic TCR signaling in the absence of foreign antigens. This is consistent with the decreased T-cell responsiveness and impaired immune synapse formation in the absence of MHC-expressing DCs (Hochweller, Wabnitz *et al.* 2010). Interestingly, hyporesponsive T-cells which lack MHC expressing DCs are able to quickly restore their antigen sensitivity if pre-incubated with DCs 30 minutes before stimulation with SEA (Hochweller, Wabnitz *et al.* 2010).

### 1.3 Restoring transiently lost TGN1412 reactivity of circulating CD4 memory T-cells

An extreme case illustrating the effect of tonic TCR signaling on subsequent T-cell activation is the dramatic difference in the response of tissue-resident versus circulating human T-cells to the CD28 superagonist TGN1412 (now called TAB08 (Tabares, Berr *et al.* 2014)). TGN1412 binds bivalently to laterally exposed determinants of the co-stimulatory molecule CD28, resulting in CD28 crosslinking (Luhder, Huang *et al.* 2003). While conventional PBMC cultures from circulating cells which lack cellular interactions fail to respond to this CD28-specific monoclonal Ab (mAb) in soluble form (Figure 1.3, middle) (Duff 2006), its application to healthy volunteers in a phase 1 study in 2006 resulted in a life-threatening cytokine release syndrome (Figure 1.3, left) (Suntharalingam, Perry *et al.* 2006). The molecular basis for this all-or-nothing effect is the dependence of CD28-driven T-cell activation on a pre-activated TCR signaling machinery which is amplified by the co-stimulatory signal at the level of the SLP76 signalosome (Dennehy, Elias *et al.* 2007).



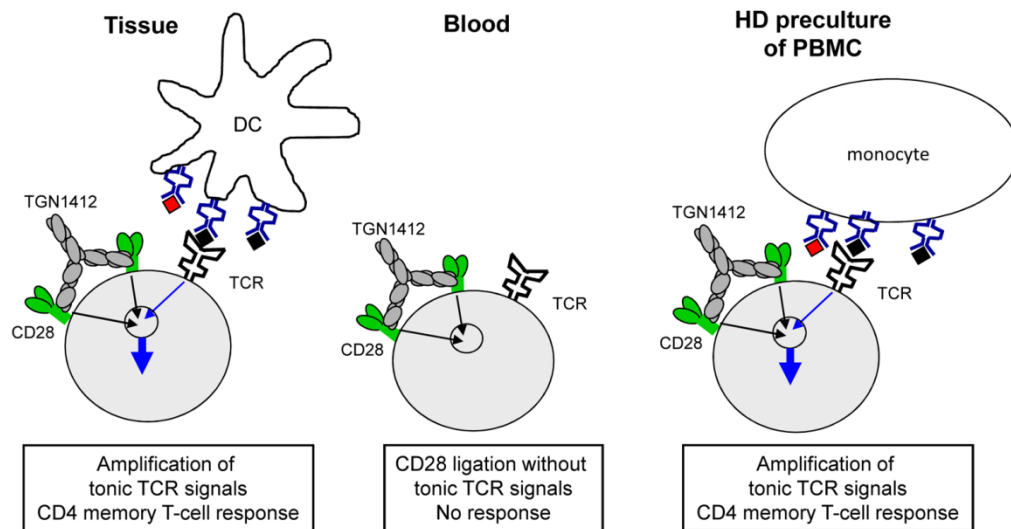


Figure 1.3: **Soluble TGN1412/TAB08-mediated T-cell responses.** (Left) Tonic TCR signals are induced by TCR-HLA/self-peptide complexes between T-cells and professional APCs, mainly DCs, and are amplified by the co-stimulatory signal at the level of the SLP76 signalosome in lymphoid tissue. (Middle) This phenomenon does not occur in freshly isolated PBMC as cell-cell contacts are missing in the circulation. (Right) T-cells in high-density (HD) precultured PBMC receive tonic TCR signals by actively scanning for HLA/self-peptide complexes on monocytes which mature during short term culture. Modified from Hünig 2011

### 1.3.1 HD preculture of PBMCs allows *in-vitro* responses of human CD4 T-cells to soluble TGN1412

Interestingly, TGN1412 reactivity is lost when entering the blood circulation but can be subsequently restored by “parking” PBMC in cultures at a 10-fold higher cell density ( $10^7$  cells/ml) than is used for conventional PBMC assays ( $10^6$  cells/ml) for 48 hours at 37 °C and 5 % CO<sub>2</sub> (Romer, Berr *et al.* 2011). This high-density (HD) preculture step, also known as the RESTORE protocol for RESetting T-cells to Original REactivity, allows human T-cells to continuously scan HLA/self-peptide complexes on the surface of other blood-derived mononuclear cells in the absence of cognate antigen (Figure 1.3, right) (Romer, Berr *et al.* 2011). In contrast to T-cell crawling in lymphoid organs, where DCs function as professional APCs presenting HLA/self-peptide complexes to T-cells (Hochweller, Wabnitz *et al.* 2010, Garbi and Kreutzberg 2012), T-cell-monocyte interactions are required for the acquisition of T-cell function in HD precultures of human PBMCs (Romer, Berr *et al.* 2011). Rapid functional recovery of hyporesponsive murine T-cells in the presence of DCs occurs within only 30 minutes (Hochweller, Wabnitz *et al.* 2010), however, 48 hours are needed for functional maturation of human monocytes. Upon HD preculture of PBMCs, the monocytes upregulate HLA class I molecules and the co-stimulatory molecule CD86 and thereby improve their features as accessory cells (Romer, Berr *et al.* 2011). Shorter HD preculture steps of only 24 hours are insufficient to restore TGN1412-reactivity of CD4 memory T-cells and longer preculture steps of up to three days do not further improve CD4 memory T-cell responses to TGN1412 (Romer, Berr *et al.* 2011).

### **1.3.2 HD preculture of PBMCs induces tonic TCR signaling for amplification by TGN1412**

Römer *et al.* confirmed the hypothesis that blood-derived CD4 T-cells lost their primed status, but that this status could be later restored during HD preculture by resuming cellular interactions, which provided tonic TCR signals for the amplification by TGN1412 (Romer, Berr *et al.* 2011). Colocalization of the TCR/CD3 with tyrosine-phosphorylated proteins by confocal microscopy was shown in human LN sections and HD precultured PBMCs, but not in fresh PBMCs (Romer, Berr *et al.* 2011). Moreover, scanning of HLA/self-peptide complexes by T-cells during HD preculture of PBMCs was blocked by the addition of monovalent Fab fragments directed against HLA class I and HLA class II. This addition resulted in a dramatic reduction of the cytokine response to TGN1412 by CD4 memory T-cells (Romer, Berr *et al.* 2011). Finally, the importance of cellular interactions leading to the acquisition of TGN1412 reactivity was investigated using LN-resident human CD4 memory T-cells (Romer, Berr *et al.* 2011). Whereas a high proliferative capacity in response to CD28 superagonist was observed for *ex-vivo* CD4 memory T-cells which were kept on ice in order to avoid the loss of the pre-activated T-cell status, interruption of cellular contacts in dispersed LN cultures for only 1 hour at body temperature led to a dramatic loss of TGN1412 reactivity (Romer, Berr *et al.* 2011).

## **1.4 The RESTORE protocol – a tool for reliable monitoring of T-cell responses directed to viral and tumor antigens?**

### **1.4.1 Monitoring of human T-cell responses specific for viral and tumor antigens**

Monitoring of blood-derived T-cell responses directed to viral or tumor antigens is an essential component of immunological research, translational science and even clinical settings. The evaluation of vaccine efficiency represents only one of multiple applications (Seder, Darrah *et al.* 2008). Many different assays are available that allow the assessment of the immune system for a variety of phenotypes and functions. CD8 T-cells specific for viral or tumor antigens can either be detected through HLA/peptide multimer staining, an option only available at considerable cost and requiring knowledge of the relevant allelic HLA molecules and antigenic peptides involved, or through the detection of functional responses to peptide pools, usually the production of the pro-inflammatory cytokine interferon- $\gamma$  (IFN- $\gamma$ ). Cytokine production of T-cells upon antigen contact can be evaluated by Enzyme Linked Immuno Spot (ELISPOT) assays, cytokine secretion assays or intracellular cytokine staining. A key element for the functional evaluation of T-cell responses is the integrity of the sample, which depends on multiple preparation steps, such as the anti-coagulant (Mallone, Mannering *et al.* 2011), the time frame between blood drawn and PBMC isolation (Bull, Lee *et al.* 2007, Afonso, Scotto *et al.* 2010), the storage temperature of unprocessed blood (Olson, Smolkin *et al.* 2011), the optimal cryopreservation and thawing of PBMCs (Filbert, Attig *et al.* 2013) and the cultivation of blood-derived mononuclear cells. With regards to the latter, overnight resting of suspended PBMCs in a tube stored with an open lid in an incubator at 37 °C and 5 % CO<sub>2</sub> is a common technique used to improve T-cell

performance by removing apoptotic cells generated as a result of freezing/thawing (Kutscher, Dembek *et al.* 2013, Santos, Buying *et al.* 2014). In contrast to the RESTORE protocol developed by Römer *et al.* (Romer, Berr *et al.* 2011), overnight resting takes place for only 1 day at an undefined cell density. Even if the integrity of the sample is optimal, the loss of a functional signaling platform in blood samples in comparison to tissue samples has to be considered for reliable immunomonitoring (Stebbing, Findlay *et al.* 2007).

### 1.4.2 Aims of this study

A tissue-like *in-vitro* response of CD8 T-cell to viral and tumor-associated antigens would be highly desirable for immunomonitoring and could improve the generation of CD8 T-cell lines and clones for cellular immunotherapy. Therefore, we posed the question as to whether HD preculture of human PBMCs would also allow for more sensitive detection of CD8 T-cell responses to viral and tumor-derived antigens. In the first part of this study (Chapter 4.1, 4.4), I will show that this is indeed the case for a broad range of virus-specific peptides and peptide pools derived from human cytomegalovirus (HCMV), Epstein-Barr virus (EBV), Influenza A virus and adenovirus (AdV). The determination of the optimal preculture conditions for monitoring of antigenic CD8 T-cell responses (Chapter 4.2) is followed by studies on cellular interactions underlying the RESTORE protocol (Chapter 4.3) and a comparison of antigen-specific T-cell responses in blood and tissue of the same individual (Chapter 4.5). The promising results obtained from virus-specific T-cell responses encouraged me to test whether HD preculture of PBMCs from leukemia patients that had received an allogeneic hematopoietic stem cell transplantation (HSCT) facilitates CD8 T-cell responses to the tumor-associated antigen Wilms tumor 1 (WT1) and whether the protocol can be applied for chronological monitoring of WT1-derived T-cell responses arising after transplantation (Chapter 4.6) as well as for the generation of CD8 T-cell lines with an improved representation of clones responding to low antigen concentrations (Chapter 4.7). Finally, I investigated whether the dramatic increase in antigen sensitivity of “restored” CD8 T-cells compared to freshly isolated CD8 T-cells correlates with “tonic signaling”, i.e. enhanced tyrosine phosphorylation of proximal TCR signaling components (Chapter 4.8), and with a change in gene expression profile tested by ribonucleic acid (RNA) microarray (Chapter 4.9, 4.10).

## 1.5 Introductory statement on contributions and previous publication

This thesis was conducted in the research laboratory of Prof. Dr. Thomas Hünig at the Institute for Virology and Immunobiology of the University of Würzburg. Experimental procedures of this PhD thesis were performed by myself, with the exception of microarray hybridization (technical assistance Margareta Göbel), Western blotting (technical assistance Hemant Kumar Joshi) and flow cytometry based isolation of CD8 memory T-cells (technical assistance Christian Linden). Dr. Claus-Jürgen Scholz (Group Leader, Core Unit SysMed) analyzed the microarray data. PD Dr. Götz Ulrich Grigoleit

(Department of Internal Medicine II, University Hospital of Würzburg) provided blood samples of leukemia patients, Priv.-Doz. Dr. Stephan Hackenberg (Department of Oto-Rhino-Laryngology, Plastic, Aesthetic and Reconstructive Head and Neck Surgery, University Hospital of Würzburg) provided human blood and paired tonsils, and Priv.-Doz. Dr. Christian Jurowich (Department of General, Visceral, Vascular and Paediatric Surgery, University Hospital of Würzburg) provided human blood and small intestine. Synthetic peptides were a kind gift from Prof. Dr. Stefan Stevanović (Interfaculty Institute for Cell Biology, Department of Immunology, University of Tübingen) and the antibody TAB08 from TheraMAB LLC. Dr. Paula Römer (former PhD student in the laboratory of Prof. Dr. Thomas Hünig) optimized the RESTORE protocol for circulating human CD4 T-cells. The major part of this research is published in the Journal of the American Society of Hematology (Wegner, Hackenberg *et al.* 2015), which grants permission to use this published material for my doctoral thesis.

Wegner, J., S. Hackenberg, C. J. Scholz, S. Chuvpilo, D. Tyrsin, A. A. Matskevich, G. U. Grigoleit, S. Stevanovic and T. Hunig (2015). "High-density preculture of PBMC restores defective sensitivity of circulating CD8 T-cells to virus- and tumor-derived antigens." Blood.

## 2 Material

### 2.1 Equipment and supplies

Equipment / Supplies	Manufacturer	Specifications
10 µl tips	Roth	
1000 µl blue tips	Roth	
200 µl yellow tips	Roth	
24 well plates	Greiner Bio-One	Flat bottom cell culture
48 well plates	Greiner Bio-One	Flat bottom cell culture
96 well plates	Greiner Bio-One	Flat bottom cell culture
96 well plates	Greiner Bio-One	U bottom suspension culture
Autoclave	Melag	
BioAnalyzer	Agilent	
Cell counting chamber	Neubauer	
Cell strainer	BD Falcon	70 µm nylon mesh
Centrifuge	Eppendorf	Eppendorf centrifuge 5804 R
Centrifuge	Heraeus	Heraeus Megafuge 1.0R
Centrifuge tubes	Greiner Bio-One	15, 50 ml polypropylene
Cryotubes	Nunc	Cryotube Vials 1.8 ml
Dark Box	FUJIFILM	Intellight Dark Box
Dispenser tips	Brand	1.25 ml, 2.5 ml
ELISPOT plates	Millipore	MultiScreen Filter plates (white)
ELISPOT reader	CTL	ImmunoSpot S5 Versa Analyzer
Eppendorf tubes	Sarstedt	1.5 ml
	Greiner	2.0 ml
FACS tubes	BD Biosciences	REF 352052
Flow Cytometer	BD Biosciences	FACSCalibur, FACS Aria III
Flow hood	Heraeus	Laminar HBB2448
Freezer	Forma Scientific	-80 °C
Freezing container	Nalgene	“Mr Frosty”, 18 vials
Harvester	Perkin Elmer LAS GmbH	
Heat block	Eppendorf	Thermomixer comfort
Hera Cell	Hera	safe hood
Humidified incubator	Thermo Scientific	HERA Cell 150
Ice maker	Scotsmann	

Leucosep tubes	Greiner Bio-One	50 ml
Liquid scintillation counter	Perkin Elmer LAS GmbH	
pH-meter	Hanna Instruments	HI 1280
Refrigerator	Liebherr	4 °C, -20 °C
Separation columns	Miltenyi Biotec	25 LS and LD
Water bath	Lauda	
Western blot equipment	BIO-RAD	
Western blot membrane	Roth	Roti-PVDF membrane

## 2.2 Software

Software	Application	Reference
Adobe Photoshop CS3	Figure preparation	Adobe
CELLQuest v3.3	FACS data acquisition on FACSCalibur flow cytometer	BD Biosciences
EndNote X5	Reference management	Thomson Reuters
FCAP Array software v2.0	CBA results analysis <a href="http://www.fcaparray.com">www.fcaparray.com</a>	SoftFlow Inc,
FlowJo v9.5.2	FACS data analysis	TreeStar, Inc
Graphpad Prism v5	Graphs and Statistical analysis	<a href="http://www.graphpad.com">www.graphpad.com</a>
Image Reader LAS-3000 v2.0	Dark Box image acquisition	Fujifilm
ImmunoSpot reader systems	Read ELISPOT plates	CTL
ImmunoSpot software v4.0	Analyze ELISPOT images	CTL
Microsoft Office 2011 for MAC	Data management and Manuscript preparation	Microsoft

## 2.3 Chemicals and reagents

Name	Manufacturer
7-AAD	BD Biosciences
10X Permeabilization Buffer	eBioscience
Acrylamid 4K Solution (30 %)	AppliChem
Ammonium persulfate	AppliChem
Annexin V stain	ImmunoTools
Anti-mouse horseradish peroxidase (HRP)	BD Biosciences
Anti-PE Microbeads	Miltenyi Biotec

Anti-rabbit HRP	BD Biosciences
Amphotericin B	AppliChem
BD FACSRinse Solution	BD Biosciences
Bovine Serum Albumin (BSA)	Roth
Brefeldin A	Sigma Aldrich
Ciprofloxacin	AppliChem, Fresenius Kabi
Chloroform	Sigma Aldrich
Collagenase type IV	Sigma Aldrich
Cotrim-ratiopharm Ampoules SF480 mg/ 5 ml	Ratiopharm
Dimethylsulfoxide (DMSO)	AppliChem
Dithiothreitol (DTT)	AppliChem
DNase type I	Sigma Aldrich
Ethanol	AppliChem
Ethylenediaminetetraacetic acid (EDTA)	Roth
Fetal calf serum (FCS)	Gibco
Gentamicin sulfate	AppliChem
Glycerol	AppliChem
HBSS, no Calcium, no Magnesium	Gibco
HEPES	AppliChem
Human Serum Type AB from Male AB	Sigma Aldrich
Isopropanol	Roth
Lymphocyte separation medium	PAA, CEDARLANE
Milk powder	Real
Methanol	Sigma Aldrich
NBT/BCIP Liquid Substrate System	Sigma Aldrich
Non-essential amino acids	Invitrogen
NP-40	AppliChem
Paraformaldehyde	Sigma Aldrich
Penicillin	INFECTOPHARM
Percoll	GE Healthcare Life Sciences
Phosphatase inhibitor Cocktail 2	Sigma Aldrich
Pro5 <sup>®</sup> Recombinant HLA-A0201 Pentamer	Proimmune
Pro5 <sup>®</sup> Recombinant PP65_HCMV 495-503 Pentamer	Proimmune
Protease inhibitor Cocktail	Sigma Aldrich
RNAse Zap	Sigma Aldrich
RPMI Medium 1640	Gibco
RPMI Medium 1640 - L-Glutamine	Gibco
Sodium acetate (NaOAc)	AppliChem
Sodium azide (NaN <sub>3</sub> )	Roth

Sodium chloride (NaCl)	Sigma Aldrich
Sodium deoxycholate	Roth
Sodium dodecyl sulfate (SDS)	Roth
$\beta$ -Mercaptoethanol	Invitrogen
Streptavidin-AP	Southern Biotech
Streptomycin sulfate	AppliChem
TEMED	AppliChem
Tris	AppliChem
Triton X-100	Roth
Trypan blue	Sigma Aldrich
Tween-20	AppliChem
TRIzol reagent	Ambion
Water, Ampuwa	Fresenius Kabi
Water, RNase-free, DEPC treated	Affymetrix
WesternBright Chemiluminescent HRP Substrate	Biozym Scientific

## 2.4 Buffers, media and solutions

### **BSS (balanced salt solution) / 0.2 % BSA (bovine serum albumin) (BSS/BSA)**

BSS I	1100 ml
BSS II	1100 ml
BSA	20.0 g
ddH <sub>2</sub> O ad	10.0 l

#### **BSS I**

Glucose	100 g
KH <sub>2</sub> PO <sub>4</sub>	6.0 g
Na <sub>2</sub> HPO <sub>4</sub> ·2H <sub>2</sub> O	23.8 g
Phenol red	1.0 g
ddH <sub>2</sub> O ad	10.0 l

#### **BSS II**

CaCl <sub>2</sub> ·2H <sub>2</sub> O	18.6 g
KCl	40.0 g
NaCl	800 g
MgCl <sub>2</sub> ·6H <sub>2</sub> O	20.0 g
MgSO <sub>4</sub> ·7H <sub>2</sub> O	20.0 g
ddH <sub>2</sub> O ad	10.0 l



**FACS (fluorescence-activated cell sorting) buffer**

BSA	0.1 %
Sodium azide	0.01 % in PBS

**Freezing medium**

Heat-inactivated human AB serum	50 %
AB medium	40 %
DMSO	10 %

**HBSS (Hank's balanced salt solution) /PSGABC**

HBSS	500 ml
Penicillin / Streptomycin	100 IU/ml
Gentamicin sulfate	50 µg/ml
Amphotericin B	2.5 µg/ml
Co-trimoxazol (Bactrim)	96 µg/ml
Ciprofloxacin	2 µg/ml

**Isotonic Percoll 100 %**

Percoll	378 ml
PBS 10x	42 ml

**Laemmli 5x buffer**

1.25M Tris	2.5 ml
Glycerol	5.0 ml
SDS	1.0 g
DTT	0.8 g
Bromphenol Blue (1 % solution)	1.0 ml
ddH <sub>2</sub> O ad	10.0 ml, pH 6.8

**RIPA (Radio Immuno Precipitation Assay) buffer**

NaCl	150 mM
NP-40	1.0 %
Sodium deoxycholate	0.5 %
SDS	0.1 %
Tris	50 mM, in ddH <sub>2</sub> O, pH 8.0

**PBS (Phosphate buffered saline)**

NaCl	80.0 g
KCl	2.0 g

KH <sub>2</sub> PO <sub>4</sub>	2.0 g
Na <sub>2</sub> HPO <sub>4</sub>	11.5 g
ddH <sub>2</sub> O ad	10.0 l, pH 7.4

**Percoll 67 %**

Isotonic Percoll 100 %	378 ml
RPMI Medium 1640	65 ml

**Percoll 30 %**

Isotonic Percoll 100 %	60 ml
PBS 1x	140 ml

**Resolving buffer**

Tris	91.0 g
ddH <sub>2</sub> O ad	300 ml, pH 8.8
ddH <sub>2</sub> O ad	200 ml
SDS	2.0 g

**RPMI Medium 1640 - L-Glutamine + 10 % AB serum (AB medium)**

RPMI Medium 1640 - L-Glutamine	500 ml
Penicillin / Streptomycin (100 IU/ml)	1.2 ml
Non-essential amino acids (100X MEM)	5.0 ml
Na-Pyruvate (100 mM)	5.0 ml
β-Mercaptoethanol (50 mM)	500 µl
HEPES (1 M)	5.0 ml
10 % heat inactivated human AB serum	50 ml

**RPMI Medium 1640 - L-Glutamine + 10 % (2 %) FCS**

RPMI Medium 1640 - L-Glutamine	500 ml
Penicillin / Streptomycin (100 IU/ml)	1.2 ml
10 % FCS (2 %)	50 ml (10 ml)

**RPMI Medium 1640 /PSGABC**

RPMI Medium 1640	500 ml
Penicillin / Streptomycin	100 IU/ml
Gentamicin sulfate	50 µg/ml
Amphotericin B	2.5 µg/ml
Co-trimoxazol	96 µg/ml
Ciprofloxacin	2 µg/ml

**RPMI Medium 1640 - L-Glutamine + 2 % FCS /PSGABC + Enzymes**

(Digestion of the lamina propria)

RPMI Medium 1640 - L-Glutamine	500 ml
2 % FCS	10 ml
Penicillin / Streptomycin	100 IU/ml
Gentamicin sulfate	50 µg/ml
Amphotericin B	2.5 µg/ml
Co-trimoxazol	96 µg/ml
Ciprofloxacin	2 µg/ml
Collagenase type IV	22.5 IU/ml
DNase type I	13.5 IU/ml

**Stacking buffer**

Tris	6.05 g
ddH <sub>2</sub> O ad	40 ml, pH 6.8
ddH <sub>2</sub> O ad	60 ml
SDS	0.4 g

**TBS 10x buffer**

Tris-HCl	24.23 g
NaCl	80.06 g
ddH <sub>2</sub> O ad	1.0 l, pH 7.4

**TBST (TBS-Tween) buffer**

Tween-20	1 ml
TBS 10x buffer	100 ml
ddH <sub>2</sub> O ad	1.0 l

**Transfer buffer**

Tris	15.1 g
Glycine	72 g
ddH <sub>2</sub> O ad	4.0 l
Methanol ad	1.0 l

**Versene**

KCl	1.0 g
KH <sub>2</sub> PO <sub>4</sub>	1.0 g
NaHPO <sub>4</sub>	2.84 g

NaCl	41.0 g
Versene	1.0 g
ddH <sub>2</sub> O ad	5.0 l

## 2.5 Commercial kits

Kit	Manufacturer
C&E version ExpressArt TR <i>nucleotide</i> mRNA amplification Pico kit	AmpTec
CD8 <sup>+</sup> T Cell Isolation Kit, human	Miltenyi Biotec
Human IFN- $\gamma$ ELISPOT Pair	BD Biosciences
IFN- $\gamma$ Secretion Assay - Detection Kit (PE)	Miltenyi Biotec
IVT PLUS kit	Affymetrix
Monocyte Isolation Ki II, human	Miltenyi Biotec
PrimeView™ Human Gene Expression Arrays	Affymetrix
RNeasy Plus Micro Kit	QIAGEN

## 2.6 Anti-human antibodies

Antigen	Clone/poly	Conjugation	Isotype	Manufacturer
CD137	4B4-1	PE	Mouse IgG1, $\kappa$	Miltenyi Biotec
CD14	M5E2	PE	Mouse IgG2b, $\kappa$	BD Biosciences
CD152 (CTLA-4)	L3D10	PE	Mouse IgG1, $\kappa$	Biolegend
CD25	M-A251	PE	Mouse IgG1, $\kappa$	BD Biosciences
CD279 (PD1)	EH12.2H7	PerCP/Cy5.5	Mouse IgG1, $\kappa$	Biolegend
CD28	15E8	Purified	Mouse IgG1, $\kappa$	Miltenyi Biotec
CD28	CD28.2	PE-Cy™5	Mouse IgG1, $\kappa$	BD Biosciences
CD3	BW264/56	Purified	Mouse IgG2a, $\kappa$	Miltenyi Biotec
CD3	MEM-57	APC	Mouse IgG2a, $\kappa$	ImmunoTools
CD3	UCHT1	Alexa647	Mouse IgG1, $\kappa$	BD Biosciences
CD357 (GITR)	621	PE	Mouse IgG1, $\kappa$	Biolegend
CD3- $\xi$	6B10.2	Purified	Mouse IgG2a, $\kappa$	Santa Cruz
CD4	MEM-241	PE	Mouse IgG1, $\kappa$	ImmunoTools
CD4	RPA-TA	PECy5	Mouse IgG1, $\kappa$	Biolegend
CD45R0	UCHL1	FITC	Mouse IgG2a, $\kappa$	BD Biosciences

CD62L	LT-TD180	APC	Mouse IgG1, $\kappa$	ImmunoTools
CD62L	LT-TD180	PE	Mouse IgG1, $\kappa$	ImmunoTools
CD8	RPA-T8	APC	Mouse IgG1, $\kappa$	BD Biosciences
CD8	RPA-T8	PE	Mouse IgG1, $\kappa$	BD Biosciences
CD8	UCHT-4	FITC	Mouse IgG2a, $\kappa$	ImmunoTools
CD80	B7-1	FITC	Mouse IgM, $\kappa$	BD Biosciences
CD86	2331 (FUN-1)	PE-Cy <sup>TM</sup> 5	Mouse IgG1, $\kappa$	BD Biosciences
ERK1/2	polyclonal	Purified	Rabbit	Life Technologies
GLUT1	202915	PE	Mouse IgG2b,	R&D Systems
HLA-ABC	G46-26	PE-Cy <sup>TM</sup> 5	Mouse IgG1, $\kappa$	BD Biosciences
HLA-DR, DP, DQ	Tü39	FITC	Mouse IgG2a, $\kappa$	BD Biosciences
IFN- $\gamma$	4S.B3	PE	Mouse IgG1, $\kappa$	BD Biosciences
Lck	polyclonal	Purified	Rabbit	Cell Signaling
pCD3- $\xi$ (Tyr142)	K25-407.69	Purified	Mouse IgG2a, $\kappa$	BD Biosciences
Phosphotyrosine	4G10	Purified	Mouse IgG2b, $\kappa$	Millipore
pSrc family (Tyr416)	polyclonal	Purified	Rabbit	Cell Signaling
pZAP-70 (Tyr319)/Syk (Tyr352)		Purified	Rabbit	Cell Signaling
ZAP-70	polyclonal	Purified	Rabbit	Cell Signaling

## 2.7 Cell stimulation reagents

Name	Manufacturer
E1A_ADE02 19-27	Kind gift of Prof. Stevanović
HEX_ADE02 37-45	Kind gift of Prof. Stevanović
HEX_ADE02 901-910	Kind gift of Prof. Stevanović
HIV-1 pol 476-484	Kind gift of Prof. Stevanović
Human IL-15	Pepto Tech
Human IL-17	Pepto Tech
Human IL-2 (Proleukine)	Chiron
Muromonab-CD3 (OKT3)	Janssen-Cilag
PepMix <sup>TM</sup> CEF standard	JPT Peptide Technologies
PepMix <sup>TM</sup> CEFT standard	JPT Peptide Technologies
PepMix <sup>TM</sup> Human Actin	JPT Peptide Technologies
PepMix <sup>TM</sup> Influenza A MP1 (H1N1)	JPT Peptide Technologies
PepMix <sup>TM</sup> Influenza A NP (H3N2)	JPT Peptide Technologies
PP65_HCMVA 495-503	Kind gift of Prof. Stevanović
TGN1412/ TAB08	Theramab GmbH

WT1\_HUMAN 126-134

Kind gift of Prof. Stevanović

WT1\_HUMAN 356-364

Kind gift of Prof. Stevanović

## 2.8 Human material

Cell type	Source	Location
PBMCs	Venous blood	Transfusion Medicine and Hemotherapy Department of Internal Medicine II University Hospital Würzburg
	Of healthy individuals	
LPMCs	Of patients with hematological malignant disorders	Department of Visceral Surgery University Hospital Würzburg
	Mucosa of the small intestine	
TMCs	Of obese patients undergoing gastric bypass operation	Department of Oto-Rhino-Laryngology, Plastic, Aesthetic and Reconstructive Head and Neck Surgery University Hospital Würzburg
	Uninfected tonsils	
	Of children undergoing tonsillotomy	

## **3 Methods**

### **3.1 Cellular methods**

#### **3.1.1 Isolation of human lymphoid cells from blood and tissue**

##### **3.1.1.1 From blood**

Human PBMCs were either prepared from healthy donors as a byproduct of platelet concentrates obtained with leukoreduction system chambers (LRS-C) (Dietz, Bulur *et al.* 2006) or as heparinized venous blood from patients with hematological malignant disorders who had undergone myeloablation and allogeneic hematopoietic stem cell transplantation. All patients were in complete hematological remission at the time of blood sampling. The average time between stem cell transplantation and sampling was 814 days; from 166 to 2372 days. PBMCs were obtained by density gradient centrifugation with lymphocyte separation medium. Upon washing with ice-cold BSS/ 0.2 % BSA, cells were kept on ice until use within one hour or were cryopreserved until analysis. The term “fresh” refers to freshly isolated PBMCs tested either directly or after freezing/thawing, which yielded identical results (see Figure 4.14).

##### **3.1.1.2 From lamina propria of the small intestine**

Lamina propria mononuclear cells (LPMCs) were isolated according to a modified method of Bull and Bookman (Bull and Bookman 1977). In brief, the mucosal layer was dissected from the fresh tissue and washed extensively in antibiotics supplemented culture medium (RPMI Medium 1640 /PSGABC). Mucus as well as part of the epithelial cells were removed by carefully scraping the tissue surface with a scalpel. Subsequently, the mucosa was cut into 2-4 mm pieces and incubated in a shaking water bath at 37 °C with 0.7 mM EDTA in HBSS/PSGABC for 45 minutes to remove epithelial cells. This incubation was repeated twice. After extensive washing the tissue was incubated in collagenase type IV and DNase type I containing digestion medium in a shaking water bath at 37 °C for totally 10-12 hours. The resulting cell suspension was separated from undigested tissue by filtration through a coarse-meshed sieve and finally through a 70 µm nylon mesh. For further isolation of LPMCs, the cell suspension was subjected to Percoll density gradient centrifugation and viable mononuclear cells were isolated via density gradient centrifugation using lymphocyte separation medium. Cells were washed and resuspended in ice-cold RPMI Medium 1640 supplemented with L-Glutamine and 10 % FCS until frozen or used.

### 3.1.1.3 From tonsils

Uninfected fresh tonsils were collected from children undergoing tonsillotomy at the University Hospital Würzburg. Single-cell suspensions were prepared by cutting the lymphoid tissue into 2-4 mm pieces, digestion with collagenase type IV (0.5 mg/ ml) and DNase type I (0.02 mg/ ml) in a shaking water bath at 37 °C for 40 minutes, followed by filtration through a 45 µm nylon mesh. Viable tonsillar mononuclear cells (TMCs) were isolated by density gradient centrifugation with lymphocyte separation medium and were washed with ice-cold BSS/BSA before cells were frozen or used. The applied protocol was first described for the isolation of mononuclear cells from liver graft biopsies (33).

### 3.1.1.4 Study approval

Studies using human material were approved by the University of Würzburg Committee on Human Research (study numbers 85/13 and 159/13) and by the institutional review board of the University of Würzburg. The informed consent was obtained in accordance with the guidelines of the World Medical Association's Declaration of Helsinki. Written Informed consent was obtained from donors prior to inclusion in the study.

## 3.1.2 Freezing and thawing of mononuclear cells

Human PBMCs, LPMCs and TMCs were cryopreserved at a concentration of  $5 \times 10^6$  cells per 1 ml of freezing media. The cell suspension was transferred into cryotubes, which were immediately placed in a pre-cooled (4 °C) "Mr. Frosty" Cryogenic Freezing Container filled with isopropanol, stored at -80 °C for 24 hours and were then transferred to a -140 °C freezer.

Cryopreserved vials were briefly thawed in a 37 °C water bath until there was a pea-sized piece of ice remaining. Tubes were disinfected before opening under sterile conditions and 1 ml of pre-warmed culture medium was added drop wise. The diluted cell suspension was transferred to a 15 ml Falcon tube containing 8 ml of pre-warmed culture medium, incubated for 10 minutes at room temperature (RT), centrifuged and washed once with medium, resuspended in media and was then kept on ice until used.

## 3.1.3 Isolation and depletion of subpopulations

### 3.1.3.1 Isolation of CD8 T-cells and monocytes

Circulating CD8 T-cells and monocytes were isolated to  $\geq 95$  % purity by using the negative CD8 T-cell Isolation Kit and the positive Monocyte Isolation Kit II from Miltenyi Biotec. Manufacturer's instructions were followed with the only modification of using BSS/BSA instead of the recommended buffer. CD8 T-cells from TMCs were positively isolated by using anti-human CD8-phycoerythrin (PE) and anti-PE-Microbeads as attempts to isolate tonsillar CD8 T-cells by using the negative CD8 T-cell Isolation Kit for human PBMC failed. LS columns were used for all selections. To confirm isolation purity cells were labeled with anti-hCD8-PE or anti-hCD14-PE and analyzed by flow cytometry.



Besides magnetic activated cell sorting, flow cytometric cell sorting was used as a further method to isolate CD8 memory T-cells from PBMCs or TMCs to  $\geq 99$  % purity. CD8<sup>+</sup>CD45R0<sup>+</sup> cells were enriched via labeling of the cells with the conjugates anti-CD8-APC and anti-CD45R0-fluorescein isothiocyanate (FITC).

### 3.1.3.2 Depletion of regulatory T-cells

Human regulatory T-cells that constitutively express CD25 on the cell surface were depleted from unstimulated fresh or HD precultured PBMCs by using anti-hCD25-PE and anti-PE-Microbeads. Purity was confirmed by staining for Foxp3<sup>+</sup>CD25<sup>+</sup>CD4<sup>+</sup> cells before and after depletion ( $\geq 98$  % purity).

## 3.1.4 Cell culture and stimulation assays

### 3.1.4.1 Standard PBMC cultures and T-cell stimulation

Cells were cultured in RPMI Medium 1640 supplemented with 10 % AB serum, L-glutamine, penicillin, streptomycin, non-essential amino acids, Na-pyruvate,  $\beta$ -mercaptoethanol and HEPES (defined as “AB medium”, concentrations of the supplements are given in chapter 2.4) in a humidified incubator at 37 °C with 5 % CO<sub>2</sub>. The cell density for standard T-cell stimulation assays was  $2 \times 10^5$  cells/ 200  $\mu$ l in a flat-bottom 96-well culture plate or a MultiScreen® 96-Well ELISPOT plate.

Virus-specific recall responses were investigated to titrated PepMix™ CEF standard, containing HLA-class I restricted T-cell epitopes from human cytomegalovirus (HCMV), Epstein-Barr virus (EBV) and Influenza A virus, and to a 1:1 combination of the PepMix™ Influenza A MP1 (H1N1) and the PepMix™ Influenza A NP (H3N2). The PepMix™ Human Actin was used a negative control pool. Synthetic peptides from human cytomegalovirus (PP65\_HCMVA 495-503), human immunodeficiency virus (HIV-1 pol 476-484), human adenovirus 2 (HEX\_ADE02 901-910, HEX\_ADE02 37-45 and E1A\_ADE02 19-27) and Wilms tumor 1 protein (WT1\_HUMAN 126-134, WT1\_HUMAN 356-364) were synthesized by an automated peptide synthesizer 433A following the Fmoc/tBu strategy. Synthesis products were analyzed by HPLC and ESI\_TOF mass spectrometry. The minimum purity of the peptide pools and synthesized peptides was 90 %. Clinical grade of TAB08 and purified anti-CD3 (OKT3) was used at 1  $\mu$ g/ ml, *Staphylococcus aureus* enterotoxin B (SEB) at 0.25  $\mu$ g/ ml.

### 3.1.4.2 RESTORE protocol for human PBMCs

For RESetting T-cells to Original REactivity, the RESTORE protocol as described by Römer *et al.* (Römer, Berr *et al.* 2011) was followed. In brief, PBMCs were precultured in AB medium for 2 days at high cell density (HD;  $1.5 \times 10^7$  cells/ 1.5 ml in 24-well suspension culture plates) [1.9 cm<sup>2</sup>] to allow tissue-like interactions of the cells. Upon HD preculture of PBMCs, cells were harvested and prepared for conventional T-cell stimulation assays.

### 3.1.4.3 *In-vitro* expansion assay

For *in-vitro* expansion of antigen-specific CD8 T-cells from fresh or HD precultured PBMCs, cells were stimulated at a cell density of  $2 \times 10^6$  cells/ ml with 1  $\mu\text{g}/\text{ml}$  of the peptide WT1\_HUMAN 356-364, 0.1  $\mu\text{g}/\text{ml}$  of the PepMix™ CEF standard or the control pool Human Actin (0.1  $\mu\text{g}/\text{ml}$ ). On day 3 of the culture, recombinant human IL-2 (50 IU/ ml), IL-7 and IL-15 (10 IU/ ml) were added. Half-media change and supplementation of cytokines were performed every 2-3 days until day 14. Restimulation was performed in MultiScreen® 96-Well ELISPOT plates with titrated amounts of the respective stimuli.

## 3.2 Immunological methods

### 3.2.1 Flow cytometry (phenotyping)

Phenotypic analysis of T-cells and monocytes from fresh or HD precultured PBMCs was performed by using fluorochrome-conjugated antibodies directed to the surface molecules CD3, CD4, CD8, CD45R0, CD62L, CD137, CD28, GITR, CTLA-4, CD14, CD80, CD86, HLA-A, -B, -C and HLA-DR, -DP, -DQ. Cells were washed with FACS buffer, stained with the appropriate antibody conjugates for 15 minutes at 4 °C, washed with FACS buffer and were fixed with 2 % paraformaldehyde. If surface staining was followed by intracellular staining, cells were incubated with Fix/Perm for 30 minutes, washed 1x with FACS buffer, 1x with Perm/Wash and incubated with antibody conjugates against the transcription factors PD-1 and Foxp3 diluted in Perm/Wash for 30 minutes at 4 °C in the dark. Cells were washed and resuspended in FACS buffer for flow cytometry using a FACSCalibur flow cytometer. Data were analyzed using FlowJo Version 8.8.7. In combination with intracellular IFN- $\gamma$  secretion (see Chapter 3.2.2.1), CD137 surface expression was used to type activated human CD8 T-cells.

### 3.2.2 Quantification of IFN- $\gamma$ releasing cells

IFN- $\gamma$  secreting T-cells were quantified by three methods: intracellular IFN- $\gamma$  staining, IFN- $\gamma$  Enzyme-Linked ImmunoSpot (ELISPOT) assay and IFN- $\gamma$  secretion assay.

#### 3.2.2.1 Intracellular IFN- $\gamma$ staining

To analyze intracellular IFN- $\gamma$  production upon T-cell activation, cytokine secretion was blocked with 2  $\mu\text{g}/\text{ml}$  Brefeldin A one hour after stimulation. After incubation for another 15 hours, cells were stained for surface markers, washed with FACS buffer, permeabilized with Fix/Perm for 30 minutes, washed 1x with FACS buffer, 1x with Perm/Wash and incubated with anti-IFN- $\gamma$ -PE diluted in Perm/Wash for 30 minutes at 4 °C in the dark. Cells were washed and resuspended in FACS buffer for flow cytometry.

### 3.2.2.2 IFN- $\gamma$ ELISPOT assay

IFN- $\gamma$  Enzyme-Linked ImmunoSpot (ELISPOT) assays were performed with MultiScreen® 96-Well Plates following the instructions of Merck Millipore. Fresh or HD precultured PBMCs were stimulated in the presence or absence of the respective stimuli for 16 hours. Negative and positive controls were included in each test. For the assay the plate was coated with 5  $\mu\text{g}/\text{ml}$  purified anti-human IFN- $\gamma$  Capture Antibody. Cytokine secreting cells were detected by adding 2  $\mu\text{g}/\text{ml}$  biotinylated anti-human IFN- $\gamma$  Detection Antibody, 1  $\mu\text{g}/\text{ml}$  AP-Streptavidin Conjugate and ready-to-use NBT/BCIP Liquid Substrate System. The number of spot-forming cells per well was determined by an ImmunoSpot® S5 Versa ELISPOT Analyzer.

### 3.2.2.3 IFN- $\gamma$ secretion assay

IFN- $\gamma$  secretion assays were used to quantify IFN- $\gamma$  releasing CD4 and CD8 T-cells from lamina propria. The assay was performed following the instructions of Miltenyi Biotec. In brief, LPMCs were prepared for *in-vitro* stimulation. Cells were resuspended in AB medium and stimulated with titrated TAB08 for 16 hours in a humidified incubator at 37 °C with 5 % CO<sub>2</sub>. As a negative control LPMCs remained unstimulated. As a positive control cells were stimulated with 0.25  $\mu\text{g}/\text{ml}$  SEB. Subsequently, an IFN- $\gamma$  specific Catch Reagent was attached to the cell surface of LPMCs, whereas each sample contained  $1 \times 10^6$  cells. The cells were then incubated for 45 minutes at 37 °C to allow cytokine secretion. The secreted IFN- $\gamma$  was bound to the IFN- $\gamma$  Catch Reagent on the positive, secreting cells. These cells were subsequently labeled with a second IFN- $\gamma$ -specific antibody, the IFN- $\gamma$  Detection Antibody conjugated to the fluorochrome PE for sensitive detection by flow cytometry. For further phenotypic characterization of IFN- $\gamma$  secreting cells, LPMCs were also stained for CD4 and CD8.

## 3.3 Molecular methods

### 3.3.1 Western blotting

#### 3.3.1.1 Sample preparation

Isolated CD8 T-cells from fresh or HD precultured PBMCs or TMCs ( $3 \times 10^6$  each) were washed twice with ice-cold PBS and lysed in 100  $\mu\text{l}$  of RIPA buffer supplemented with Protease Inhibitor Cocktail, Phosphatase inhibitor Cocktail 2 and 1 mM DTT on a shaker at 4 °C for 10 minutes. The lysate was centrifuged at 13.000 rpm at 4 °C for 15 minutes and 80  $\mu\text{l}$  of the supernatant was then mixed with 20  $\mu\text{l}$  of Laemmli 5x buffer prior to boiling at 95 °C for 8 minutes. Denatured, reduced samples were frozen at -20 °C for later use.

### 3.3.1.2 SDS-polyacrylamide gel electrophoresis

Protein extracts were separated on 15 % SDS polyacrylamide gels under reducing conditions. The separating gel mix was prepared, poured into the gel apparatus, and overlaid with water. After the gel polymerized, the water was descanted and the stacking gel was poured. 14  $\mu$ l of protein samples were loaded, and ran in 1x SDS PAGE running buffer.

### 3.3.1.3 Transfer of proteins and staining

Separated proteins from the SDS-PAGE gel were blotted to a PVDF membrane at 12 V (140 mA) for 80 min using a semi-dry transfer system. After the transfer, the membrane was washed with methanol for 5 min, and was blocked with 5 % milk powder in TBST buffer for 1 hour at RT on a rocker platform. The PVDF membrane was then incubated with the primary Ab diluted in TBST buffer plus 5 % milk powder overnight at 4 °C. The membrane was washed 3x with TBST buffer for 10 minutes each time, on the rocker platform at RT, then incubated with a horseradish-peroxidase (HRP) secondary Ab for 2 hours, and washed 3x with TBST buffer for 10 minutes each time. The membrane was treated with the WesternBright chemiluminescent HRP substrate and developed in the dark box.

## 3.3.2 Microarray analysis

### 3.3.2.1 Total RNA isolation and ethanol precipitation of nucleic acids

Total RNA was extracted from isolated CD8<sup>+</sup>CD45R0<sup>+</sup> cells from either fresh or HD precultured PBMCs (donor 1-3) or from fresh PBMCs or TMCs (donor 4-6) by the TRIzol method according to the instructions of Ambion® Life Technologies. To further purify the isolated nucleic acids, 1/10 volume of 3M sodium acetate, pH 5.2 and 2-3 volumes of 100 % ethanol were added to each sample, mixed and frozen at -80 °C for 20 minutes. Samples were centrifuged at full speed for 30 minutes at 4 °C. The supernatant was discarded and 200  $\mu$ l of 70 % ethanol were added. Samples were again spun down at full speed for 5 minutes at 4 °C, supernatant was discarded and the pellet was dried with an open lid in a heat block set at 55 °C for approximately 5 minutes. The RNA pellet was resuspended in 10  $\mu$ l RNase-free water in a heat block for 10 minutes. High RNA quality was checked using a Bioanalyzer 2100 and samples were frozen at -20 °C.

### 3.3.2.2 Gene Array

Expression profiling of RNA from blood and tissue-derived CD8 memory T-cells was performed with GeneChip® PrimeView™ Human Gene Expression Arrays. RNA samples were amplified using the C&E version ExpressArt TRInucleotide mRNA amplification Pico kit. For the third round of *in-vitro* transcription, we used the IVT PLUS kit for incorporation of biotin-labeled nucleotides. Samples were hybridized to GeneChip® PrimeView™ Human Gene Expression Arrays. Data were analyzed using the statistical software environment R version 3.1.2 ([www.r-project.org](http://www.r-project.org)) and extensions from the Bioconductor project ([www.bioconductor.org](http://www.bioconductor.org)). Raw signal intensities were normalized by variance stabilization (Huber, von Heydebreck *et al.* 2002). Statistical analysis to select differentially expressed

genes was performed using the Linear Models of Microarray Analysis (LIMMA) package (Andersen, Svane *et al.* 2005); we here required a nominal  $P < .05$  and an absolute log fold change of at least 1. DAVID was used to search for enriched KEGG pathways (Huang, Sherman *et al.* 2007). The microarray data are available in the Gene Expression Omnibus (GEO) database (<http://www.ncbi.nlm.nih.gov/geo>) under the accession number GSE63430.

### 3.4 Statistical analysis

Data are presented as mean  $\pm$  SD or median with interquartile range. Statistical significance was analyzed by unpaired t test, Wilcoxon matched-paired signed rank test or Mann-Whitney test using GraphPad Prism Software. Values of  $P < .05$  were considered to be statistically significant.

## 4 Results

### 4.1 HD preculture of PBMCs enhances anti-viral IFN- $\gamma$ responses in human CD8 memory T-cells

As previously reported, PBMC CD4 T-cells fail to respond to the CD28 superagonist TGN1412 (now called TAB08) unless they are first returned to a tissue-like functional status by HD preculture of PBMCs for 2 days ((Romer, Berr *et al.* 2011), Figure 4.1A). It was now asked whether the responsiveness of circulating CD8 T-cells to viral antigens is also improved by this preculture procedure.

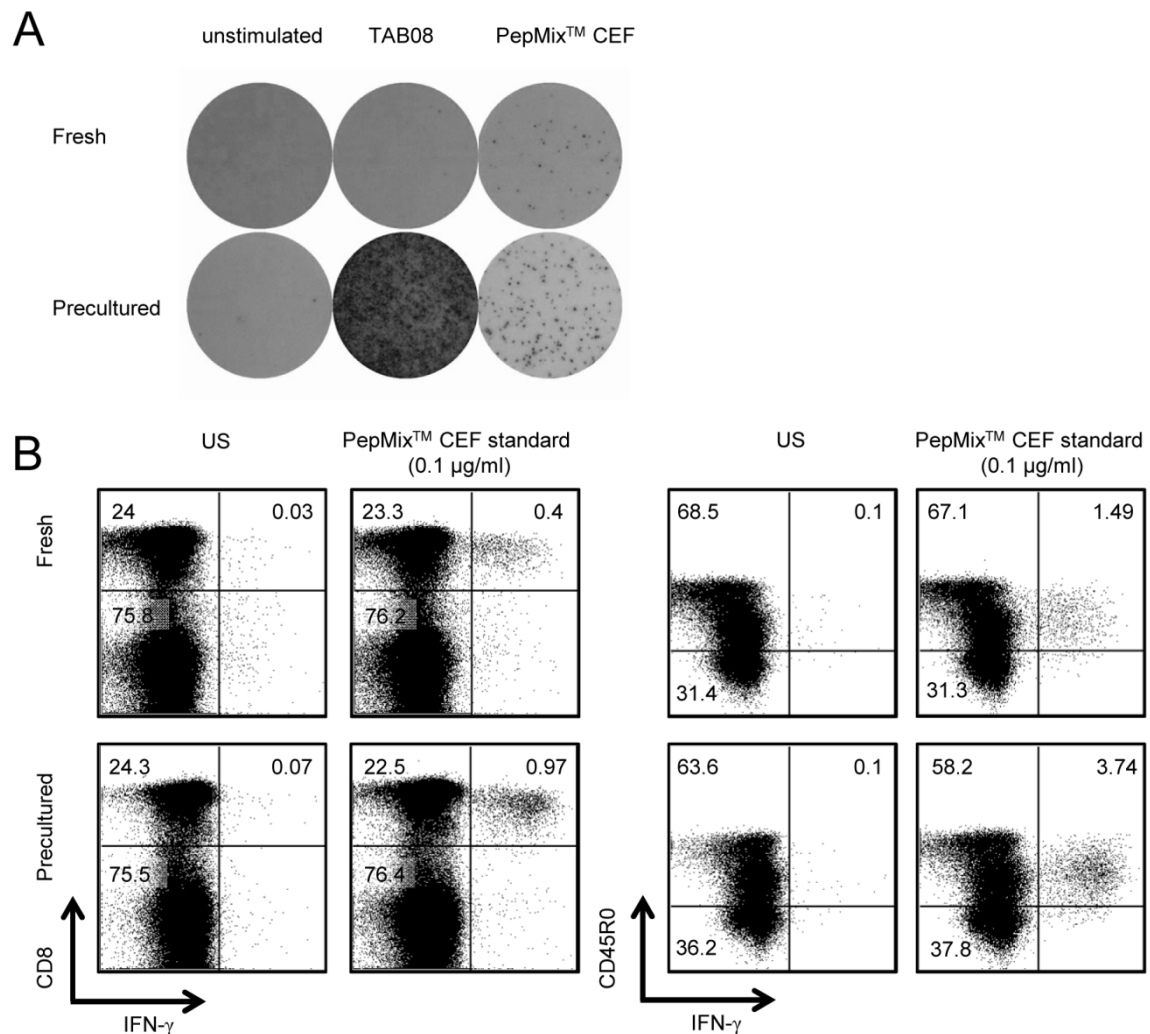


**Figure 4.1: Enhanced anti-viral IFN- $\gamma$  response in HD precultured human CD8 memory T-cells by HD preculture of PBMCs.** (A) Representative IFN- $\gamma$  ELISPOT assay of fresh or HD precultured PBMCs. Cytokine release after stimulation with 1  $\mu$ g/ml CD28 superagonist TAB08 (previously: TGN1412) and 0.1  $\mu$ g/ml PepMix<sup>TM</sup> CEF standard was assessed after 16 hours. Unstimulated fresh and HD precultured PBMCs were used as negative controls. (B) Intracellular IFN- $\gamma$  staining of fresh and HD precultured PBMCs after stimulation with 0.1  $\mu$ g/ml PepMix<sup>TM</sup> CEF standard for 16 hours. Gating was performed on (left) viable lymphocytes and (right) CD8 T-cells. Experiments were repeated  $\geq 3$  times.

For this purpose, the frequencies of CD8 T-cells responding with IFN- $\gamma$  release to 0.1  $\mu\text{g}/\text{ml}$  of the virus-specific PepMix™ CEF standard, containing HLA-class I restricted overlapping 9-mer peptides derived from HCMV, EBV and Influenza A proteins, were compared between fresh and HD precultured PBMCs by a standard ELISPOT assay in a pilot experiment (Figure 4.1A). Antigen-independent spot formation was neither observed in fresh nor in precultured PBMCs. Interestingly, HD preculture of human PBMCs affected not only CD4 T-cell reactivity to soluble TAB08, but also the reactivity of virus-specific CD8 T-cells. Thus, HD precultured PBMCs showed a distinctly higher IFN- $\gamma$  response to the PepMix™ CEF standard relative to fresh PBMCs, indicating that their reactivity to viral antigens had increased. Of note, the HD preculture step did not alter the frequency of CD8 T-cells in the PBMC preparation (Romer, Berr *et al.* 2011). A further example is given in Table 4.1. Whereas 12.0 % CD3<sup>+</sup>CD8<sup>+</sup> T-cells were detected in fresh PBMCs, 11.6 % CD3<sup>+</sup>CD8<sup>+</sup> T-cells were detected in HD precultured PBMCs of the same individual.

The elevated virus-specific IFN- $\gamma$  response of precultured PBMCs relative to fresh PBMCs was confirmed by intracellular cytokine staining, in which CD8 memory cells (CD8<sup>+</sup>CD45R0<sup>+</sup> cells) were identified as the main cytokine source (Figure 4.1B).

## 4.2 Determination of optimal preculture conditions for increasing the sensitivity of CD8 T-cell responses

As it was important to know whether the preculture conditions established in the original report describing the RESTORE protocol for TGN1412-directed CD4 T-cell responses, i.e. 2 days at  $1 \times 10^7$  cells/ ml (Romer, Berr *et al.* 2011) are also optimal for monitoring of virus-specific blood-derived CD8 T-cell responses using IFN- $\gamma$  ELISPOT assays, preculture conditions were varied with regard to time (from 1 - 3 days) and cell density (from  $1.1 - 30 \times 10^6$  cells/ ml, titration 1:3). High sample integrity was the basis for all experiments of this study. As described in chapter 3.1, heparinized venous blood was stored at RT, processed within a time frame of eight hours, followed by immediate cryopreservation or cell culture. All steps are fixed in a standard operation procedure (SOP) developed in the research group of Prof. Dr. Thomas Hünig, Institute for Virology and Immunobiology, University of Würzburg.

The effect of PBMC preculture on virus-directed CD8 T-cell responses turned out to be highly dependent on time and density during preculture (Figure 4.2). Unstimulated cells from all preculture conditions tested did not release IFN- $\gamma$ . Preculture at a cell density ( $\geq 3.3 \times 10^6$  cells/ ml) improved the T-cell performance in comparison to fresh PBMCs or PBMCs that were precultured at  $1.1 \times 10^6$  cells/ ml. However, preculture was not only dependent on the cell density, but also on the time span of preculture. Whereas the highest IFN- $\gamma$  responses were detected in PBMC precultures for 2 days, precultures for 1 day or 3 days, respectively at the same cell density were less efficient. Hence, shorter preculture steps of only 1 day that would be desirable with regard to time management were less effective in comparison to 2 day preculture steps, even if an extremely high cell density ( $3 \times 10^7$  cells/ ml) was chosen. Preculture steps for 3 days at a high cell density ( $\geq 1 \times 10^7$  cells/ ml) were less efficient

in comparison to 2 day precultures at a similar high cell density. One possible explanation might be a lack of nutrients and oxygen, especially during the third day of preculture indicated by a strong pH shift of the indicator phenol red to yellow.

Hence, the preculture conditions established in the RESTORE protocol, i.e. 2 days at  $1 \times 10^7$  cells/ml (Romer, Berr *et al.* 2011) were confirmed as optimal for the detection of antigenic CD8 T-cell responses and were used in all further experiments, if not otherwise stated.

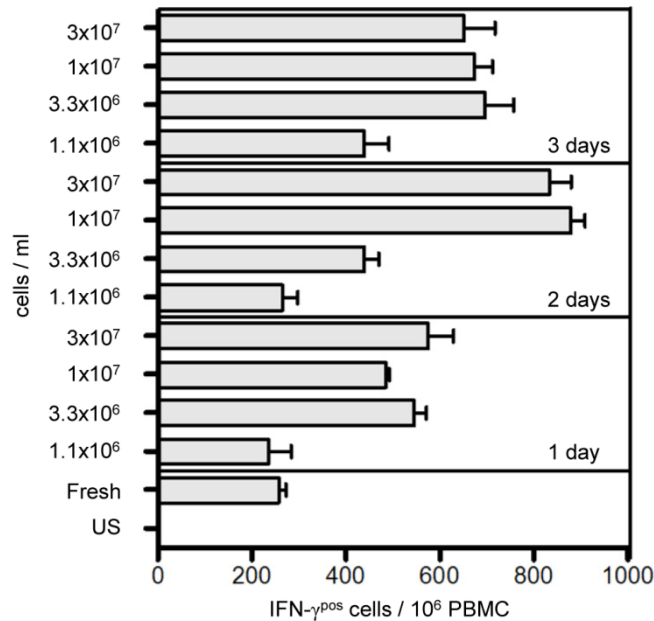


**Figure 4.2: Time and density-dependence of the PBMC preculture effect on virus-directed CD8 T-cell responses.** CD8 T-cell responses of a healthy donor to  $0.1 \mu\text{g/ml}$  of the PepMix<sup>TM</sup> CEF standard were obtained by IFN- $\gamma$  ELISPOT assay. PBMC preculture conditions were tested by varying time and cell densities. Unstimulated cells from all preculture conditions tested did not release IFN- $\gamma$ . Data represent mean  $\pm$  SD for triplicate samples. Experiment was repeated  $\geq 3$  times.

## 4.3 Mechanistic studies on restored virus-specific CD8 T-cell responses

### 4.3.1 Functional maturation of human CD8 T-cells and monocytes contribute to the HD preculture effect

Next, it was tested whether the enhanced IFN- $\gamma$  response of blood-derived CD8 memory T-cells to the PepMix<sup>TM</sup> CEF standard requires interaction with matured monocytes that develop during the preculture step (Romer, Berr *et al.* 2011). CD8 T-cells and monocytes were purified from fresh or precultured PBMCs and were stimulated for 16 hours in ELISPOT plates in the presence or absence of CD14<sup>+</sup> monocytes isolated from fresh or HD precultured PBMCs of the same individual (Figure 4.3). In agreement with the results reported above, CD8 T-cells present in unseparated precultured PBMCs showed a dramatic increase in the IFN- $\gamma$  response upon stimulation with  $0.1 \mu\text{g/ml}$  of the virus-specific PepMix<sup>TM</sup> CEF standard as compared to fresh PBMCs. Similarly high responses to the PepMix<sup>TM</sup> CEF standard were observed in 1:1 co-cultures of CD8 T-cells and monocytes if both had



been purified from precultured PBMCs, indicating that the maturation of the monocytes during HD preculture of PBMCs is required for the strong cytokine response observed after antigen contact. In addition, however, HD preculture also pre-sensitizes the CD8 T-cells themselves for the subsequent virus-specific response. Thus, purified CD8 T-cells isolated from fresh PBMCs that were co-cultured with monocytes prepared from precultured PBMCs showed a response which was as low as that of fresh PBMCs. In the absence of monocytes, only CD8 T-cells purified from precultured PBMCs, but not from fresh PBMCs showed a small but significant response which is probably due to presentation of the virus-derived peptides by the T-cells themselves. Of note, and in agreement with Römer *et al.* (Römer, Berr *et al.* 2011) the OKT3 response did not discriminate between fresh and HD precultured PBMCs. This is explained by the high-affinity interaction of the monoclonal Ab with the TCR complex (Adair, Athwal *et al.* 1994), which obviates the need for priming of the TCR signaling machinery by scanning of HLA/self-peptide complexes.

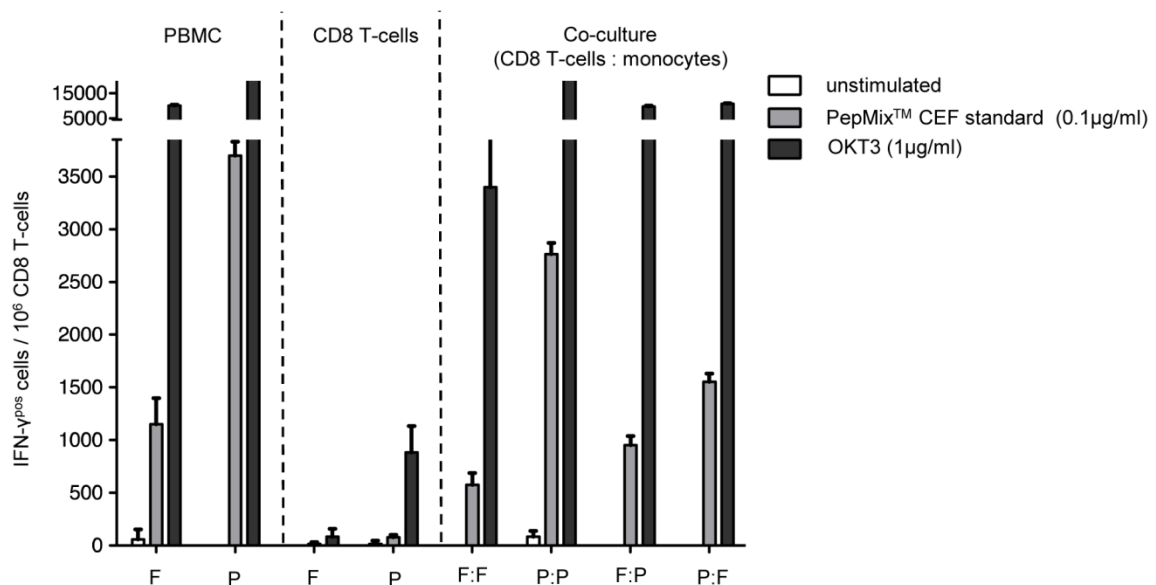


**Figure 4.3: Functional maturation of CD8 T-cells and monocytes contributes to the HD preculture effect.** CD8 T-cells and monocytes were purified from fresh (F) and precultured (P) PBMCs of the same donor by magnetic sorting (MACS) and co-cultured under standard conditions at a 1:1 ratio in the presence of either 0.1 μg/ml PepMix™ CEF standard or 1 μg/ml OKT3, and were assessed by IFN-γ ELISPOT 16 hours after stimulation. Data represent mean ± SD for triplicate samples for one representative donor out of three.

As the results presented in Figure 4.3 indicate functional maturation of not only monocytes (Römer, Berr *et al.* 2011), but also CD8 memory cells that additionally contribute to improved virus-specific responses, the expression or down regulation of surface molecules and transcription factors allowing CD8 T-cells to perform their function was tested by flow cytometry. Phenotypic analysis of CD8 T-cells revealed that expression of molecules associated with co-stimulation (CD28) or co-inhibition (cytotoxic T-lymphocyte-associated protein 4: CTLA-4), apoptosis (Annexin V binding, 7-AAD incorporation) or exhaustion (programmed cell death 1: PD-1) remained unaffected by HD preculture of PBMCs, whereas GITR surface expression, a glucocorticoid-induced tumor necrosis factor receptor (Ronchetti, Zollo *et al.* 2004, Ronchetti, Nocentini *et al.* 2012) increased and CD3 was slightly down regulated, possibly as a consequence of MHC scanning (Table 4.1). With regard to CD14<sup>+</sup> monocytes,

maturation was confirmed by an enhanced expression level ( $\Delta$ MFI: mean fluorescence intensity) of HLA class I (HLA-A, -B, -C) and class II molecules (HLA-DR, -DP, -DQ) and the co-stimulatory ligand CD86 upon HD preculture of PBMCs, facilitating cellular interactions between monocytes and T-cells. CD80 expression on monocytes of HD precultured PBMCs relative to fresh PBMCs was not increased (Table 4.1).

**Table 4.1: Phenotyping of CD8 T-cells and monocytes from fresh or HD precultured PBMCs.** Expression of the memory (CD45R0), co-stimulation or co-inhibition (CD28, GITR and CTLA-4), exhaustion (PD-1) or cell death (7-AAD, Annexin V) markers on CD8 T-cells as well as the co-stimulation (CD80, CD86) and HLA markers on CD14 positive monocytes are given as frequencies (%) and  $\Delta$ MFI: MFI (specific marker) – MFI (unstained control).

within	marker	%		$\Delta$ MFI	
		Fresh	Precultured	Fresh	Precultured
lymphocytes	CD3 CD8	12.0	11.6	117.8	88.8
CD8 T-cells	CD45R0	38.5	38.0	2.9	4.0
	CD28	74.9	80.5	85.6	91.8
	GITR	56.0	73.4	9.9	17.9
	PD-1	49.5	48.8	27.0	26.0
	CTLA-4	*	*	4.8	6.7
	7-AAD	0.8	0.6	2.0	1.8
	Annexin V	0.3	0.7	6.0	6.8
monocytes	CD80	4.3	3.0	5.4	7.4
	CD86	99.1	98.5	261.4	500.2
	HLA-A,-B,-C	99.6	97.9	465.4	1067.4
	HLA-DR, -DP, -DQ	99.4	98.5	546.4	926.2

\* no distinct population

### 4.3.2 RESTORE effect is not due to a reduction in Treg activity

To address the mechanistic question whether HD preculture of PBMC induces a gain in reactivity, rather than a loss of suppression, *e.g.* due to an underrepresentation of Treg cells after the preculture step, the following experiment was performed. Frequencies of CD25<sup>+</sup>Foxp3<sup>+</sup> cells were compared for one representative healthy individual by intracellular staining followed by flow cytometry and turned out to be comparable (1.7 % in CD4 T-cells from fresh PBMCs, 1.8 % in CD4 T-cells from

precultured PBMCs, Figure 4.4A, left column). Treg cells were depleted from fresh or precultured PBMCs by magnetically labeling CD25 positive cells (Figure 4.4A, right column). In agreement with the result reported above, HD precultured PBMCs showed a significantly higher reactivity to 0.033-0.3  $\mu\text{g/ml}$  of the PepMix™ CEF standard as compared to fresh PBMCs (IFN- $\gamma$  ELISPOT assay, Figure 4.4B). The reactivity of fresh PBMCs was unchanged if Treg cells were removed prior to the assay and it was equally high between CD25 depleted and non-depleted precultured PBMCs. Hence, the increased response of HD precultured PBMCs is due to a gain in virus-specific T-cell reactivity rather than a reduction in Treg-mediated suppression.

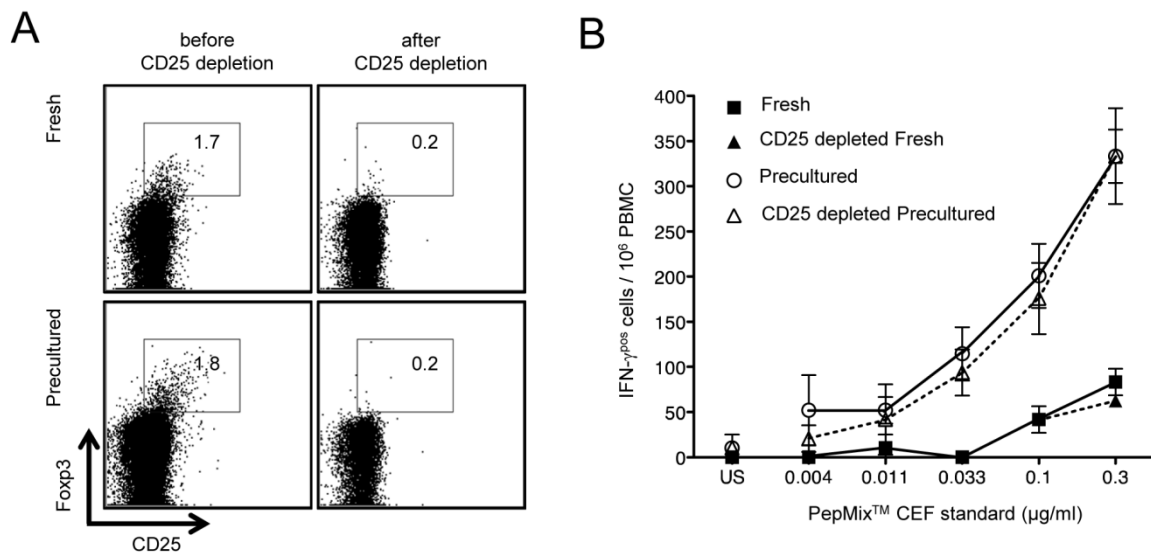


**Figure 4.4: RESTORE effect is not due to a reduction in Treg activity.** (A, Left) Similar frequencies of regulatory T-cells in unstimulated fresh and precultured PBMCs of a representative healthy donor. Intracellular staining and flow cytometry of regulatory T-cells; Gating of Foxp3<sup>+</sup>CD25<sup>+</sup> cells was performed on viable CD4<sup>+</sup> T-cells. (Right) Regulatory T-cells were depleted from fresh or precultured PBMCs by magnetically labeling CD25 positive cells. (B) Similar increase in virus-specific CD8 T-cell responses upon HD preculture of total and CD25-depleted PBMCs. Cells from Panel A were stimulated with titrated PepMix™ CEF standard in IFN- $\gamma$  ELISPOT assays. Responses of fresh/ CD25 depleted fresh PBMCs and precultured/ CD25 depleted precultured PBMCs, respectively were compared by an unpaired *t* test: n.s.; Significantly enhanced IFN- $\gamma$  secretion of CD8 T-cells upon HD preculture of total or CD25 depleted PBMCs relative to fresh or CD25 depleted fresh PBMCs were detected after stimulation with 0.033  $\mu\text{g/ml}$  (unpaired *t* test: \*\* *P* < .005), 0.1  $\mu\text{g/ml}$  (\* *P* < .05) and 0.3  $\mu\text{g/ml}$  (\*\* *P* < .005) of the PepMix™ CEF standard. Data represent mean  $\pm$  SD for triplicate samples. Experiment was repeated 3 times.

### 4.3.3 HD preculture prepares T-cells to better respond to antigen, but does not increase the frequency of antigen-specific cells

In order to test if the improved T-cell reactivity upon HD preculture of PBMCs results from an increase in frequency of detectable antigen specific CD8 T-cells during the preculture step, HLA pentamer staining was performed. Unstimulated fresh, high density (HD:  $1 \times 10^7/\text{ml}$ ) or low density (LD:  $1 \times 10^6/\text{ml}$ ) precultured PBMCs of one representative HLA-A0201 positive healthy donor were stained for PP65\_HCMV 495-503-specific CD8 T-cells (Figure 4.5). The frequency of CD8 T-cells expressing the relevant antigen/MHC specificity remained unchanged independent of the preculture step. Pentamer HLA-A0201 was used as a negative control and revealed only a low level of unspecific staining.

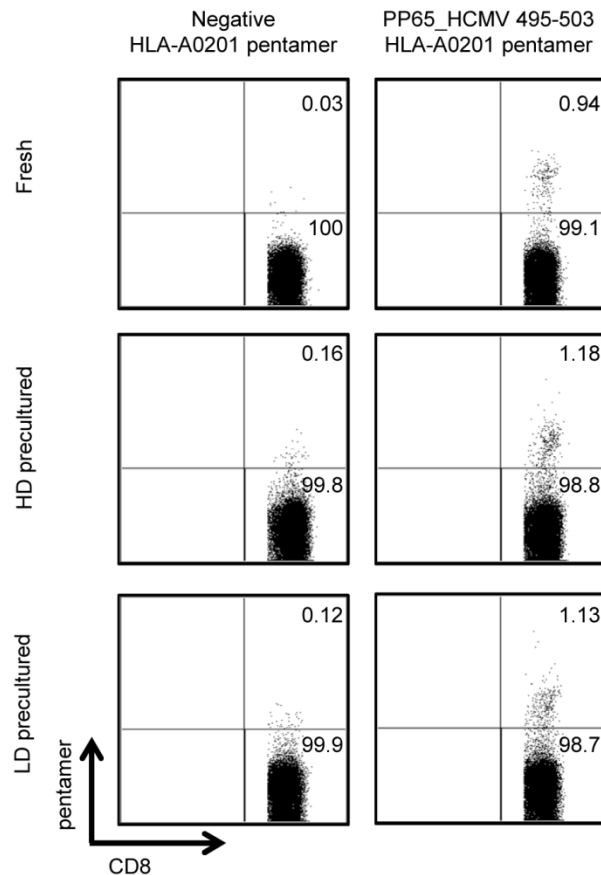


*Figure 4.5: HD preculture prepares T-cells to better respond to antigen, but does not increase the frequency of antigen-specific cells. Similar frequencies of PP65\_HCMV 495-503-specific T-cells were detected in unstimulated Fresh, HD and LD precultured PBMCs by flow cytometry upon pentamer staining. An HLA-A0201-restricted pentamer was used as a negative control. Gating was performed on viable CD8 T-cells. Experiment was repeated with 2 HLA-A0201 positive healthy donors.*

Taken together, mechanistic studies on “restored” CD8 T-cells have shown that both, monocytes and T-cells gain in reactivity upon HD preculture of PBMCs (Figure 4.3, Table 4.1), whereas restored T-cell performance was independent of Treg-mediated suppression (Figure 4.4) and changes in antigen-specific CD8 T-cell frequency (Figure 4.5).

#### 4.4 HD preculture of PBMCs boosts antigen sensitivity of virus-specific CD8 T-cells

The effect of PBMC preculture at HD on the sensitivity of the CD8 T-cell response was then quantified by titrating PepMix™ Influenza A (Figure 4.6A) and PP65\_HCMV 495-503 (Figure 4.6B). IFN- $\gamma$  responses were tested with freshly prepared PBMCs of healthy individuals, and again after 2 days of HD preculture. PBMCs were isolated from HLA-A0201 CMV-seropositive donors that were used for stimulation with the peptide PP65\_HCMV 495-503. Application of the RESTORE protocol strongly increased the responsiveness of CD8 T-cells to titrated amounts of the influenza and HCMV derived peptides relative to fresh PBMCs as presented for one representative donor in Figure 4.6A and B. The displacement of the titration curves of precultured as compared to fresh PBMCs indicates a 5-

10 fold gain in sensitivity to matrix and nucleocapsid peptides of the Influenza A virus compared to fresh PBMCs (Figure 4.6A). Similarly high increases in the sensitivity of CD8 T-cells from precultured PBMCs were observed upon stimulation with titrated amounts of PP65\_HCMV 495-503 (Figure 4.6B). Here, HD preculture allowed the detection of a CD8 T-cell response to as little as 0.001  $\mu\text{g}/\text{ml}$  of that peptide, whereas fresh cells failed to respond with IFN- $\gamma$  secretion at that antigen concentration. Data compiled from six donors showed a significantly increased IFN- $\gamma$  recall response to the PepMix™ Influenza A when HD precultured PBMCs were compared to fresh PBMCs (Figure 4.6B). The average fold-increase in the response of CD8 T-cells from precultured relative to fresh PBMCs is presented as the median with interquartile range after stimulation with titrated PepMix™ Influenza A. Three out of nine tested donors did not show IFN- $\gamma$  responses to PepMix™ Influenza A, neither in fresh nor in HD precultured PBMCs and were not included in the summary Figure 4.6B. Unresponsiveness of the three excluded donors can be explained by the assumption that those individuals have never been in contact with Influenza A-specific peptides, either by previous virus infections nor by vaccination prior to this *in-vitro* test. Responses to titrated PP65\_HCMV 495-503 of five donors were compiled in Figure 4.6D and presented as in Figure 4.6B. Fold-increases could not be calculated for the concentrations 0.0001 and 0.001  $\mu\text{g}/\text{ml}$  where no response was detectable in fresh PBMCs. Average fold-increases in the HCMV-specific CD8 T-cell response from HD precultured PBMCs relative to fresh PBMCs were highly significant ( $P < .005$ ) if cells were stimulated with 0.01-1  $\mu\text{g}/\text{ml}$  of peptide PP65\_HCMV 495-503.

Since adenovirus-specific CD8 memory T-cells are usually rare in peripheral blood, monitoring of patients at high risk for infection, *e.g.* after allogeneic HSCT is difficult without prior *in-vitro* expansion, which, however, exaggerates their *in-vivo* representation (Geyeregger, Freimuller *et al.* 2013). It was therefore investigated whether HD preculture of PBMCs also enhances the responsiveness of human adenovirus-specific CD8 T-cells to more readily detectable levels. Indeed, CD8 T-cells from seven tested healthy individuals showed strongly enhanced IFN- $\gamma$  responses to the epitopes HEX 901-910 presented on HLA-A01, E1A 19-45 presented on HLA-A02 or HEX 37-45 presented on HLA-A24 molecules from the clinically important strain ADE02 (Figure 4.6E, F).

In order to obtain a larger data set allowing a statistical assessment of the effects of HD preculture on the detection of anti-viral responses within a test population, fresh or precultured PBMCs from 22 healthy individuals were stimulated with titrated amounts of the virus-specific PepMix™ CEF standard. An example of these responses is shown in Figure 4.7A, where CD8 T-cells in precultured PBMCs stimulated with 0.033  $\mu\text{g}/\text{ml}$  of the PepMix™ CEF standard showed an IFN- $\gamma$  recall response comparable to that of CD8 T-cells in fresh PBMCs stimulated with 0.3  $\mu\text{g}/\text{ml}$  of the same peptide pool, indicating a 10-fold gain in sensitivity through the HD preculture step. To evaluate whether this procedure renders CD8 T-cells responsive to self-peptides that they are usually tolerant of, fresh and precultured PBMCs of the same individual as in Figure 4.7A were stimulated with titrated amounts of the PepMix™ pool Human Actin (Figure 4.7B).

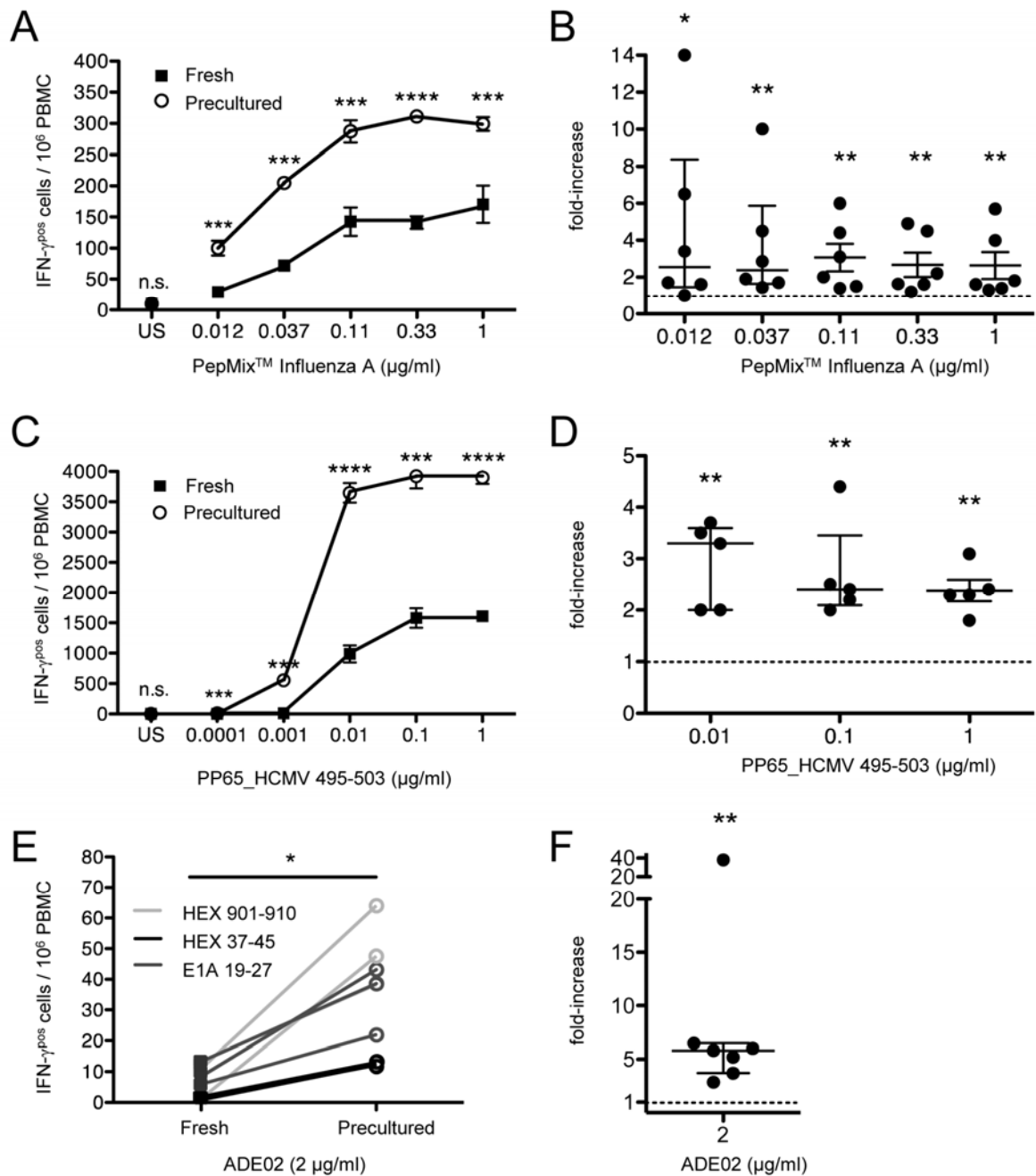


**Figure 4.6: Enhanced sensitivity of human CD8 T-cells to defined viral antigens by HD preculture of PBMCs.** (A) IFN- $\gamma$  responses of CD8 T-cells from fresh or precultured PBMCs from a representative healthy donor were directly compared by ELISPOT assay after stimulation with titrated PepMix<sup>TM</sup> Influenza A. Unpaired *t* test: \*\*\*  $P < .0005$ ; \*\*\*\*  $P < .0001$ ; (B) Compiled data from 6 healthy donors tested as in Figure 2A. Data represent the mean fold-increase in IFN- $\gamma$  responses of CD8 T-cells from precultured PBMCs relative to CD8 T-cells from fresh PBMCs after stimulation with the PepMix<sup>TM</sup> Influenza A. Mann-Whitney test: \*  $P < .05$ ; \*\*  $P < .01$ . Data represent median with interquartile range. (C) IFN- $\gamma$  responses of CD8 T-cells from fresh or precultured PBMCs from a CMV-seropositive healthy donor after stimulation with titrated PP65\_HCMV 495-503. (D) Compiled data from 5 donors tested as in Figure 2C. Data presentation as in Figure 2B. Fold increase could not be calculated for the concentrations 0.0001 and 0.001  $\mu$ g/ml where no response was detectable in fresh PBMCs. (E) CD8 T-cell responses in fresh and precultured PBMCs to 2  $\mu$ g/ml of three different adenovirus-derived peptides. (F) Compiled data from 7 HLA-A01 (HEX\_ADE02 901-910), -A02 (E1A\_ADE02 19-27) or -A24 (HEX\_ADE02 37-45) positive healthy individuals. Data presentation as in Figure 2B.

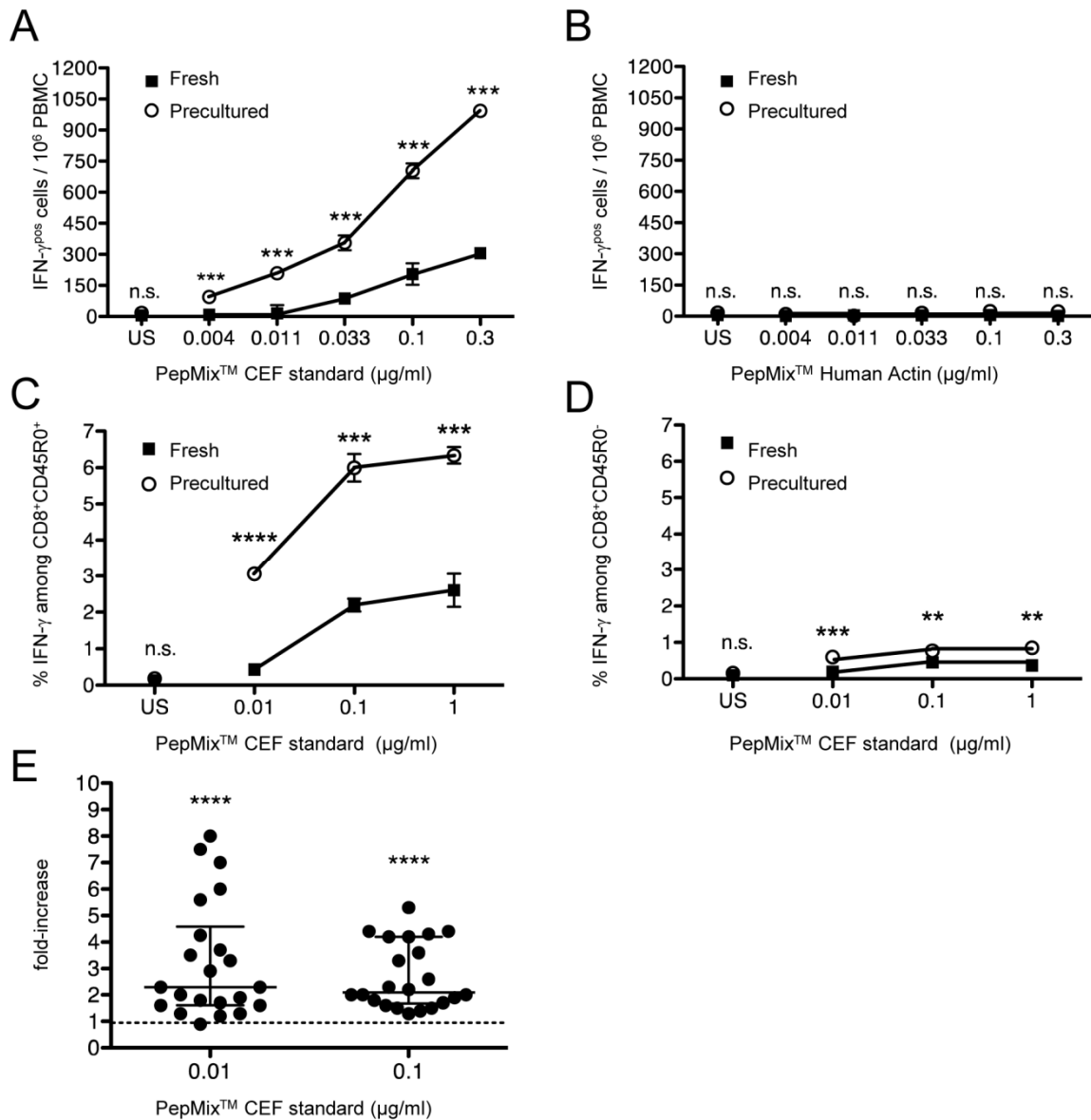


**Figure 4.7: Enhanced recall responses of HD precultured CD8 T-cells to virus-derived peptide pools.** (A) IFN- $\gamma$  ELISPOT responses of fresh or precultured PBMCs of one representative healthy donor to titrated amounts of the HLA-class I restricted PepMix™ CEF standard. (B) Response of the same donor as shown in Figure 3A to titrated amounts of the negative control pool PepMix™ Human Actin. Unpaired *t* test: \*  $P < .05$ ; \*\*  $P < .005$ ; \*\*\*  $P < .0005$ . Data represent mean  $\pm$  SD for triplicate samples. (C, D) Identification of memory CD8 T-cells as source of for IFN- $\gamma$  production by intracellular cytokine staining of fresh and precultured PBMCs of one representative donor that is different from Figure 3A, B. Results are shown as percentage of IFN- $\gamma$ -positive cells among CD8<sup>+</sup>CD45R0<sup>+</sup> cells and CD8<sup>+</sup>CD45R0<sup>-</sup> cells. (E) Compiled data from 22 healthy donors tested as in Figure 2A and presented as in Figure 2B.

The unresponsiveness of both fresh and precultured PBMCs to even high concentrations of 9-mer peptides of the actin protein demonstrates that HD preculture of PBMCs does not create responses to tolerated self-antigens.

Next, intracellular IFN- $\gamma$  staining was performed to test whether the boost in antigen sensitivity observed over the whole titration range is a feature of the CD8 memory compartment (Figure 4.7C, D). Indeed, CD8 memory cells (CD8<sup>+</sup>CD45R0<sup>+</sup>) were not only identified as the T-cell subset being responsible for the enhanced reactivity to 0.1  $\mu$ g/ml of the PepMix™ CEF standard (Figure 4.1B), but

also as being responsible for the increased sensitivity of the response (Figure 4.7C). CD8 naive T-cells (CD8<sup>+</sup>CD45R0<sup>-</sup>) did not contribute to the enhanced T-cell sensitivity to PepMix™ CEF if PBMC were HD precultured prior to the stimulation assay (Figure 4.7D).

Data were then compiled from 22 individuals and showed an increased IFN- $\gamma$  recall response to the PepMix™ CEF standard when CD8 T-cells received cell-cell contacts during HD preculture of PBMCs prior to stimulation with the viral peptide mix (Figure 4.7E). The average fold-increase in the response of CD8 T-cells from precultured PBMCs relative to fresh PBMCs is presented as in Figure 4.6B. The median with interquartile range (IQR) was found highly significant ( $P < .0001$ ) after stimulation with 0.01  $\mu\text{g}/\text{ml}$  (2.3, IQR = 3.0) or 0.1  $\mu\text{g}/\text{ml}$  (2.1, IQR = 2.5) of the PepMix™ CEF standard. While for some responders, little or no increase (but never a decrease) was seen after HD preculture, 5/22 individuals revealed 4-fold or higher increments at both peptide concentrations tested. As pointed out above, such increases in detectable IFN- $\gamma$  responses at individual antigen concentrations translate into even higher increases in antigen sensitivity, *e.g.* the HD precultured cells shown in Figure 4.7A have an at least 10-fold higher sensitivity than the non-precultured ones as evidenced by the requirement for more than 10-fold higher peptide concentrations of the latter to reach comparable responses.

## 4.5 Comparison of T-cell responses in blood and tissue

Continuous cellular interactions in murine (Stefanova, Dorfman *et al.* 2002) and human (Romer, Berr *et al.* 2011) lymphoid tissue are essential for high sensitivity of CD4 T-cells to peptide antigens. In the following chapter 4.5, CD4 and CD8 T-cell functionality measured by IFN- $\gamma$  secretion was compared between blood and tissue. Tissue samples were obtained from lamina propria of the small intestine of obese patients undergoing gastric bypass operation at the University Hospital Würzburg. Lamina propria mononuclear cells (LPMCs) were isolated in parallel to PBMCs of the same individual, followed by phenotyping of T-cell subpopulations and *ex-vivo* stimulation assays.

### 4.5.1 Phenotyping of CD4 and CD8 T-cells from LPMCs and HD precultured PBMCs

As already mentioned in the introduction (chapter 1.1.3), T-cell subsets exhibit distinct phenotypic properties depending on their location in the human body, but stay remarkably constant between individuals (Sathaliyawala, Kubota *et al.* 2013). Unstimulated T-cells from blood and lamina propria were now characterized by the expression of the common leukocyte antigen isoform CD45R0 and the homing receptor L-selectin (Figure 4.8). Results from HD precultured PBMCs and LPMCs originate from the same type 2 diabetes negative obese patient (Figure 4.8, upper and middle line). Of note, distribution of cell subsets in the blood is independent of HD preculture ((Romer, Berr *et al.* 2011) and data not shown). Hence, results are shown exclusively for HD precultured PBMCs, but not for fresh PBMCs. Gating was performed on viable mononuclear cells (MCs, Figure 4.8, left column), CD4 T-



cells (Figure 4.8, middle column) and CD8 T-cells (Figure 4.8, right column). In blood and LPMCs, CD4 T-cell frequencies were higher compared to those of CD8 T-cells. As expected, unequal proportions of CD4 memory T-cells (CD45R0<sup>+</sup> cells) were found in blood (39.1 %) and lamina propria (94.3 %) (Schroder-Braunstein, Pavlov *et al.* 2012). In contrast, naive T-cells (CD62L<sup>+</sup> cells) were almost absent in LPMCs (Figure 4.8, middle line), confirming that memory CD4<sup>+</sup> T cells represent the major subset in mucosal tissues (Sathaliyawala, Kubota *et al.* 2013).

In contrast to CD4 T-cell subsets, CD8 T-cell subsets are maintained as effector or central memory CD8<sup>+</sup> T-cells mainly in mucosal sites *e.g.* lamina propria (99.5 % within CD8 T-cells) (Sathaliyawala, Kubota *et al.* 2013).

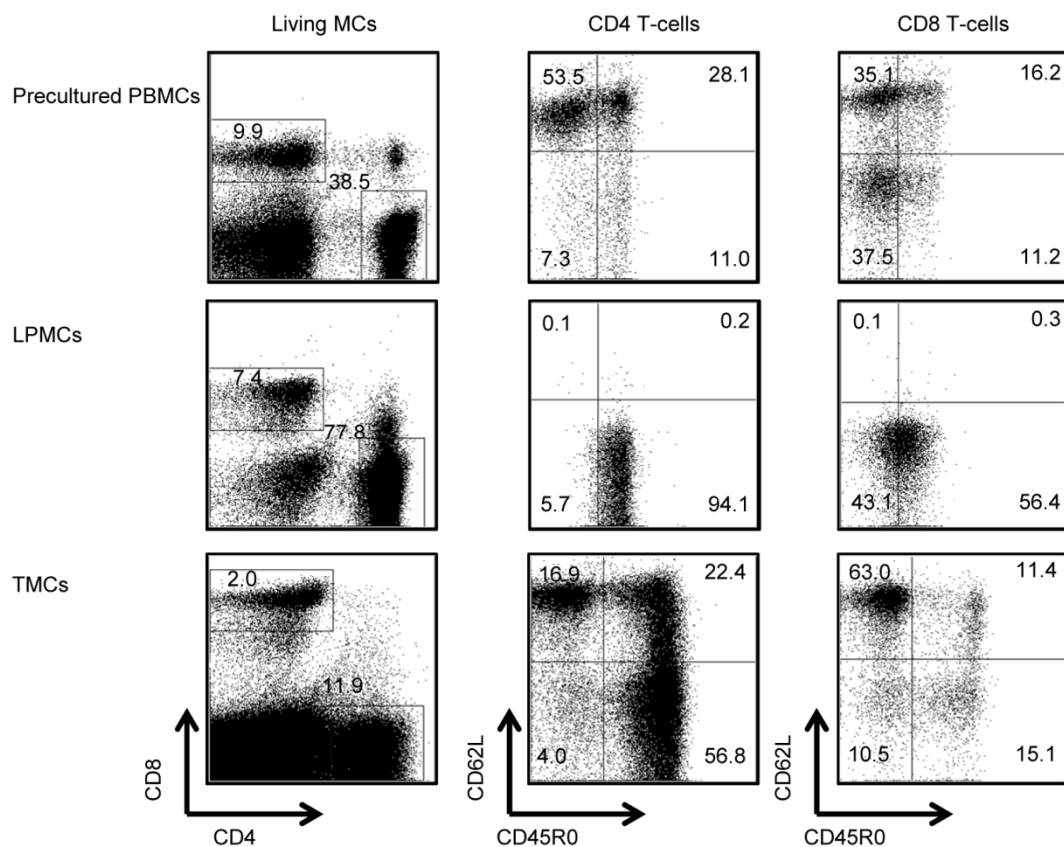


**Figure 4.8: Phenotyping of HD precultured PBMCs, LPMCs and TMCs.** Unstimulated mononuclear cells (MCs) from the blood (PBMCs), lamina propria of the small intestine (LPMCs) or tonsils (TMCs) were stained with the given antibodies to determine their frequency of naive (CD62L<sup>+</sup> CD45R0<sup>-</sup>), effector (CD62L<sup>-</sup> CD45R0<sup>-</sup>), central memory (CD62L<sup>+</sup> CD45R0<sup>+</sup>) and effector memory (CD62L<sup>-</sup> CD45R0<sup>+</sup>) CD4 or CD8 T-cells within living MCs. Results from HD precultured PBMCs and LPMCs originate from the same representative obese patient without type 2 diabetes. Results from TMCs are of another representative tonsil and blood donor. Experiment was repeated  $\geq 8$  individuals.

#### 4.5.2 Loss of T-cell sensitivity to TAB08 in dispersed LPMC cultures

Experiments from Römer *et al.* have shown that CD4 T-cells from LNs and HD precultures of PBMCs respond to TGN1412 (Römer, Berr *et al.* 2011). I now compared the results of human LN-derived CD4 T-cells with those of lamina propria-derived CD4 T-cells and additionally tested LPMCs for virus-specific T-cell responses.

Cytokine release was compared by IFN- $\gamma$  ELISPOT assay between blood and mucosal cells upon stimulation with 1  $\mu\text{g/ml}$  TAB08 or 1  $\mu\text{g/ml}$  OKT3, respectively. Unstimulated MCs derived from blood or lamina propria were used as negative controls and revealed no unspecific responses (Figure 4.9A). As expected, *ex-vivo* CD4 T-cell responses to the CD28 superagonist TAB08 were detected in human lamina propria and in blood-derived T-cells that were first reset to tissue-like conditions by HD preculture of PBMCs, but TAB08-reactivity was absent in fresh PBMCs. According to Figure 4.3, T-cell responses induced by high-affinity OKT3 binding to the TCR complex are independent of HD preculture of PBMCs. IFN- $\gamma$  responses were next compared to titrated TAB08 (dilution 1:10) between LPMCs with those of fresh or precultured PBMCs of the same individual presented in Figure 4.9A, and correlated to the frequencies of CD4 T-cells in MCs from blood and mucosal tissue as determined by flow cytometry (Figure 4.9B). HD preculture of PBMCs dramatically enhanced the reactivity of CD4 T-cells to 0.1 or 1  $\mu\text{g/ml}$  TAB08 to a level that was even higher than for lamina propria T-cells.

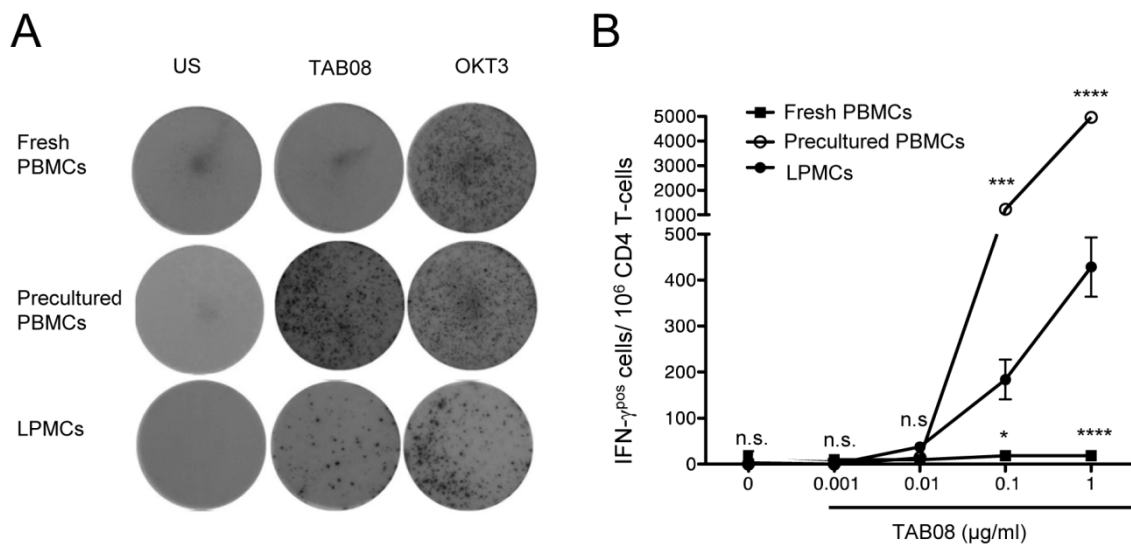


**Figure 4.9: IFN- $\gamma$  release in HD precultured PBMCs and LPMCs in response to TAB08.** (A) Representative IFN- $\gamma$  ELISPOT assay of fresh or precultured PBMCs as well as LPMCs of one patient with morbid obesity. Cytokine release after stimulation with 1  $\mu\text{g/ml}$  TAB08 (previously: TGN1412) or 1  $\mu\text{g/ml}$  OKT3 was assessed after 16 hours. Unstimulated MCs were used as negative controls. (B) IFN- $\gamma$  responses to titrated TAB08 were detected by IFN- $\gamma$  ELISPOT assays, and correlated to the frequencies of CD4 T-cells in MCs from blood or lamina propria as determined by flow cytometry. Statistical comparison of CD4 T-cell responses from LPMCs with those of fresh or HD precultured PBMCs. Unpaired *t* test: \*\*\*\*  $P \leq 0.0001$ , \*\*\*  $P \leq 0.0005$ , \*  $P \leq 0.05$ . Data represent mean  $\pm$  SD for triplicate samples of one representative patient out of five.

In order to investigate the loss of high functionality through loss of cellular interactions when entering the circulation, LPMCs were either kept dispersed in suspension ( $1 \times 10^6$  cells/ml) for 2 hours at 37  $^{\circ}\text{C}$  and 5 %  $\text{CO}_2$  to simulate tissue exit or were kept on ice (4  $^{\circ}\text{C}$ ) for the same time to maintain high T-cell sensitivity (Figure 4.10). IFN- $\gamma$  releases were tested by IFN- $\gamma$  secretion assay for CD4 (Figure 4.10A) and CD8 (Figure 4.10B) T-cells of the small intestine to titrated TAB08 (titration 1:5) and 0.25  $\mu\text{g/ml}$  of the bacterial superantigen *Staphylococcus aureus* enterotoxin B (SEB) that stimulates all T-cells expressing TCRs belonging to the V $\beta$ 3 family (Niedergang, Hemar *et al.* 1995). Unstimulated cells were used as a negative control. After stimulation for 16 hours, the IFN- $\gamma$  secretion assay protocol was performed as described in chapter 3.2.2.3. In order to determine the phenotype of IFN- $\gamma$  secreting

cells, LPMCs were additionally stained for CD4 and CD8. Indeed, interruption of cellular contacts at 37 °C resulted in a significant reduction in the frequency of IFN- $\gamma$  secreting T-cells to both tested stimuli. In contrast to results from HD precultured blood cells (Romer, Berr *et al.* 2011), TAB08-directed responses were not exclusively observed in CD4 T-cells (Figure 4.10A), but also to a low extent in mucosal CD8 T-cells (Figure 4.10B).

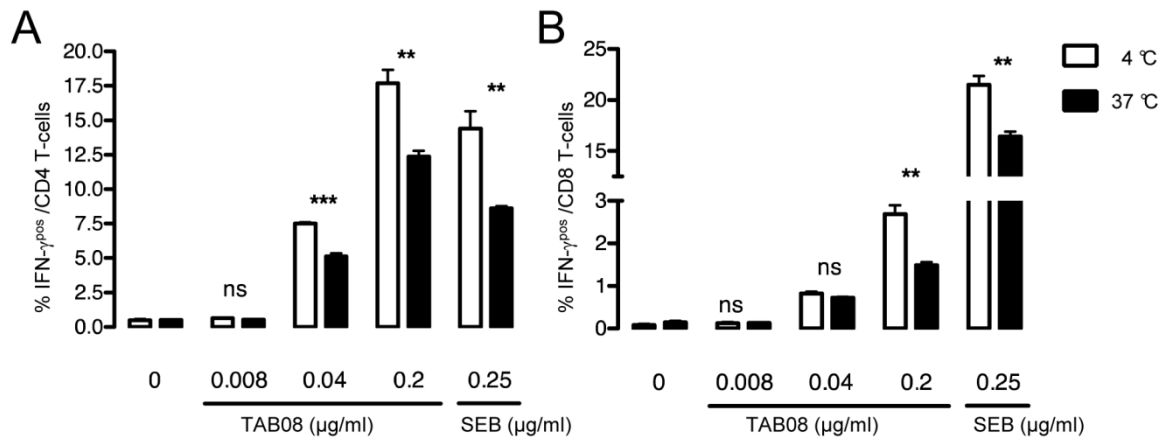


Figure 4.10: **Loss of T-cell reactivity to TAB08 and SEB in LD cultures of LPMCs.** LPMCs were either kept on ice or dispersed in suspension ( $1 \times 10^6$  cells/ ml) for 2 hours at 37 °C (5 % CO<sub>2</sub>) to simulate tissue exit. IFN- $\gamma$  responses of T-cells to titrated amounts of TAB08 (previously: TGN1412) and 0.25  $\mu\text{g/ml}$  SEB were analyzed by an IFN- $\gamma$  secretion assay after stimulation for 16 hours. The IFN- $\gamma$  secretion assay was combined with surface staining for (A) CD4 and (B) CD8 T-cells in order to determine the subtype of IFN- $\gamma$  cells. Unpaired *t* test: \*\*\*  $P < .0005$ , \*\*  $P < .005$ . Data represent mean  $\pm$  SD for triplicate samples of one representative patient with morbid obesity out of two.

The data support once more the concept that tissue-resident CD4 T-cells, particular lamina propria cells or LN cells (Romer, Berr *et al.* 2011) receive tonic T-cell signals that are amplified upon stimulation. Importantly, pre-activation was lost by suspension culture at body temperature, namely interruption of cellular interactions.

Unfortunately, no T-cell responses to viral peptides *e.g.* to the PepMix™ CEF standard or peptide pools of the Varicella-Zoster virus (IE-62, -63, JPT Peptide Technologies) could not be detected in *ex-vivo* studies using LPMCs. Therefore, I used uninfected human tonsils as a source of virus-specific tissue-resident CD8 T-cells. As viruses enter the human body mainly via the respiratory tract, I expected a higher frequency of virus-specific T-cells in tonsil pairs (one of the sites of viral clearance) compared to the lamina propria of the small intestine.

### 4.5.3 Phenotyping of CD4 and CD8 T-cells from TMCs and HD precultured PBMCs

Tonsillar mononuclear cells (TMCs) were isolated from uninfected tonsils of children undergoing tonsillotomy at the University Hospital Würzburg. PBMCs of the same individual were isolated in parallel to TMCs, followed by phenotyping of T-cell subpopulations. Gating was performed on viable TMCs (Figure 4.8, bottom line left), tonsillar CD4 T-cells (Figure 4.8, bottom line middle) and tonsillar CD8 T-cells (Figure 4.8, bottom line right).

Similar to the situation in blood and LPMCs, CD4 T-cell frequencies in TMCs (11.9 % within viable TMCs) were higher compared to CD8 T-cell frequencies (2 % within viable TMCs, Figure 4.8, left column). CD4 T-cell subsets in TMCs were phenotypically much more comparable to those of PBMCs, relative to those of LPMCs (Figure 4.8, middle column). Beside effector memory CD4 T-cells (56.8 %, CD62L-CD45R0<sup>+</sup>), naive (16.9 %, CD62L<sup>+</sup>CD45R0<sup>-</sup>), effector (4 %, CD62L-CD45R0<sup>-</sup>) and central memory CD4 T-cells (22.4 %, CD62L<sup>+</sup>CD45R0<sup>+</sup>) were detected.

In contrast to CD4 T-cell subsets, CD8 T-cell subsets are mainly maintained as naive cells in lymphoid compartments *e.g.* tonsils (63 % within CD8 T-cells) (Sathaliyawala, Kubota *et al.* 2013). Hence, antigen-experienced CD8 memory T-cells (26.5 % within CD8 T-cells) are rare in TMCs. Upon phenotyping of T-cell subpopulations in TMCs, *ex-vivo* stimulation assays were performed.

#### 4.5.4 Loss of anti-viral CD8 T-cell sensitivity in dispersed TMC cultures

Initially, virus-specific CD8 memory T-cell responses to titrated PepMix<sup>TM</sup> CEF standard (titration 1:10) were compared by IFN- $\gamma$  ELISPOT assay between TMCs that were kept on ice or in suspension at body temperature. Frequencies of CD8 memory T-cells in TMCs were determined by flow cytometry. Interruption of cellular contacts at 37 °C for 2 hours resulted in a 5- to 10-fold reduction in antigen sensitivity which can be seen by the displacement of the titration curves in Figure 4.11A. Loss in cell viability was not observed (data not shown).

Next, the *ex-vivo* responsiveness of tonsillar CD8 memory T-cells to PepMix<sup>TM</sup> CEF standard was compared to that of CD8 memory T-cells in fresh and HD precultured PBMCs of the same individual (Figure 4.11B). As predicted from their previous cellular interactions in the lymphatic tissue, CD8 memory T-cells contained a much (about 10-fold) higher frequency of IFN- $\gamma$  producers in response to 0.04 or 0.4  $\mu$ g/ml of the viral peptide mix as compared to fresh PBMCs. While homing of virus-specific CD8 memory T-cells to this strategically important site may explain part of this huge difference, disablement by loss of tissue context during circulation seems to play an important role as evidenced by the strong response of HD precultured PBMCs, which did, however, not reach that measured for TMCs of the same individual (Figure 4.11B).

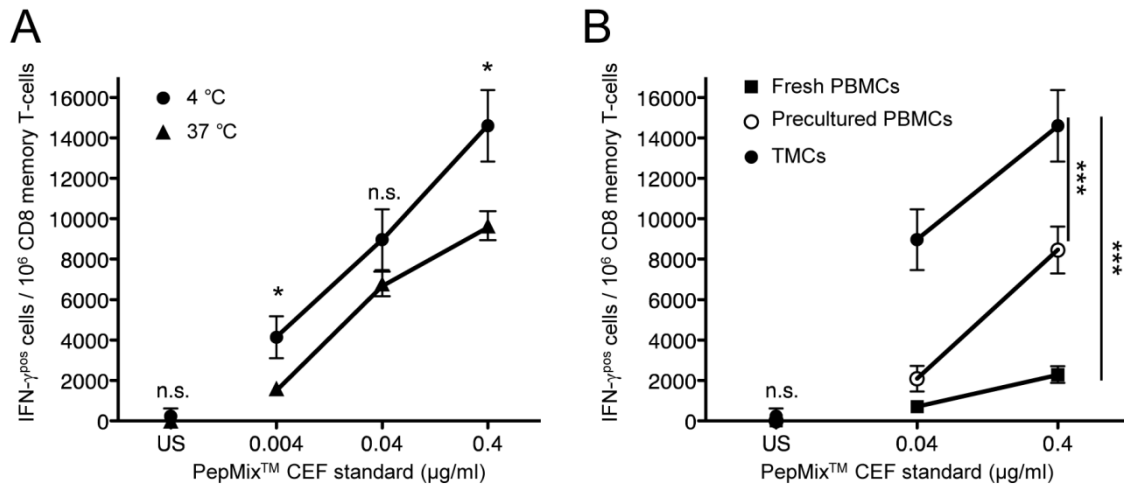


**Figure 4.11: Loss of virus-specific CD8 T-cell reactivity in dispersed TMCs.** (A) Tonsillar mononuclear cells (TMCs) were prepared from uninfected fresh human tonsils and were either kept on ice or dispersed in suspension ( $1 \times 10^6$  cells/ml) for 2 hours at 37 °C (5 % CO<sub>2</sub>) to simulate tissue exit. IFN- $\gamma$  responses to titrated amounts of the HLA-class I restricted PepMix™ CEF standard were analyzed by an IFN- $\gamma$  ELISPOT assay, and the frequency of CD8 memory T-cells in TMC was determined by flow cytometry. Unpaired *t* test: \*  $P < .05$ . (B) Virus-specific IFN- $\gamma$  responses to 0.04 or 0.4  $\mu$ g/ml of the peptide pool were compared between CD8 memory T-cells from TMCs with those of fresh and HD precultured PBMCs of the same individual as presented in Figure 4A. Similar results were obtained after repetition of the experiment. 2way ANOVA \*\*\*  $P < .0005$ . Data represent mean  $\pm$  SD for triplicate samples.

Taken together, CD8 T-cell reactivity in blood to viruses is decreased in comparison to tissue resident T-cells from tonsils, but high antigen sensitivity of circulating CD8 T-cells was restored upon HD preculture of PBMCs allowing cellular interactions that were lost when leaving the tissue context to enter the circulation.

## 4.6 Facilitation of CD8 T-cell responses to the tumor-associated antigen WT1 by HD preculture of PBMCs from leukemia patients after allogeneic HSCT

The enhanced sensitivity of CD8 T-cells from HD precultured PBMCs to multiple virus-specific antigens, relative to CD8 T-cells from fresh PBMCs (Figure 4.6, Figure 4.7), led to the important question whether HD preculture of PBMCs also improves the detection of tumor-directed CD8 T-cells. An improvement in the detection of tumor-directed CD8 T-cell responses would be highly desirable for immunomonitoring of patients with tumors since blood represents the only routinely available source of immune cells. For this study, peptide antigens derived from the extensively studied human protein Wilms tumor 1 (WT1\_HUMAN) were selected. WT1-specific T-cell responses have been elicited in normal donors and implicated in the graft versus leukemia (GVL) effect against acute lymphoblastic leukemia (ALL) or acute myeloid leukemia (AML) after myeloablation and allogeneic HSCT (Oka, Tsuboi *et al.* 2002, Rezvani, Brenchley *et al.* 2005, Rezvani, Yong *et al.* 2007, Tsuboi, Oka *et al.* 2012). Consistent with published results, it was found that the frequency of IFN- $\gamma$  secreting T-cells specific for peptides derived from the tumor-associated antigen WT1\_HUMAN was often low as compared to high-avidity CD8 T-cell responses to HCMV, EBV or influenza A (Figure 4.6) (Villacres,

Lacey *et al.* 2003, McMahan and Slansky 2007). As shown in Figure 4.12A, B, “restored” T-cells from representative HLA-A-0201 positive AML patients displayed dramatically higher IFN- $\gamma$  recall responses to titrated amounts of the peptides WT1\_HUMAN 126-134 and 356-364 than T-cells from fresh PBMCs ( $P < .0005$ ).

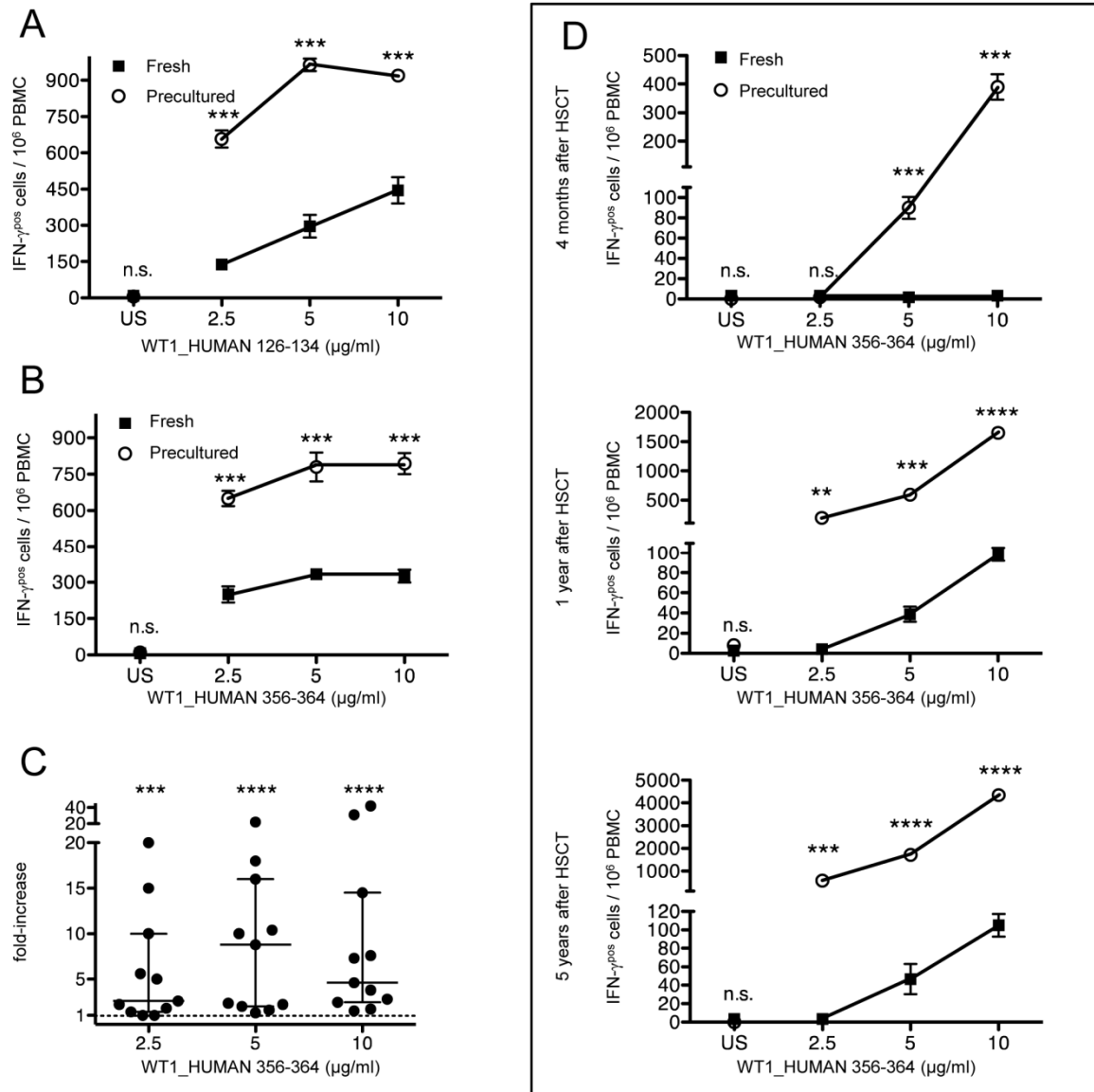


**Figure 4.12: HD preculture enhances the recall responses of PBMCs to WT1-derived antigens.** (A, B) IFN- $\gamma$  T-cell responses from fresh or precultured PBMCs of one representative HLA-A0201 positive HSCT patient to titrated amounts of the peptide WT1\_HUMAN 126-134 or WT1\_HUMAN 356-364, respectively. Unpaired *t* test: \*\*\*  $P < .0005$ . Data represent mean  $\pm$  SD for triplicate samples. The experiment presented in Figure 5A was repeated for two different patients. (C) Compiled data from Figure 4B from 11 patients. Average time between stem cell transplantation and sampling: 814 days; from 166 to 2372 days. Data are presented as in Figure 2B. (D) Improved monitoring of anti-WT1-directed T-cell responses from an HLA-A0201 positive patient 4 months, 1 year and 5 years after HSCT upon HD preculture of PBMCs. Unpaired *t* test: \*\*  $P < .005$ ; \*\*\*  $P < .0005$ ; \*\*\*\*  $P < .0001$ . Data represent mean  $\pm$  SD for triplicate samples.

To demonstrate the specificity of the HLA-A0201-restricted WT1 responses, PBMCs of the human immunodeficiency virus (HIV)-seronegative patients presented in Figure 4.12A, B were also treated with the HLA-A0201-restricted peptide HIV-1 pol 476-484 (Figure 4.13A, B), and showed no

response. Nonspecific effects of WT1 peptides were additionally excluded by the unresponsiveness of PBMCs from an HLA-A0201 negative healthy donor with WT1\_HUMAN 126-134 and 356-364 (Figure 4.13C). Restoration of high T-cell functionality was demonstrated by TAB08 responses exclusively in HD precultured PBMCs, but not in fresh PBMCs of all tested patients (Figure 4.13A, B) and healthy donors (Figure 4.13C).

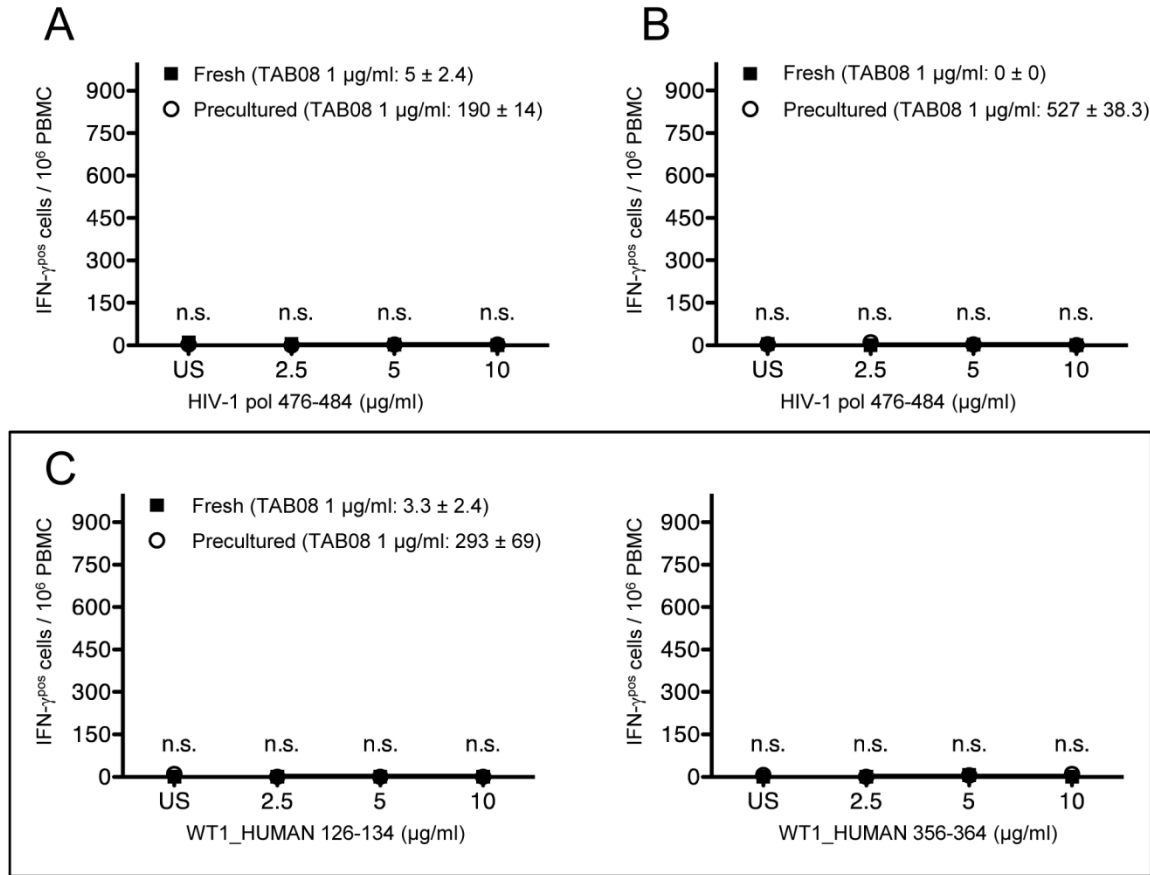


Figure 4.13: **Specificity controls of the T-cell responses presented in Figure 4.12 (WT1\_HUMAN 126-134/ HLA-A0201, WT1\_HUMAN 356-364/ HLA-A0201).** (A, B) PBMC of HIV sero-negative hematopoietic stem cell transplanted patients that show WT1 dependent IFN- $\gamma$  releases to WT1\_HUMAN 126-134 (Figure 4.12A) or WT1\_HUMAN 356-364 (Figure 4.12B) were also treated in IFN- $\gamma$  ELISPOT assays with titrated amounts of the irrelevant HLA-A0201-restricted peptide HIV-1 pol 476-484. (C) Nonspecific effects of WT1 peptide stimulation were excluded by treating PBMCs of an HLA-A0201 negative healthy donor with titrated WT1\_HUMAN 126-134 or 356-364. No unspecific responses were detected. Unpaired *t* test: n.s.; The RESTORE effect was demonstrated by TAB08 responses, exclusively in HD precultured PBMCs, but not in fresh PBMCs of all tested patients (A, B) and healthy donors (C). Data represent mean  $\pm$  SD for triplicate samples.

CD8 T-cell responses to titrated WT1\_HUMAN 356-364 (titration 1:2) were compiled from 11 HLA-A0201 positive AML patients. The average time between allogeneic HSCT and blood sampling was 814 days, varying from 166 to 2372 days (Figure 4.12C). High fold-increases ( $P < .0005$  or  $P < .0001$ ) in tumor-directed CD8 T-cell responses of precultured PBMCs relative to fresh PBMCs were detected after stimulation with 2.5  $\mu\text{g/ml}$  (3.6, IQR = 10.0) 5  $\mu\text{g/ml}$  (9.4, IQR = 14.6) or 10  $\mu\text{g/ml}$  (5.9, IQR = 14.1) of WT1\_HUMAN 356-364. These increases were even higher than the gain in T-cell reactivity upon stimulation with the viral peptide mix presented in Figure 4.7E and might be explained by the low-avidity TCR repertoire recognizing tumor-associated antigens.

The usefulness of the RESTORE protocol for monitoring of anti-tumor T-cell responses of AML patients who underwent allogeneic HSCT was tested next. WT1\_HUMAN 356-364-specific CD8 T-cell responses in fresh or HD precultured PBMCs of one representative HLA-A0201 positive AML patient were chronologically followed upon transplantation (Figure 4.12D). Anti-tumor responses were detected already 4 months after allogeneic HSCT only if the RESTORE protocol, but not if the conventional T-cell stimulation assay was used. A dramatically increased WT1 reactivity was observed in HD precultured PBMCs relative to fresh PBMCs 1 year after transplantation and was still detectable 5 years after transplantation (Figure 4.12D).

As monitoring of tumor-directed T-cell responses is often performed with cryopreserved PBMCs because of technical reasons, it was important to test whether an additional freeze/thaw step influences the restored T-cell functionality. As presented in an IFN- $\gamma$  ELISPOT assay for one representative HLA-A0201 positive AML patient in Figure 4.14, identical results were obtained in (non)-cryopreserved cells after stimulation with titrated WT1\_HUMAN 356-364 (titration 1:2).

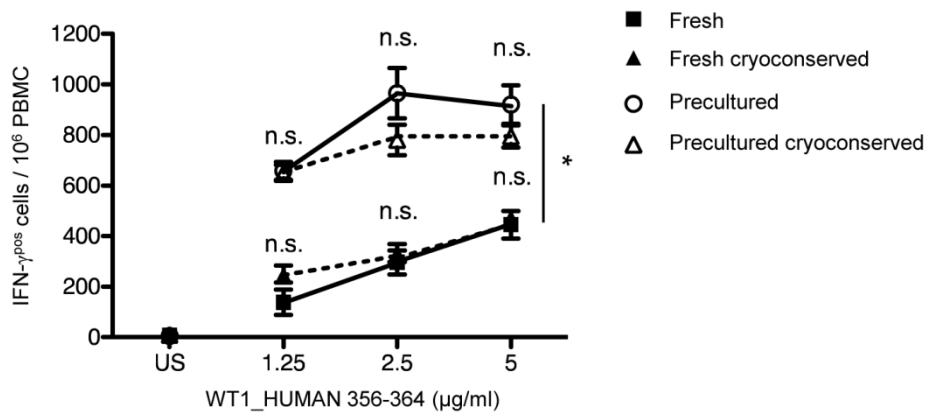


Figure 4.14: **The RESTORE effect is independent of cryopreservation.** PBMCs of a representative leukemia patient were frozen, thawed and tested with or without the HD preculture step. IFN- $\gamma$  secretion of cryoconserved and non-cryoconserved fresh or HD precultured samples were compared by an unpaired *t* test: n.s.; The RESTORE effect was significantly analyzed by 2way ANOVA. Experiment was repeated  $\geq 3$  times.

Taken together, the results presented in Figure 4.12 - Figure 4.14 demonstrate that cellular interactions induced by HD preculture of PBMCs dramatically enhance CD8 T-cell sensitivity to the low-avidity antigens WT1\_HUMAN 126-134 and 356-364.

#### 4.7 HD preculture allows the generation of CD8 T-cell lines with an improved representation of clones responding to low antigen concentrations

Repeated antigen stimulation in the presence of growth-promoting cytokines is often used to generate T-cell lines and clones for both analytical and therapeutic purposes. The gain in antigen sensitivity during the first round of *in-vitro* stimulation as a result of HD preculture suggested that without this step, CD8 T-cells able to respond to low antigen concentrations if appropriately pre-sensitized by cell contacts may be lost from the population and hence be under-represented during later rounds of



stimulation. Recall responses of fresh or precultured PBMCs to titrated amounts of the peptide WT1\_HUMAN 356-364 (titration 1:2) were analyzed before and after antigen-specific CD8 T-cell expansion in the presence of the cytokines IL-2, -7 and -15 (Figure 4.15A). Whereas circulating functional WT1-specific CD8 T-cell responses were absent or barely measurable in fresh PBMCs of a representative HLA-A0201 positive AML patient, CD8 T-cell responses from precultured PBMCs of the same individual were easily detectable (Figure 4.15A, left). Importantly, the enhancing effect of HD preculture before the first round of stimulation with WT1\_HUMAN 356-364 was apparent even after long-term culture (Figure 4.15A, right). CD8 T-cells from expanded precultured PBMCs displayed a much higher sensitivity (up to 10-fold) after restimulation with titrated peptide WT1\_HUMAN 356-364 (titration 1:2) in comparison to CD8 T-cells from fresh PBMCs that were cultured under the same conditions. Of note, the increase in the CD8 T-cell response was particularly striking at low antigen doses, suggesting that indeed, the HD preculture step had allowed presensitization-dependent clones to participate in the antigen-driven expansion protocol. No responses were observed to PepMix™ Human Actin, illustrating the maintenance of peptide specificity (Figure 4.15A, right). To rule out the possibility that the observed increase in sensitivity is due to differences in absolute cell number or frequency to CD8 T-cells in fresh versus precultured PBMCs after 2 weeks of expansion, flow cytometry analyses was performed of fresh or precultured PBMC. After 2 weeks of expansion, the absolute cell number decreased from  $2 \times 10^6$  PBMC to  $1.5 \times 10^6$  in peptide/cytokine expanded fresh and  $1.2 \times 10^6$  precultured PBMC, respectively. CD8 T-cells in viable fresh PBMCs (69 %) were similar in frequency as CD8 T-cells in viable precultured PBMCs (68 %, data not shown). To confirm the enhanced responsiveness of CD8 T-cells from precultured PBMCs after long-term culture, relative to expanded CD8 T-cells derived from fresh PBMCs, CD137 expression was used as a second readout for CD8 T-cell activation (Figure 4.16). Whereas only 2.0 % of CD8 T-cells from the fresh PBMC-derived cultures expressed CD137 upon restimulation with 10  $\mu\text{g}/\text{ml}$  of the peptide WT1\_HUMAN 356-364, the frequency of CD137 expressing CD8 T-cells from precultured PBMC-derived cultures was increased by a factor of four (8.2 %). Unstimulated CD8 T-cells were negative for CD137 expression.

An analogous set of experiments was also performed regarding the generation of virus-specific CD8 T-cell lines. CD8 T-cells from precultured PBMCs specific for multiple virus-specific peptides showed a significantly higher IFN- $\gamma$  recall response to titrated amounts of the PepMix™ CEF standard (titration 1:5) as compared to CD8 T-cells from fresh PBMCs (Figure 4.15B, left). Even after dramatic expansion of virus-specific CD8 T-cells during long-term culture, the enhanced responsiveness of CD8 T-cells expanded from precultured PBMCs was maintained if cells were restimulated with low concentrations of peptides (0.004 to 0.1  $\mu\text{g}/\text{ml}$ , Figure 4.15B, middle). Of note, this enhanced response of cells expanded from HD precultured PBMCs remained strictly antigen-dependent. Moreover, expansion and re-stimulation with peptides derived from human actin yielded only minute responses to this self-antigen using both protocols (Figure 4.15B, right). Together the data indicate that CD8 T-cells that receive tissue-like interactions during HD preculture of PBMCs gain in sensitivity to virus- and tumor-derived antigens. Sensitization-dependent CD8 T-cells from HD precultured PBMCs

expanded during the first round of stimulation are maintained during long-term cultures, contributing to a stronger recall response when the expanded CD8 T-cell populations are confronted with antigens, e.g. upon adoptive T-cell transfer, especially those that are presented at a low level.

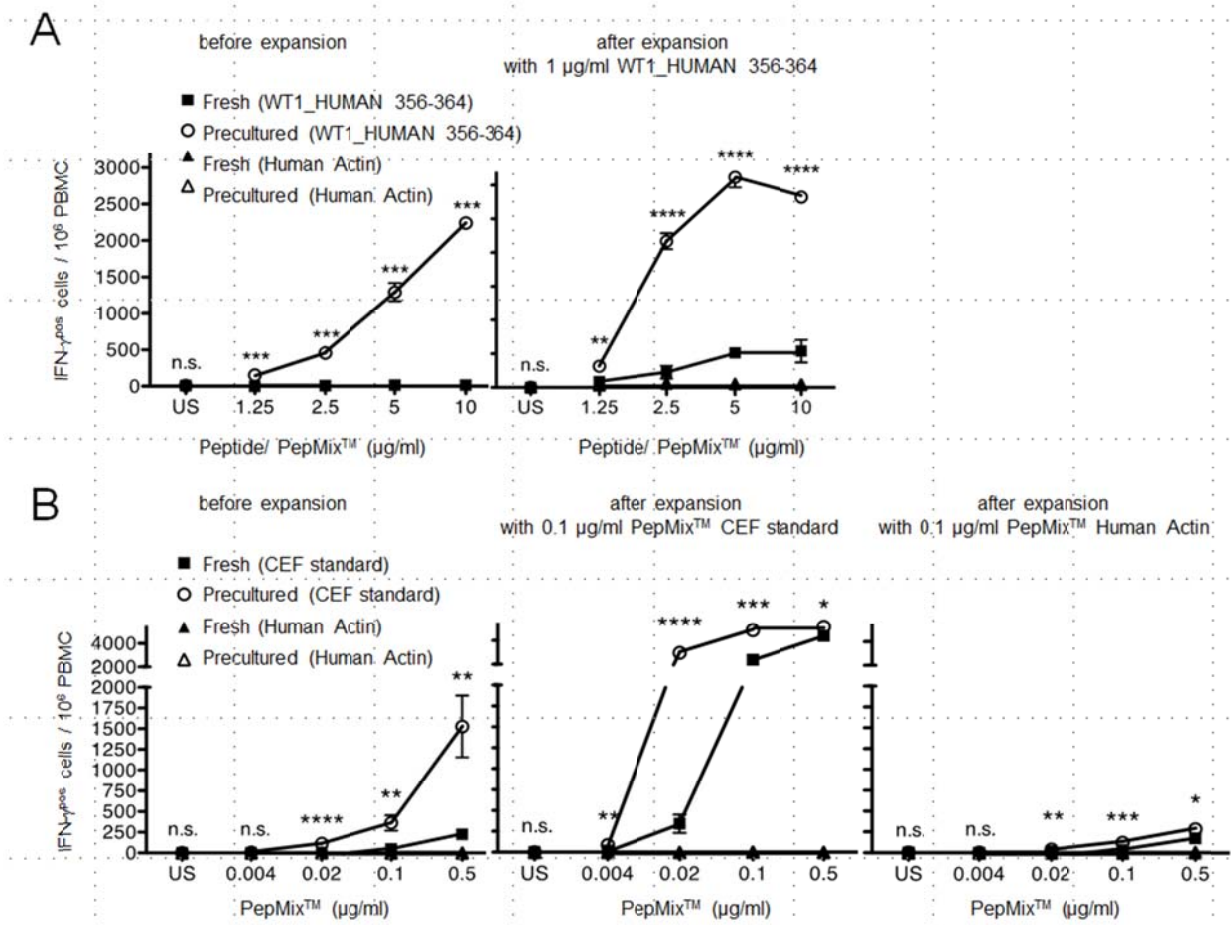


**Figure 4.15: HD preculture of PBMCs allows generation of CD8 T-cell lines with an improved representation of clones responding to low antigen concentrations.** (A, Left) IFN- $\gamma$  responses of CD8 T-cells from fresh or precultured PBMCs of one HLA-A\*0201 positive patient to titrated amounts of the peptide WT1\_HUMAN 356-364 before expansion. (Right) Fresh or precultured PBMCs of the same patient were stimulated with 1 µg/ml of the peptide WT1\_HUMAN 356-364 in a final cell density of  $2 \times 10^6$  cells/ml and were expanded in the presence of IL-2, IL-7 and IL-15 for 2 weeks. After expansion, cells were restimulated with titrated amounts of the peptide WT1\_HUMAN 356-364 or the control pool Human Actin in IFN- $\gamma$  ELISPOT plates for 16 hours. (B, Left) IFN- $\gamma$  responses of CD8 T-cells from fresh or precultured PBMCs of one representative healthy donor to titrated amounts of the HLA-class I restricted PepMix<sup>TM</sup> CEF standard and the control pool Human Actin before expansion. Fresh or precultured PBMCs of the same donor were stimulated with 0.1 µg/ml of (middle) the PepMix<sup>TM</sup> CEF standard or the PepMix<sup>TM</sup> Human Actin (right) and were expanded under the same conditions as presented in Figure 4.15A. After expansion, virus-specific CD8 T-cells were restimulated with titrated amounts of the PepMix<sup>TM</sup> CEF standard or the control pool Human Actin in IFN- $\gamma$  ELISPOT plates for 16 hours, respectively. Unpaired *t* test: \*  $P < .05$ ; \*\*  $P < .005$ ; \*\*\*  $P < .0005$ ; \*\*\*\*  $P < .0001$ . Data represent mean  $\pm$  SD for triplicate samples. Experiments were repeated 4 times.

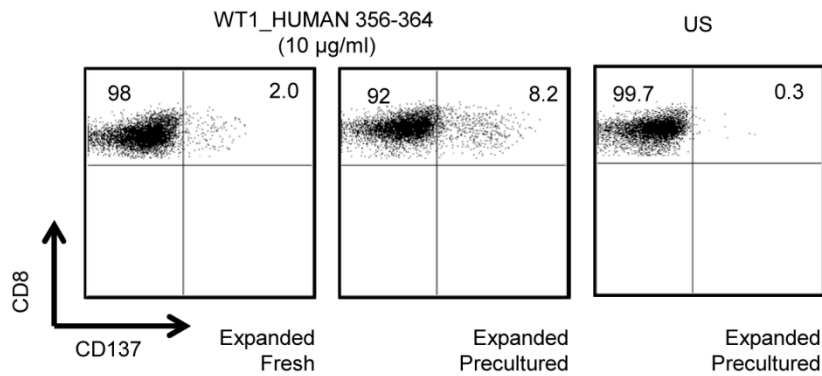


Figure 4.16: **CD137 expression on CD8 T-cells from fresh or precultured PBMCs after WT1-specific T-cell expansion.** Fresh or precultured PBMCs of the same HLA-A0201-positive AML patient were simultaneously stimulated with 1 µg/ml of the peptide WT1\_HUMAN 356-364 in a final cell density of  $2 \times 10^6$  cells/ml and were expanded in the presence of IL-2, IL-7 and IL-15 for 2 weeks. After expansion, cells were restimulated with 10 µg/ml WT1\_HUMAN 356-364 for 16 hours and stained for CD3, CD8 and CD137. Gating was performed on viable CD8 T-cells.

## 4.8 Phosphorylation of proximal TCR signaling components upon HD preculture of PBMCs

As previously reported, Stefanová *et al.* have demonstrated that tonic TCR signaling induced by frequent MHC-recognition maintains the sensitivity of murine T-cells towards subsequent foreign antigens in the tissue environment (Stefanova, Dorfman *et al.* 2002). In this studies tonic TCR signaling was measured by the phosphorylation level of the ZAP-70 associated TCR  $\zeta$  chains using immunoprecipitation (IP) assays. Phosphorylation levels were enhanced in LN-resident TCR transgenic CD4 T-cells, relative to freshly prepared, blood-derived cells from the same animal (Stefanova, Dorfman *et al.* 2002). In the present study Western blotting was performed to compare tyrosine phosphorylation of proximal components of the TCR signaling machinery presented in Figure 1.1 between human CD8 T-cells from fresh PBMCs and those that were first “restored” at HD (Figure 4.17). In a pilot experiment, CD8 T-cell and monocyte co-cultures (1:1) were lysed, proteins were separated under reducing conditions using a 15 % polyacrylamide gel and membranes were finally probed with the primary antibody 4G10, which recognizes total tyrosine-phosphorylated proteins in CD8 T-cells and monocytes (Figure 4.17A). Several phosphorylated proteins were detected with stronger tyrosine phosphorylation in HD precultured co-cultures (P) compared to co-cultures of fresh CD8 T-cells and monocytes (F). A band that presented stronger tyrosine phosphorylation in precultured cells relative to fresh cells presented a molecular weight of around 19 kDa (Figure 4.17A). This 19 kDa band was tested for correspondence to the CD3  $\zeta$  chains that undergo multistep tyrosine phosphorylated upon TCR engagement resulting in a shift in electrophoretic mobility from 16-21 kDa (Koyasu, McConkey *et al.* 1992, van Oers 1999). Indeed, when using CD3  $\zeta$  p-142-specific mAb a much higher phosphorylation level in HD precultured-derived CD8 T-cells as compared to freshly isolated CD8 T-cells was observed, whereas total CD3  $\zeta$  levels remained unchanged (Figure 4.17B). As it was shown in mice that different types of TCR engagement are translated into defined CD3  $\zeta$

phosphorylation patterns that regulate thresholds for T-cell activation (Kersh, Shaw *et al.* 1998), frequent formation of low-avidity TCR/MHC-self-peptide complexes during HD preculture of PBMCs might establish lower thresholds for CD8 T-cell activation compared to CD8 T-cells that lose cellular interactions by entering the circulation. In addition, Lck p-Y394 which is required for tyrosine phosphorylation of the CD3  $\zeta$  chains (Molina, Kishihara *et al.* 1992, Straus and Weiss 1992) was much more pronounced in CD8 T-cells from precultured PBMCs as compared to CD8 T-cells from fresh PBMCs (Figure 4.17B), whereas total Lck levels remained unchanged. This result correlates with the finding that addition of the Lck inhibitor protein phosphatase 1 (PP1) strongly reduces TGN1412-specific CD4 T-cell reactivity when added during HD preculture or subsequent stimulation culture, whereas a brief pulse before harvest of HD precultures was without effect (Romer, Berr *et al.* 2011).

A second band that presented strong tyrosine phosphorylation in precultured relative to fresh cells presented a molecular weight of around 70 kDa (Figure 4.17A). This 70 kDa band was tested for correspondence to ZAP-70 tyrosine kinase activity. Phosphorylation of Tyr319 is known to be required for the positive regulation of ZAP-70 function upon TCR triggering (Di Bartolo, Mege *et al.* 1999). Total ZAP-70 levels were comparable in HD precultured-derived CD8 T-cells and freshly isolated CD8 T-cells (Figure 4.17B).

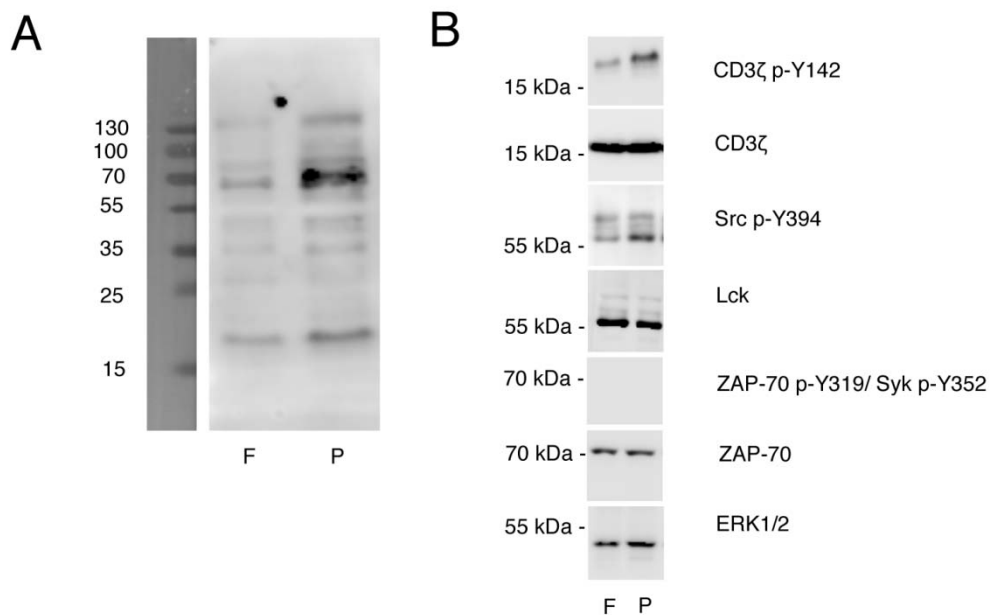


**Figure 4.17: HD preculture of PBMCs affects TCR signaling of CD8 T-cells.** (A) Total tyrosine phosphorylation patterns were compared by Western blotting between freshly isolated CD8 T-cells and monocytes (1:1, F) and HD precultured co-cultured CD8 T-cells and monocytes (1:1, P) of one representative donor. After cell lysis, proteins were separated under reducing conditions using a 15% polyacrylamide gel. Membranes were probed with 4G10 antibody (anti-pTyr). (B) Phosphorylation of proximal TCR signaling components was compared between CD8 T-cells from fresh and precultured PBMCs. Membranes were probed with antibodies against CD3 $\zeta$  p-Y142, CD3 $\zeta$ , Src p-Y394, Lck, ZAP-70 p-Y319/ Syk p-Y352 and ZAP-70 as indicated. ERK1/2 served as a loading control. Experiment was repeated  $\geq 3$  times with the exceptions that membranes were probed with antibody against ZAP-70 p-Y319/ Syk p-Y352 only once.

Tyrosine phosphorylation of ZAP-70 was not observed using ZAP-70 p-Y319/ Syk p-Y352 antibody which detects endogenous ZAP-70 only when phosphorylated at Tyr319 and also cross-reacts with

endogenous tyrosine kinase (Syk) when phosphorylated at Tyr352 (Figure 4.17B). To firmly conclude that HD preculture does not induce tyrosine phosphorylation of ZAP-70 and that hence, the observed band of 70 kDa in Figure 4.17A is of a different origin, further repetitions of the experiment using cells from different donors and antibodies other than ZAP-70 p-Y319/ Syk p-Y352 antibody are necessary.

Taken together, tonic TCR signaling that is shown by enhanced tyrosine phosphorylation of the proximal TCR signaling components *e.g.* CD3  $\zeta$  and Lck in human CD8 T-cells from precultured PBMCs, but not from fresh PBMCs gives an explanation for improved CD8 T-cell sensitivity to a broad range of viral and tumor-associated antigens.

## 4.9 Gene expression analysis of CD8 memory T-cells from HD precultured PBMCs and tonsils compared to fresh PBMCs

The mechanism of the RESTORE protocol was further studied using Human Gene Expression Arrays. Total RNA was prepared from flow cytometry sorted CD8 memory T-cells (CD8<sup>+</sup>CD45R0<sup>+</sup>) from fresh (F) and HD precultured (P) PBMCs of three healthy adults (donors 1-3) and from CD8 memory T-cells from fresh PBMCs and TMCs (T) of three children undergoing tonsillectomy (donors 4-6). The experimental setup contained samples from both adults and children, as only very few amounts of blood were received from children undergoing tonsillectomy. The isolation of RNA out of CD8 memory T-cells (CD8<sup>+</sup>CD45R0<sup>+</sup>) from fresh, HD precultured PBMCs and TMCs of the same child failed.

Global expression profiles were hierarchically clustered according to their similarity and presented in the dendrogram in Figure 4.18A. Expression values of differentially expressed genes were then scaled, where dark blue corresponds to the lowest expression and dark red to the highest expression level (heatmap, Figure 4.18B). Gene expression profiles of CD8 memory T-cells (CD8<sup>+</sup>CD45R0<sup>+</sup>) from fresh PBMCs were comparable between adults (F1-3) and children (F4-6) with the exception of donor 5 (F5) (Figure 4.18A, B), indicating that gene expression was independent of age. Expression profiles differed clearly between CD8 memory T-cells from HD precultured PBMCs (P1-3) and TMCs (T5-6) as CD8 memory T-cells from TMCs (T5-6) were clustered closer to the ones in fresh PBMCs (F2-4, 6) relative to the ones in HD precultured PBMCs (P1-3, Figure 4.18B).

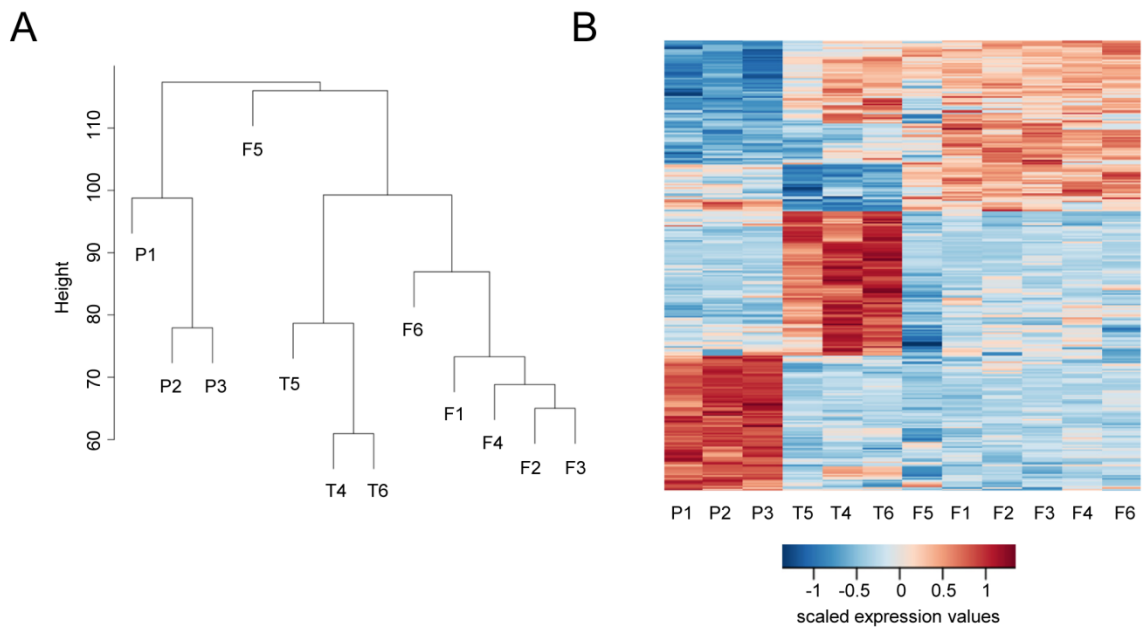


**Figure 4.18: Gene expression analysis of CD8 memory T-cells from fresh and HD precultured PBMCs and tonsils.** Total RNA was prepared for microarray analysis out of flow cytometry sorted CD8 memory T-cells ( $CD8^+CD45R0^+$ ) from fresh (F) and HD precultured (P) PBMCs of three healthy individuals (1-3) and from CD8 memory T-cells ( $CD8^+CD45R0^+$ ) from fresh PBMCs and TMCs (T) of three children undergoing tonsillectomy (4-6). (A) Agglomerative hierarchical clustering of global gene expression profiles. The cumulated length of vertical lines connecting two samples is indicative for their similarity. (B) Heatmap of differentially expressed genes showing scaled expression values, where dark blue corresponds to the lowest expression and dark red to the highest expression level.

Next, differentially expressed genes were used for enrichment analyses in order to determine pathways that could contribute to the enhanced functionality of MHC scanning cells (Figure 4.19). The radar plot in Figure 4.19A shows enriched signaling and metabolic pathways that displayed a globally significant enrichment (false discovery rate (FDR)  $<.05$ ) in at least one comparison. For 13 pathways a transformed enrichment FDR ( $-\log_{10}$  FDR) is shown. A value of 1.3 or greater corresponds to significant enrichment. Differentially expressed genes and the direction of changes are not evident from Figure 4.19A. Differentially expressed genes in CD8 memory T-cells ( $CD8^+CD45R0^+$ ) from HD precultured versus fresh PBMCs (dark grey area) belong to pathways that are associated with metabolism (proteasome, glycolysis, glyconeogenesis, fuctose and mannose metabolism, oxidative phosphorylation (OXPHOS), citrat cycle, aminoacetyl and tRNA biosynthesis) and with cellular interactions and movements (leukocyte transendothelial migration, antigen processing and presentation and actin cytoskeleton). Only few pathways (leukocyte transendothelial migration, antigen processing and presentation, intestinal immune network for IgA production, ribosome and o-glycan biosynthesis) were found if gene expression in CD8 memory T-cells ( $CD8^+CD45R0^+$ ) from TMCs was compared to that of CD8 memory T-cells from fresh PBMCs (light grey area). Among the differentially expressed genes presented in Figure 4.18, only five genes display concordant expression changes between CD8 memory T-cells from HD precultured PBMCs and from TMCs relative to fresh PBMCs. These are presented in a heatmap of scaled expression values (Figure 4.19B). While 6-phosphofructo-2-kinase/fructose-2,6-biphosphatase (*PFKFB3*, log fold change (log FC): +1.3), an important regulator of glycolysis (Maciolek, Pasternak *et al.* 2014) was upregulated in “restored” and tissue-resident CD8

memory T-cells relative to circulating cells, 4 genes were downregulated (Figure 4.19B). The latter are SAM domain and HD domain-containing protein 1 (*SAMHD1*, log FC: -1.7), a human IFN- $\gamma$  inducible protein (Li, Zhang *et al.* 2000), integrin, alpha M (*ITGAM*, log FC: -1.3) and integrin, alpha 6 (*ITGA6*, log FC: -2.2) both implicated in various adhesive interactions (Dana, Fathallah *et al.* 1991, Savino and Silva-Barbosa 1996) and vinculin (*VCL*, log FC: -1.2), a regulator of the cell structure (Ziegler, Liddington *et al.* 2006). Downregulation of vinculin was shown to enhance cell motility that might be important for frequent MHC scanning in tonsils and HD precultures (Ziegler, Liddington *et al.* 2006). As only very few genes were similarly expressed in CD8 memory T-cells from HD precultured PBMCs and from TMCs relative to fresh PBMCs no general conclusions were drawn.

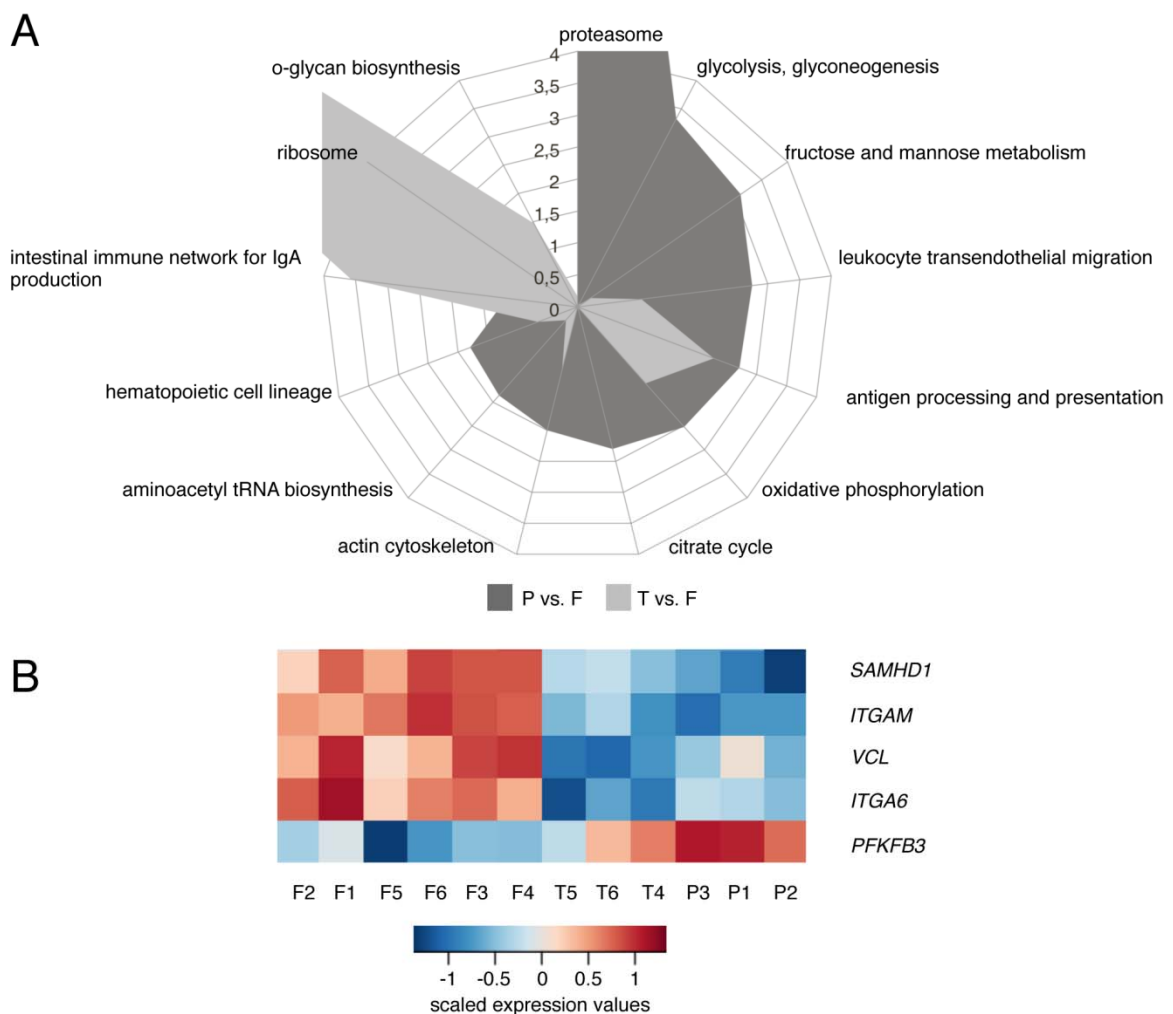


**Figure 4.19: Comparison of the expression profile of CD8 memory T-cells from HD precultured PBMCs and TMCs.** (A) Radar plot displaying gene set enrichment results from CD8 memory T-cells ( $CD8^+CD45R0^+$ ) from HD precultured PBMCs versus fresh PBMCs (dark grey area) and those from TMCs versus fresh PBMCs (light grey area). Of the 13 functional clusters / pathways shown, each displayed a globally significant (false discovery rate [FDR]  $<.05$ ) enrichment in at least one comparison. Enrichment FDRs were transformed to  $-\log_{10}(\text{FDR})$  and displayed along the axis for each pathway;  $\text{FDR} <.05$  corresponds to  $-\log_{10}(\text{FDR}) >1.3$ . (B) Heatmap of genes that display concordant expression changes between CD8 memory T-cells ( $CD8^+CD45R0^+$ ) from HD precultured PBMCs and from TMCs relative to fresh PBMCs.

When CD8 memory T-cells ( $CD8^+CD45R0^+$ ) from HD precultured PBMCs (P1-3) were compared to their fresh counterparts (F1-3) without samples from patients 4-6, multiple genes associated with metabolism were differentially expressed (Figure 4.20A). While genes involved in glycolysis (33 probe sets, 12 genes), fructolysis (9 probe sets, 7 genes) and the pentose phosphate pathway (6 probe sets, 4 genes) were strongly upregulated, expression levels of genes related to other metabolic pathways such as oxidative phosphorylation, citrate cycle, aminoacetyl and tRNA biosynthesis, lipolysis and amino acid synthesis remained largely unchanged. Interestingly, metabolic enzymes were consistently upregulated in order to facilitate the transformation from glucose-6-phosphate to pyruvate (glycolysis) that is further transformed to lactate via lactate dehydrogenase A (LDHA, lactic acid fermentation), an enzyme which also regenerates oxidized nicotinamide adenine dinucleotide ( $NAD^+$ ) needed for glyceraldehyde-3-phosphate dehydrogenase (GAPDH) (Figure 4.20B). The results indicate that CD8 memory T-cells in HD precultured PBMCs apparently reprogram their metabolism in preparation for antigenic stimulation.

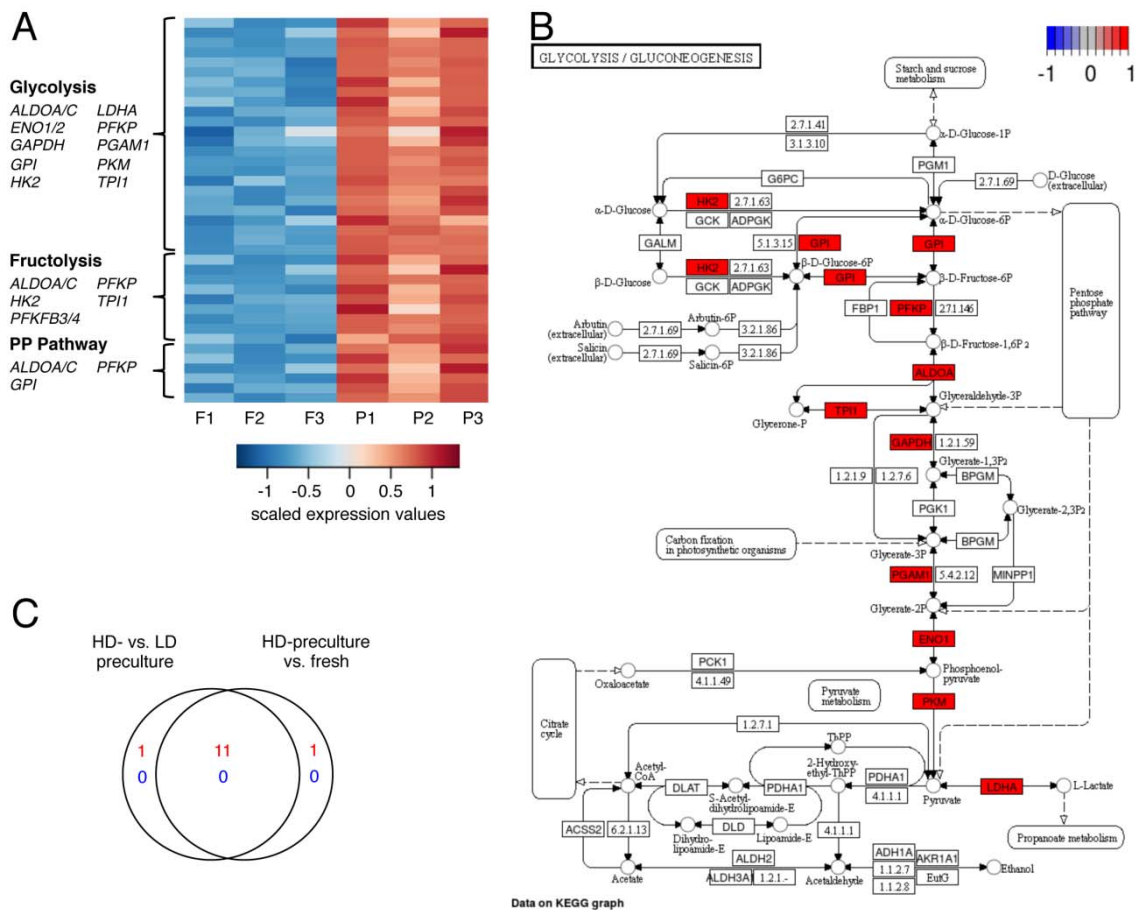


**Figure 4.20: HD preculture of PBMCs affects metabolism of CD8 memory T-cells.** Differentially expressed glycolysis pathway genes from a comparison of CD8 memory T-cells ( $CD8^+CD45R0^+$ ) from fresh and HD precultured PBMCs are shown (A) in a heatmap of scaled expression values and (B) in a KEGG pathway map with color coded log fold changes. (C) Venn Diagram indicating high concordance of changes in glycolysis-related gene expression changes between CD8 memory T-cells ( $CD8^+CD45R0^+$ ) from fresh PBMCs (presented in 7A and 7B) and pan T-cells from LD precultured PBMCs.



To exclude the possibility that the enhanced expression of glycolytic genes in CD8 memory T-cells is a result of *in-vitro* culture *per se*, rather than of the HD preculture conditions which lead to increased antigen sensitivity, results presented in Figure 4.20A, B were compared to a previous data set (GEO database, GSE51288) in which CD4 and CD8 T-cells were isolated from either high (HD) or low density (LD) precultured PBMCs (Figure 4.20C). A large overlap of 11/13 genes associated with the “glycolytic pathways” demonstrates that metabolic reprogramming of T-cells is induced specifically by cellular interactions provided by HD preculture of PBMCs.

Resting cells metabolize glucose to pyruvate, which enters the mitochondrial citrate cycle and generates reducing equivalents for fueling adenosine triphosphate (ATP) production via oxidative phosphorylation (OXPHOS). Activated lymphocytes, however, change their metabolism. They engage glycolysis where pyruvate is fermented to lactate in the cytoplasm even when sufficient oxygen is present to utilize OXPHOS, a process termed originally Warburg effect (Warburg 1956) and later aerobic glycolysis (Wang, Marquardt *et al.* 1976) (Reviewed by (Fox, Hammerman *et al.* 2005, Lunt and Vander Heiden 2011)). Although both processes generate ATP, OXPHOS is more efficient than lactic acid fermentation. As reviewed by Lunt *et al.*, OXPHOS generates 30 ATPs out of one glucose molecule, whereas glycolysis followed by lactic acid fermentation generates only two ATP molecules out of one glucose molecule. Hence, activated lymphocytes that increase glycolysis and lactic acid fermentation have to take up dramatically higher amounts of glucose compared to resting cells. Those high amounts of glucose are imported into the cell mainly via the transmembrane protein glucose transporter 1 (GLUT1) that is expressed upon TCR engagement. CD28 co-stimulation has been shown to be required for maximal GLUT1 expression (Frauwirth, Riley *et al.* 2002). GLUT1 surface expression, known to be regulated on the translational level (Chakrabarti, Jung *et al.* 1994, Maciolek, Pasternak *et al.* 2014), was next compared in CD8 memory T-cells between fresh and HD precultured PBMCs using flow cytometry. Gating was performed on viable CD8<sup>+</sup>CD45R0<sup>+</sup> cells and expression levels of GLUT1 are indicated as  $\Delta$  MFI (Figure 4.21). As presented in Figure 4.21A, GLUT1 expression was significantly increased in CD8 memory T-cells that were first precultured at HD compared to freshly isolated CD8 memory T-cells ( $P < .005$ ). However, in contrast to our expectations, strong co-stimulatory signals induced by the CD28 superagonist TAB08 did not further enhance GLUT1 expression on HD precultured CD8 memory T-cells. Moreover, already preculture of PBMCs at a low cell density (LD) in AB medium significantly increased GLUT1 expression on CD8 memory T-cells (one representative healthy donor, Figure 4.21B). Thus, enhanced GLUT1 expression cannot be explained by cellular interactions during HD preculture of PBMCs. The observed effect is likely to preculture of cells in glucose-rich cell culture media (2 mg/ml). Replication of the experiments under low glucose conditions might be useful to study the effects of HD culture on GLUT1 expression.

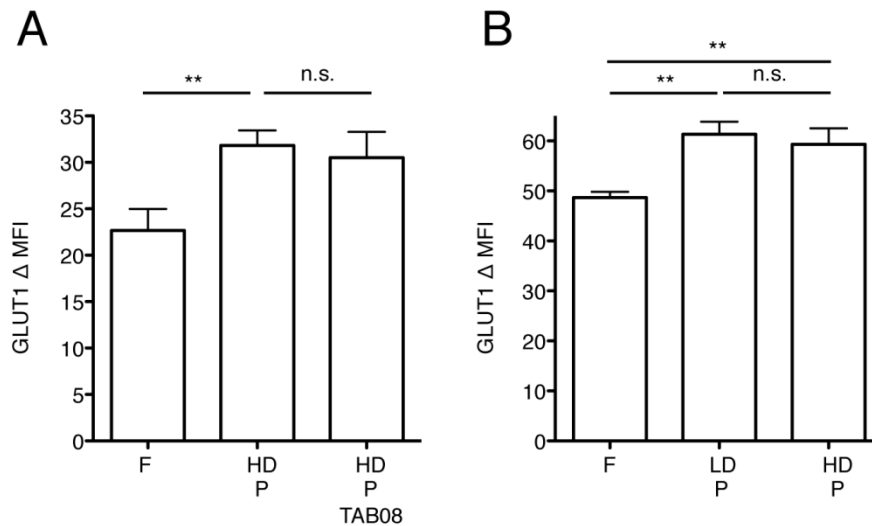


**Figure 4.21: GLUT1 expression in CD8 memory T-cells from fresh and HD precultured PBMCs.** Unstimulated fresh (F) and HD precultured (P) PBMCs were stained for the glucose transporter 1 (GLUT1). Expression values are given as  $\Delta$ MFI: MFI (GLUT1) – MFI (Isotype control). Gating was performed on viable CD8 memory T-cells (CD8<sup>+</sup>CD45R0<sup>+</sup>). (A) HD precultured PBMCs were additionally stimulated with 1  $\mu$ g/ ml TAB08. (B) PBMCs were additionally precultured at a low cell density (LD).

#### 4.10 HD preculture of PBMCs affects integrin expression

In addition to metabolism-related pathways presented in Figure 4.20A, HD preculture was found to affect the expression levels of a number of genes involved in migration (*e.g.* chemokine receptor *CXCR4*), adhesion (*e.g.* integrin *VLA-4*) and cytoskeleton regulation (*e.g.* paxillin: *PXN*, vinculin: *VCL*, actin gamma 1: *ACTG1*). Expression levels of the genes involved in migration, adhesion and cytoskeleton regulation were lower in HD precultured versus freshly prepared CD8 memory T-cells indicated by the blue boxes (Figure 4.22). This counterintuitive observation may reflect the “readiness” of circulating CD8 memory T-cells to extravasate.

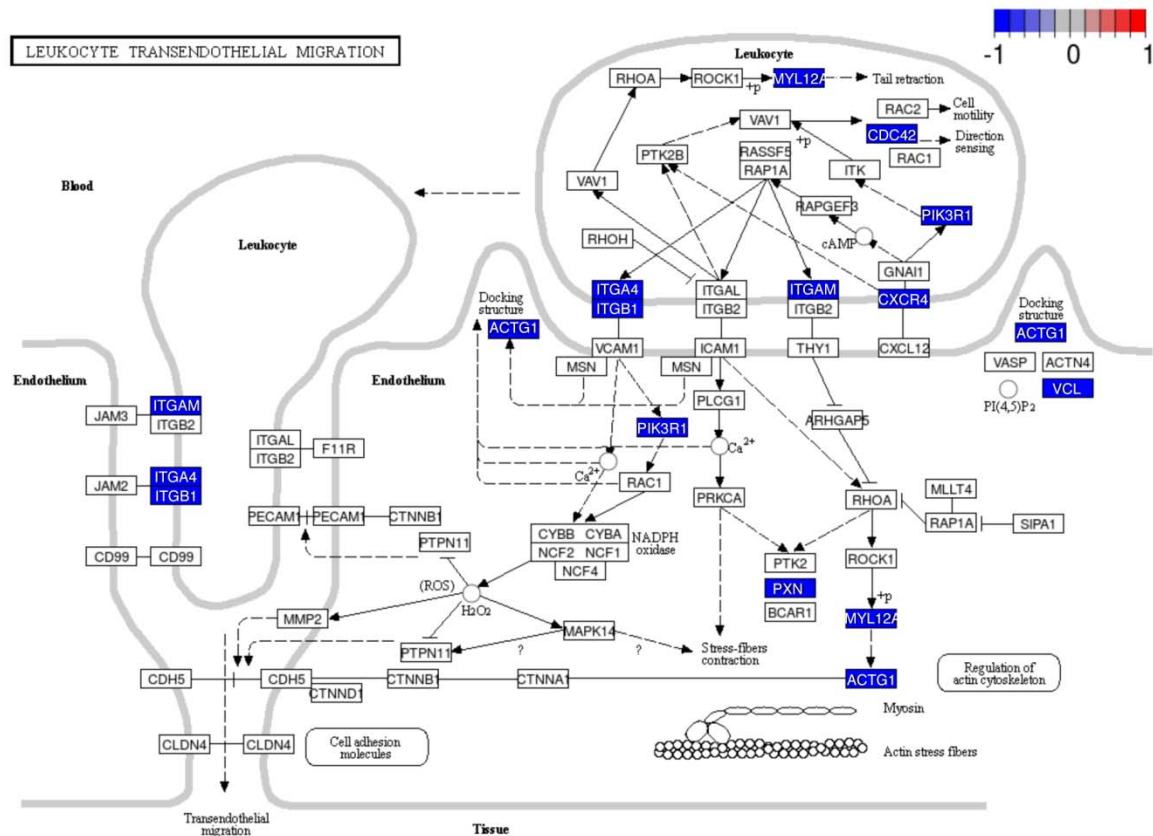


Figure 4.22: **Actin cell adhesion and mobility of CD8 memory T-cells.** Color-coded log FC of differentially expressed leukocyte transendothelial migration pathway genes from the comparison of CD8 memory T-cells ( $CD8^+CD45R0^+$ ) from fresh and HD precultured PBMCs are shown in a KEGG pathway map.

As integrin-induced T-cell adhesion is known to influence T-cell functionality (Friedl and Weigelin 2008), protein expression levels of the alpha and beta subunits of several integrins such as VLA-4 and LFA-1 on leukocytes were also investigated by FACS analysis. Very late antigen 4 (VLA-4) consists of the subunits CD49d (integrin alpha 4) and CD29 (integrin beta 1) and binds to vascular cell adhesion protein 1 (VCAM-1) or to junctional adhesion molecule B (JAM2) on endothelial cells in order to facilitate leukocyte transendothelial migration (see Figure 4.22). Lymphocyte function-associated antigen 1 (LFA-1) binds to intercellular adhesion molecule 1 (ICAM-1) on APCs and consists of the two subunits CD11a (integrin alpha L) and CD18 (integrin beta 2) (Friedl and Weigelin 2008). CD11b (integrin alpha M) forms heterodimers and is implicated in various cellular interactions.

Expression levels of the proteins CD11b, CD18, CD49d, CD29 and CD11a were compared between CD8 memory T-cells ( $CD8^+CD45R0^+$ ) from unstimulated fresh (F) and HD precultured (P) PBMCs using flow cytometry and are presented in histograms (Figure 4.23, left) as well as in bar diagrams (Figure 4.23, right). In line with the previously presented RNA microarray data (Figure 4.22), protein levels of CD11a, CD11b, CD18 and CD49d were concordantly decreased, whereas CD29 expression remained unchanged if cells were first allowed to interact at a HD.

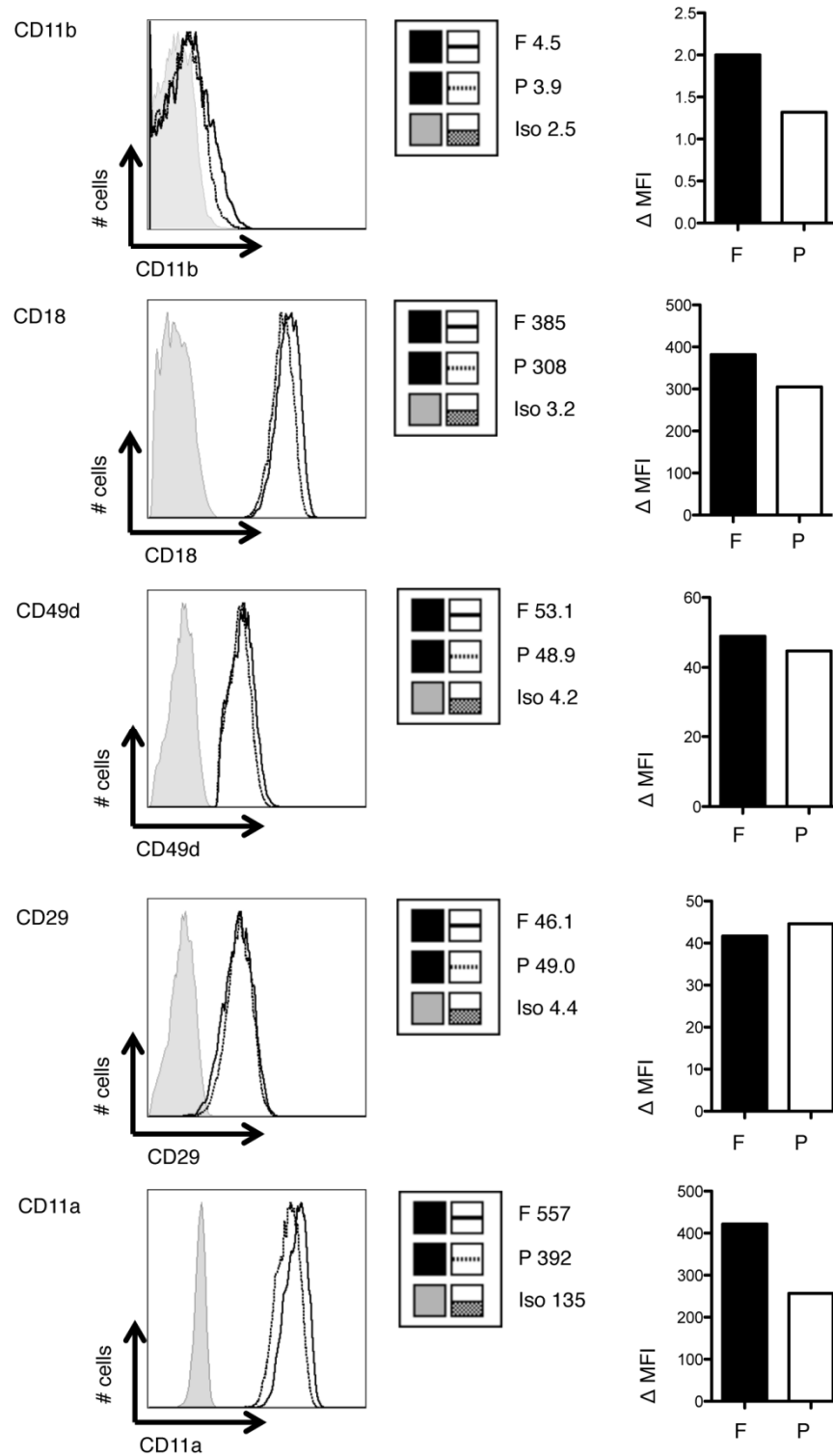


Figure 4.23: **Integrin expression of CD8 memory T-cells from fresh and precultured PBMCs.** Unstimulated fresh (F) and HD precultured (P) PBMCs of one representative healthy donor were surface stained to detect the expression of the integrins CD11b, CD18, CD49d, CD29, and CD11a within CD8 memory T-cells ( $CD8^+CD45R0^+$ ). Isotype stainings (Iso) were used as controls. Mean fluorescence intensities (MFI) are given for each staining (left column) and  $\Delta$  MFI were calculated:  $MFI(\text{Integrin}) - MFI(\text{Isotype})$ ; (right column). Staining was repeated  $\geq 3$  times with similar results.

## 5 Discussion

### 5.1 Increased antigen sensitivity of CD8 memory T-cells upon HD preculture of PBMCs

Blood provides the only routinely accessible source of human CD8 T-cells for immunomonitoring and the generation of CD8 T-cell lines and clones for cellular immunotherapy. Researchers and physicians should, however, be aware of the fact that the large majority of the body's T-cells reside in tissue, especially in bone marrow and lymphatic organs such as thymus, spleen, tonsils, Peyer's patches in the small intestine and LNs, while only 1 % of the cells circulate in the blood stream (Lee, Mandl *et al.* 2012, Sathaliyawala, Kubota *et al.* 2013), and these are transiently less prepared for antigenic stimulation (Stefanova, Dorfman *et al.* 2002). Therefore restoring tissue-like reactivity in blood-derived CD8 T-cells would be highly desirable. In this study it was tested whether short term *in-vitro* preculture of PBMCs at HD – the RESTORE protocol that was initially described for CD4 T-cell responses to the CD28 superagonist TGN1412 (Romer, Berr *et al.* 2011) – returns circulating virus- and tumor-associated CD8 T-cells to tissue-like functionality.

Indeed, a pilot experiment demonstrated that T-cells do not only present an all or nothing effect after HD preculture in response to TAB08 (previously called TGN1412) (Romer, Berr *et al.* 2011), but also an increase in responses to MHC class I-presented viral peptides (Figure 4.1A). These first observations from IFN- $\gamma$  ELISPOT assays were confirmed by intracellular cytokine staining, and antigen-experienced CD8 memory T-cells (CD8<sup>+</sup>CD45R0<sup>+</sup> cells) were identified as the main source for elevated IFN- $\gamma$  responses in HD precultured compared to fresh PBMCs (Figure 4.1B, Figure 4.7C, D). In order to exclude the possibility that the observed effect could be simply secondary to overnight resting of human PBMC in an incubator, which has been a standard method for immunological functional assays (Kutscher, Dembek *et al.* 2013, Santos, Buying *et al.* 2014), preculture conditions were varied with regard to time (from 1 – 3 days) and cell density (from 1.1 - 30x10<sup>6</sup> cells/ ml, Figure 4.2). T-cell performance was improved only if cells were allowed to interact at a high cell density ( $\geq 3.3 \times 10^6$  cells/ ml). The strongest IFN- $\gamma$  releases were detected in PBMC precultures for 2 days. Shorter preculture steps of only 1 day that are comparable to overnight resting are, of course, desirable in regard to time management. Longer preculture steps of up to 3 days were less efficient in comparison to precultures for 2 days at a similar high cell density. A lack of nutrients and oxygen, especially during the third day of preculture might be an explanation for decreased T-cell performance after 3 days of preculture. Hence, the preculture conditions established in the RESTORE protocol, i.e. 2 days at 1x10<sup>7</sup> cells/ ml (Romer, Berr *et al.* 2011) were confirmed to be optimal for the detection of antigenic CD8 T-cell responses against viruses (Figure 4.2) and tumors (data not shown). As T-cell monitoring is often performed on cryopreserved PBMCs, the influence of an additional freeze/thaw step on the restored

T-cell functionality was tested and identical results were obtained in (non)-cryopreserved cells after WT1-specific stimulation (Figure 4.14).

IFN- $\gamma$  ELISPOT assays indicated that the RESTORE protocol prepares T-cells to better respond to a broad range of virus-specific (Figure 4.6, Figure 4.7) and tumor-associated antigens (Figure 4.12). Upon HD preculture of PBMC, CD8 T-cells gained in antigen sensitivity (Figure 4.6, Figure 4.7, Figure 4.12 and Figure 4.15) whereas the frequencies of CD8 T-cells expressing the relevant antigen/MHC specificity remained unaffected (Figure 4.5). Moreover, the possibility that the observed RESTORE effect is due to a reduction in Treg activity in HD precultured PBMCs relative to fresh PBMCs, rather than due to a gain in T-cell sensitivity, was excluded (Figure 4.4B).

Antigen-independent responses were neither observed in fresh nor in HD precultured PBMC (Figure 4.1). The increase in the magnitude of CD8 T-cell responses obtained by preculturing PBMC varied somewhat between donors and the type of antigen but is overall a robust phenomenon. Thus, preculture of PBMC at HD increased the frequency of IFN- $\gamma$  producing human CD8 T-cells to virus-specific antigens by 2-fold on average (from 1.2 - 8 fold) if the whole range of antigen doses is considered (Figure 4.7E). Remarkably high increases in sensitivity were detected after stimulation with titrated amounts of defined virus-derived peptides (Figure 4.6A, C) as well as virus-derived peptide pools (Figure 4.7A, C).

While saturated T-cell responses to multiple virus-specific peptides were already obtained in the presence of 0.3  $\mu\text{g/ml}$  of peptide (Figure 4.7A), much higher peptide concentrations of 5-10  $\mu\text{g/ml}$  were necessary to trigger saturated T-cell responses to tumor-directed peptides (Figure 4.12A, B). This corroborates published results indicating a higher functional avidity of T-cells for APCs displaying virus-specific antigens as compared to over-expressed autologous tumor-derived antigens (Villacres, Lacey *et al.* 2003, McMahan and Slansky 2007). *In-vitro* HD preculture of PBMCs had no influence on the sensitivity of T-cells to non-immunogenic self-antigens, as demonstrated by the unresponsiveness of fresh and precultured PBMCs to even high concentrations of the PepMix™ Human Actin (Figure 4.7B, Figure 4.15). The importance of preceding cell-cell interactions for the responsiveness of CD8 T-cells was unambiguously demonstrated by the high ratio of precultured to fresh PBMC responses following stimulation with the HLA-A0201 restricted peptide WT1\_HUMAN 356-364 (Figure 4.12C). Importantly, the gain in sensitivity by the RESTORE protocol allowed the detection of tumor-directed CD8 T-cell responses that were undetectable in PBMC *in-vitro* tests routinely performed on human fresh PBMC (Figure 4.15A, left). High fold-increases in the magnitude of precultured PBMC relative to fresh PBMC responses (up to 4-fold) were also observed for T-cells of two HLA-A0201 positive patients specific for WT1\_HUMAN 126-134 (data not shown). The enhancing effect of preculture of PBMC at HD on antigen-specific CD8 T-cell responses to HCMV, EBV, AdV, Influenza A and WT1 is in accordance with previous investigations of Römer *et al.* CD4 T-cell responses to a combined tetanus/diphtheria toxoid preparation as well as CD4 and CD8 T-cell responses to SEB (Figure 4.10) were greatly enhanced by HD preculture of PBMCs (Römer, Berr *et al.* 2011). In contrast to all antigens tested, the recall responsiveness of CD8 T-cells to an epitope of the tumor-associated protein B-cell lymphoma 2 was comparable between fresh and HD precultured PBMC from three HLA-B0702

positive AML patients (data published in my Master Thesis). This may be explained by the remarkably high anti-BCL2\_HUMAN 214-223 CD8 T-cell responses in these patients (Fuji S. 2015), which could be secondary to high-affinity recognition by expanded clones which in turn could make them independent of cell contact-mediated priming.

Of note, the enhancing effect of HD preculture on the sensitivity of CD8 T-cells to both WT1\_HUMAN 356-364 (Figure 4.15A) and viral antigens (Figure 4.15B) was maintained after T-cell expansion, resulting in more responsive preparations for experimental or therapeutic purposes especially in the low-dose range of antigenic stimulation which may be relevant after transfer *in-vivo*. The enhanced cytokine response of CD8 T-cells expanded from HD precultured PBMC remained strictly antigen-dependent and the expansion and re-stimulation with peptides from human actin yielded only minute responses to this self-antigen independent of HD preculture prior to long-term expansion (Figure 4.15).

## 5.2 Enhanced T-cell sensitivity depends on cellular interactions

Continuous cellular interactions provided by the tissue environment or by HD preculture are important for the maintenance of full T-cell reactivity (Stefanova, Dorfman *et al.* 2002, Romer, Berr *et al.* 2011). Preculture at HD resulted in a dramatic increase in CD4 T-cell responsiveness to TAB08, approaching the sensitivity observed in lamina propria CD4 T-cells (Figure 4.9). Similar to previous experiments performed on human LN-derived CD4 T-cells (Romer, Berr *et al.* 2011), short-term suspension culture of LPMCs at body temperature led to a significant reduction in T-cell responsiveness to TAB08 and to the bacterial superantigen SEB (Figure 4.10). The findings on blood and tissue-derived CD4 T-cells were extended to anti-viral CD8 memory T-cell responses of the tonsil by demonstrating a 5- to 10-fold drop in antigen sensitivity within 2 hours of dispersed culture at body temperature (Figure 4.11A). As no information is as yet available regarding how long human T-cells remain on average in the circulation before re-entering a tissue, a relatively short time span of 2 hours was chosen. Smith and Ford studied lymphocyte recirculation in rats and found that intravenously injected cells returned to tissue 4-16 hours after injection (Smith and Ford 1983). Further experiments were performed on sheep which, like humans, have large immune systems. The mean lifetime of carboxyfluorescein succinimidyl ester (CFSE)-labeled T-cells from 17 animals in blood was calculated and ranged between 5.3-20.6 hours, whereas few labeled cells remained remarkably long (>100 hours) in blood before trans-endothelial migration to LNs (Thomas, Matejovicova *et al.* 2012). Hence, circulation periods of human T-cells are likely to take even longer than 2 hours on average, resulting in a strongly impaired readiness of T-cells to detect antigens. Decreased virus-specific cytokine responses were shown in blood-derived CD8 memory T-cells relative to tonsillar cells of the same individual (Figure 4.11B). However, the decreased responsiveness of blood-derived CD8 T-cells was partially restored upon HD preculture of PBMC allowing cellular interactions (Figure 4.11B). aaaaa

### 5.3 Maturation of monocytes and sub-threshold activation of CD8 T-cells contribute to the enhanced T-cell functionality

The importance of returning circulating T-cells to a tissue-like status before testing their antigen-reactivity cannot be over-estimated. Thus, the functional impairment of CD4 T-cells during their sojourn in the blood has been clearly demonstrated in both mice (Stefanova, Dorfman *et al.* 2002) and humans (Romer, Berr *et al.* 2011), and is associated with a reduction in the phosphorylation and polarization of signaling molecules. These phenotypic indicators of the readiness of CD4 T-cells to respond to even low numbers of cognate MHC/peptide complexes are restored by an optimized HD preculture, which not only enabled vigorous responses to the CD28 superagonist TAB08, but also enhanced responses to several tested recall antigens (Romer, Berr *et al.* 2011). There, the importance of cellular contacts involving MHC scanning for this functional maturation was demonstrated by the importance of cell density (HD > LD), the inhibitory effects of cell contact prevention by separation of low-density from high-density cultured cells by a semipermeable membrane, and the inclusion of blocking antibodies to HLA molecules (Romer, Berr *et al.* 2011). Moreover, colocalization of the TCR/CD3 with tyrosine-phosphorylated proteins was shown by confocal microscopy in HD precultured PBMCs, but not in fresh PBMCs (Romer, Berr *et al.* 2011).

With regard to the mechanisms underlying the increase in sensitivity of “restored” CD8 T-cells, the observations made for CD4 T-cells with regard to pre-activation of the TCR signaling machinery were extended by demonstrating enhanced tyrosine phosphorylation of Lck and the TCR  $\zeta$  chains (Figure 4.17B). The results obtained by Western blotting correlated with the previous finding that addition of the Lck inhibitor protein phosphatase 1 (PP1) strongly reduces TGN1412-specific CD4 T-cell reactivity when added during HD preculture or subsequent stimulation culture, whereas a brief pulse before harvest of HD preculture was without effect (Romer, Berr *et al.* 2011). Preliminary data exhibited enhanced tyrosine phosphorylation of Lck in CD8 T-cells from tonsils and from HD precultured PBMCs, but not from fresh PBMC (data not shown), supporting the concept that pre-activation of T-cells in the tissue-context depends on functional Lck.

In order to determine pathways that could additionally contribute to the enhanced functionality of HD precultured CD8 T-cells, gene expression analysis of CD8 memory T-cells from fresh and HD precultured PBMC were performed. Interestingly, multiple genes related to metabolism were differentially expressed (Figure 4.19 dark grey area, Figure 4.20). Whereas key enzymes involved in glycolysis, fructolysis and the pentose phosphate pathway were upregulated, expression levels related to oxidative phosphorylation (OXPHOS) remained largely unchanged (Figure 4.20A). Hence, CD8 memory T-cells apparently reprogram their metabolism in preparation for antigenic stimulation, similar to cancer cells (Warburg 1956), effector T-cells (Gubser, Bantug *et al.* 2013) and activated macrophages (Cheng, Quintin *et al.* 2014) that exhibit a higher rate of glycolysis even in the presence of oxygen. An overview about the metabolic reprogramming of T-cells is given in Figure 5.1 (Chang, Curtis *et al.* 2013). Non-proliferating T-cells metabolize glucose to pyruvate, which enters the mitochondrial citrate



cycle and generates reducing equivalents for fueling ATP production via OXPHOS. However, activated T cells engage glycolysis, where pyruvate is fermented to lactate in the cytoplasm even when sufficient oxygen is present to utilize OXPHOS, a process termed the Warburg effect (Warburg 1956) or aerobic glycolysis (Wang, Marquardt *et al.* 1976) (Reviewed by (Fox, Hammerman *et al.* 2005, Lunt and Vander Heiden 2011)).

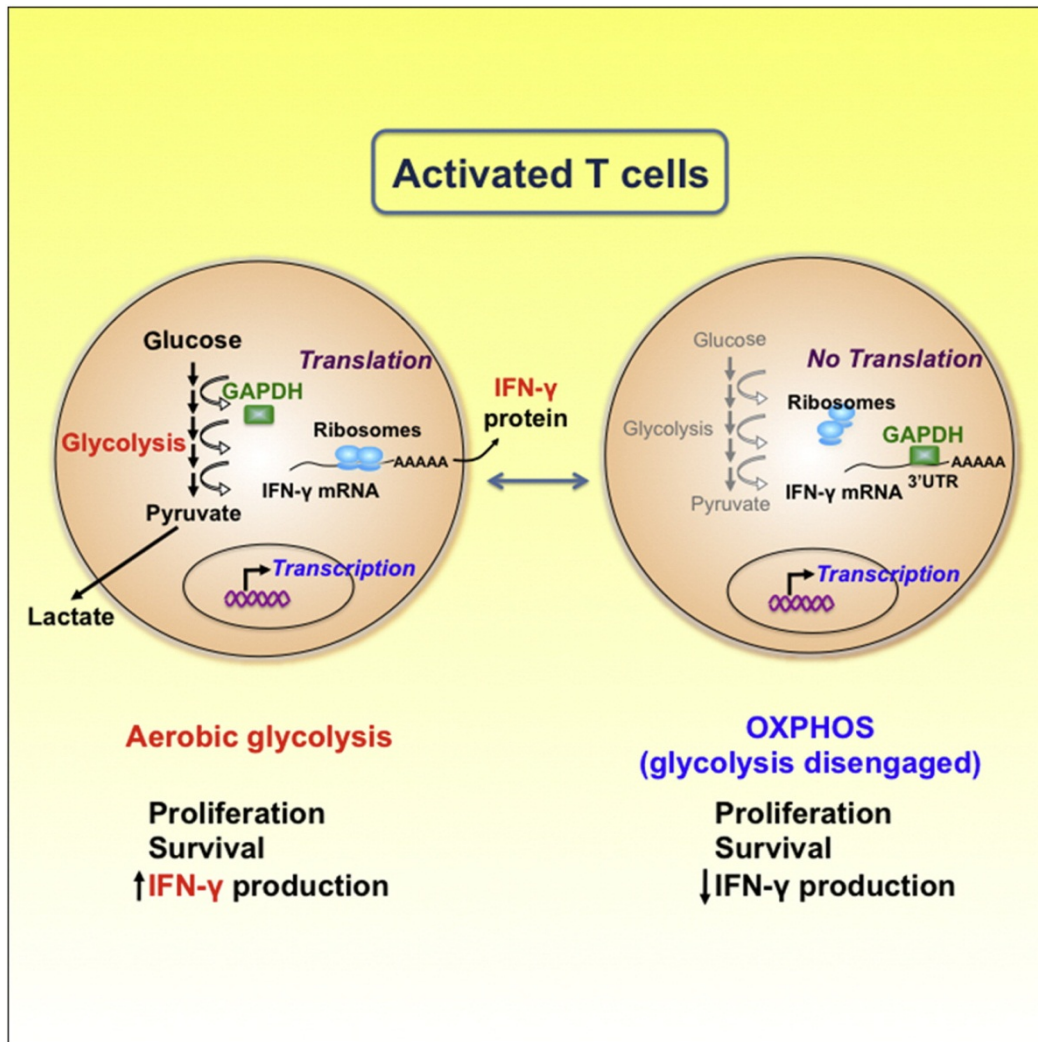


*Figure 5.1: Metabolic reprogramming in T-cells controls T-cell functionality. Resting T-cells metabolize glucose to pyruvate, which enters the mitochondrial citrate cycle and generates reducing equivalents for fueling ATP production via OXPHOS. Activated T cells engage glycolysis, where pyruvate is fermented to lactate in the cytoplasm even when sufficient oxygen is present to utilize OXPHOS (Warburg effect, aerobic glycolysis). Although both processes generate ATP, glycolysis is less efficient in producing ATP, indicating that it might provide other advantages such as uptake and incorporation of nutrients into the biomass needed for cellular proliferation. Beside T-cell proliferation, aerobic glycolysis regulates cytokine production. The key glycolytic enzyme glyceraldehyde-3-phosphate dehydrogenase (GAPDH) controls effector cytokine production on a translational level. (Chang, Curtis *et al.* 2013) © Cell Press*

Although both processes generate ATP, glycolysis is less efficient, indicating that it might provide other advantages during proliferation. It is thought that the metabolism of proliferating cells is adapted to facilitate uptake and incorporation of nutrients into the biomass needed to produce a daughter cell; i.e., aerobic glycolysis is necessary, both in terms of energy and biosynthesis, for cellular proliferation (Vander Heiden, Cantley *et al.* 2009, Lunt and Vander Heiden 2011). However, cells such as dendritic cells exhibit a high rate of glycolysis upon Toll-like receptor-induced activation but do not proliferate

(Krawczyk, Holowka *et al.* 2010). This might be also the case for “restored” CD8 T-cells which do not proliferate during HD preculture ((Romer, Berr *et al.* 2011), Figure 4.1B). This observation suggests that aerobic glycolysis may be necessary for pathways other than, or in addition to, those underlying proliferation. Recently performed studies by Chang *et al.* have shown that the key glycolytic enzyme glyceraldehyde-3-phosphate dehydrogenase (GAPDH) is also a positive translational regulator of IFN- $\gamma$  production (Chang, Curtis *et al.* 2013, Gubser, Bantug *et al.* 2013). GAPDH binds to AU-rich elements within the 3' UTR of IFN- $\gamma$  mRNA and thereby controls effector cytokine production (Chang, Curtis *et al.* 2013).

Initial observations from gene expression analysis have to be further investigated. Experiments on the cellular level might be helpful to test whether the metabolic reprogramming upon HD preculture of PBMCs is required for sub-threshold activation of CD8 T-cells. This could be tested by using an extracellular Flux Analyzer. The extracellular acidification rate (ECAR), an indicator of aerobic glycolysis, and the oxygen consumption rate (OCR), an indicator of OXPHOS can be measured in cultures containing CD8 memory T-cells from either fresh or HD precultured PBMCs. Moreover, surface expression of the glucose transporter 1 (GLUT1) on CD8 memory T-cells from fresh and HD precultured PBMCs (Figure 4.21) could be further tested using cell culture media with glucose conditions < 2 mg/ ml.

In addition to metabolism-related pathways, HD preculture also affected the expression levels of a number of genes involved in migration (*e.g.* chemokine *CXCR4*), adhesion (*e.g.* integrin *VLA-4*) and cytoskeleton regulation (*e.g.* paxillin: *PXN*, vinculin: *VCL*, actin gamma 1: *ACTG1*), where expression levels were lower in HD precultured versus freshly prepared CD8 memory T-cells (Figure 4.22). Also on the protein level, expression of integrins was decreased (Figure 4.23). Possibly, the higher integrin expression in CD8 memory T-cells from fresh relative to HD precultured PBMCs reflects “preparedness” of the circulating T-cells for the process of extravasation and migration into tissues. Moreover, Friedl *et al.* described integrin-independent migration of T-cells in three-dimensional multi-layer structures such as LNs, whereas integrin-mediated attachment of circulating T-cells to two-dimensional endothelial surfaces is highly dependent on LFA-1/ICAM-1 interactions (Friedl and Weigelin 2008). During HD preculture multiple layers of PBMCs can be observed under the microscope. Further studies are necessary to test whether T-cells migrate in an integrin-dependent manner during the preculture step.

In my study I could show that cellular interactions are important for the functional maturation of both interaction partners, CD8 T-cells and monocytes (Figure 4.3). Whereas CD8 T-cells prime their TCR signaling machinery by HLA scanning, indicated by a slight downregulation of CD3 molecules (Table 4.1) and an enhanced tyrosine phosphorylation of proximal TCR signaling components (Figure 4.17B), monocytes improve their features as accessory cells by an enhanced expression of HLA molecules and the co-stimulatory ligand CD86 (Table 4.1 and (Romer, Berr *et al.* 2011)). A brief summary of cellular maturation events occurring during HD preculture of PBMCs is given in Figure 5.2.

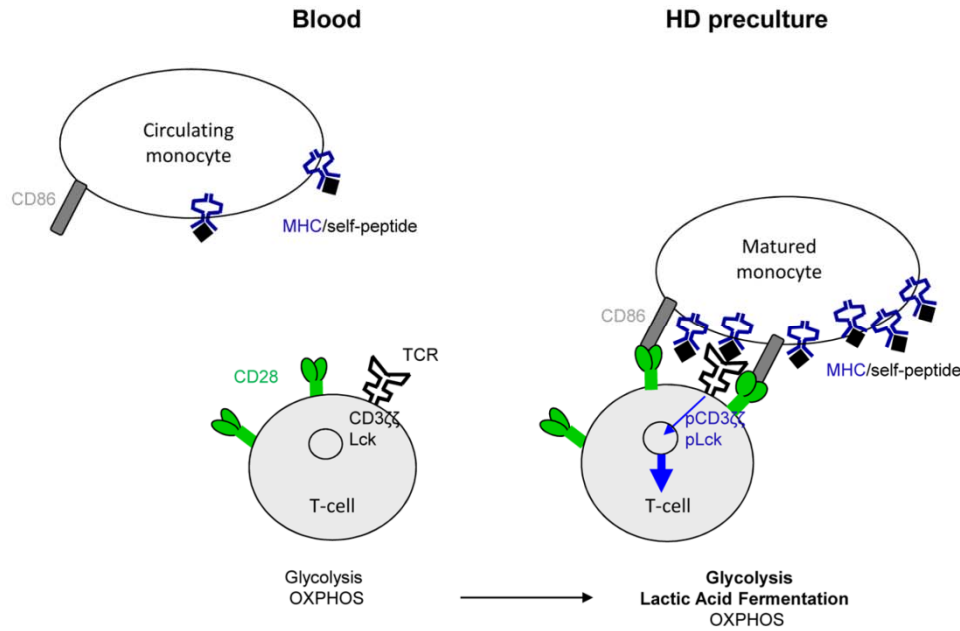


**Figure 5.2: Maturation events in blood-derived T-cells and monocytes during HD preculture.** During HD preculture of PBMCs, monocytes improve their features as accessory cells by an enhanced expression of HLA molecules and the co-stimulatory ligand CD86. T-cells frequently interact with matured monocytes by scanning of MHC molecules that are loaded with self-peptide. Frequent TCR engagement and co-stimulation (CD28-CD86) results in tonic TCR signaling indicated by an enhanced tyrosine phosphorylation of the CD3  $\zeta$  chains and Lck. The primed TCR signaling machinery of “restored” T-cells in combination with increased glycolysis and lactic acid fermentation (referred to as Warburg effect or aerobic glycolysis) which was observed only on the RNA level, but was not on the cellular level until now, lowers the threshold for full T-cell activation.

In contrast to our concept that the enhanced functionality of “restored” T-cells results from tonic TCR signaling in responder T-cells, lowering the threshold for full T-cell activation, Hussain *et al.* report that HD preculture induces strong Fc receptor expression on monocytes and that this expression provides sufficient interaction with the Fc region of the antibody TGN1412/ TAB08 to induce strong CD4 T-cell activation. It was concluded that no enhancement of T-cell sensitivity is required, whereas co-engagement with Fc receptor Fc $\gamma$ RIIb is crucial to the agonistic activity of soluble TGN1412. (Hussain, Hargreaves *et al.* 2015). However, in contrast to our study, Hussain and colleagues performed the experiments in serum-free media, artificially exposing FcRs to the added stimulatory antibody. Moreover, antigen-specific T-cell responses where Fc receptors do not play a role were not tested in fresh and HD precultured PBMCs.

## 5.4 Few genes displaying concordant expression changes between CD8 memory T-cells from tonsils and HD precultures of PBMCs

Contrary to the functionality assays, where “restored” T-cells exhibited a stronger antigen sensitivity relative to fresh cells, approaching the sensitivity observed in tissue cells (Figure 4.9, Figure 4.11), gene expression analysis revealed that expression profiles differed more between CD8 memory T-cells from

tonsillar and HD precultured PBMCs, rather than between CD8 memory T-cells from tonsillar and fresh PBMCs (Figure 4.18). Within the differentially expressed genes, only five genes displayed concordant expression changes between CD8 memory T-cells from HD precultured PBMCs and from TMCs relative to fresh PBMCs (Figure 4.19B). Only one glycolytic enzyme was upregulated in “restored” and tissue-resident CD8 memory T-cells relative to circulating cells, and 4 genes related to cell adhesion and cell structure were downregulated (Figure 4.19B). It might be interesting to test whether knockdown of these 5 genes by small interfering RNAs results in the loss of enhanced T-cell functionality in tissue and HD precultures of PBMCs relative to fresh PBMCs.

It is possible that tonsils, as secondary immunological organs, are not the optimal choice for a comparison of gene expression in CD8 memory T-cells derived from either blood or tissue. Even if tonsil pairs were removed from children that do not suffer from acute infection at the time of surgical removal of the organs, tonsillar T-cells have often previously cleared viral and bacterial infections at this strategically important site and were perhaps not in a “resting” state before tonsillotomy. As the composition of cell subsets differs depending on the location in the human body, further investigations on CD8 memory T-cells from organs different than tonsil might be helpful to detect genes that are similarly expressed in tissue and HD precultures of PBMCs.

## 5.5 The RESTORE protocol as a promising, cost-effective and reliable diagnostic and research tool

In this thesis it was shown that restoring CD8 T-cell functionality of blood-derived cells by first preculturing PBMCs at HD results in a dramatic increase in their responsiveness to various viral and tumor-associated antigens, approaching the sensitivity observed in tissue-resident CD8 T-cells. Importantly, returning blood-derived T-cells to tissue-like conditions before antigenic stimulation does not involve antigen- or cytokine-driven clonal expansion (Figure 4.5), as is used in some protocols to reveal otherwise undetectable responses (Geyeregger, Freimuller *et al.* 2013). Thus by increasing antigen sensitivity *ex-vivo*, the RESTORE protocol detects antigen-reactive T-cells at frequencies which are closer to the *in-vivo* situation as compared to secondary stimulation of conventional PBMC cultures because they are not exaggerated by prior expansion. These features make HD preculture an ideal, simple and cost-effective tool for immunomonitoring of CD8 T-cell responses to infectious agents, vaccines and cancer-associated antigens (Lutz, Worschech *et al.* 2015). An impressive example of the latter is given in Figure 4.12D, where WT1-specific CD8 T-cell responses in leukemia patients were monitored up to 5 years Post-HSCT.

Finally, it is worth mentioning that resetting of circulating T-cells to a tissue-like state before the first *in-vitro* contact with antigen avoids the loss of those antigen-specific cells which depend on pre-sensitization for an antigen-specific response. The inclusion of these cells also in long-term expanded CD8 T-cell lines and clones may improve their usefulness for analytic and therapeutic purposes by harnessing CTL which could contribute to the effectiveness of passive cellular vaccination against infectious agents and tumors.

## List of figures

- Figure 1.1: **TCR/CD3-mediated proximal signaling.** Upon TCR complex engagement a phosphorylation cascade is induced (Watanabe 2012). © Journal of Clinical & Cellular Immunology .....13
- Figure 1.2: **Model: MHC/(self-peptide) recognition enhances sensitivity of T-cells to foreign antigens.** In secondary lymphoid organs low- or intermediate affinity MHC/(self-peptide) recognition of naive T-cells on steady state DCs results in tonic TCR signaling and a pre-activated T-cell status that makes cells sensitive to MHC/foreign-peptide recognition on DCs activated by inflammatory stimuli. Modified from (Garbi, Hammerling et al. 2010).....15
- Figure 1.3: **Soluble TGN1412/TAB08-mediated T-cell responses.** (Left) Tonic TCR signals are induced by TCR-HLA/self-peptide complexes between T-cells and professional APCs, mainly DCs, and are amplified by the co-stimulatory signal at the level of the SLP76 signalosome in lymphoid tissue. (Middle) This phenomenon does not occur in freshly isolated PBMC as cell-cell contacts are missing in the circulation. (Right) T-cells in high-density (HD) precultured PBMC receive tonic TCR signals by actively scanning for HLA/self-peptide complexes on monocytes which mature during short term culture. Modified from Hünig 2011 .....17
- Figure 4.1: **Enhanced anti-viral IFN- $\gamma$  response in HD precultured human CD8 memory T-cells by HD preculture of PBMCs.** (A) Representative IFN- $\gamma$  ELISPOT assay of fresh or HD precultured PBMCs. Cytokine release after stimulation with 1 $\mu$ g/ml CD28 superagonist TAB08 (previously: TGN1412) and 0.1  $\mu$ g/ml PepMix™ CEF standard was assessed after 16 hours. Unstimulated fresh and HD precultured PBMCs were used as negative controls. (B) Intracellular IFN- $\gamma$  staining of fresh and HD precultured PBMCs after stimulation with 0.1  $\mu$ g/ml PepMix™ CEF standard for 16 hours. Gating was performed on (left) viable lymphocytes and (right) CD8 T-cells. Experiments were repeated  $\geq 3$  times. ....38
- Figure 4.2: **Time and density-dependence of the PBMC preculture effect on virus-directed CD8 T-cell responses.** CD8 T-cell responses of a healthy donor to 0.1  $\mu$ g/ml of the PepMix™ CEF standard were obtained by IFN- $\gamma$  ELISPOT assay. PBMC preculture conditions were tested by varying time and cell densities. Unstimulated cells from all preculture conditions tested did not release IFN- $\gamma$ . Data represent mean  $\pm$  SD for triplicate samples. Experiment was repeated  $\geq 3$  times. ....40
- Figure 4.3: **Functional maturation of CD8 T-cells and monocytes contributes to the HD preculture effect.** CD8 T-cells and monocytes were purified from fresh (F) and

precultured (P) PBMCs of the same donor by magnetic sorting (MACS) and co-cultured under standard conditions at a 1:1 ratio in the presence of either 0.1  $\mu\text{g}/\text{ml}$  PepMix™ CEF standard or 1  $\mu\text{g}/\text{ml}$  OKT3, and were assessed by IFN- $\gamma$  ELISPOT 16 hours after stimulation. Data represent mean  $\pm$  SD for triplicate samples for one representative donor out of three. ....41

Figure 4.4: **RESTORE effect is not due to a reduction in Treg activity.** (A, Left) Similar frequencies of regulatory T-cells in unstimulated fresh and precultured PBMCs of a representative healthy donor. Intracellular staining and flow cytometry of regulatory T-cells; Gating of Foxp3<sup>+</sup>CD25<sup>+</sup> cells was performed on viable CD4 T-cells. (Right) Regulatory T-cells were depleted from fresh or precultured PBMCs by magnetically labeling CD25 positive cells. (B) Similar increase in virus-specific CD8 T-cell responses upon HD preculture of total and CD25-depleted PBMCs. Cells from Panel A were stimulated with titrated PepMix™ CEF standard in IFN- $\gamma$  ELISPOT assays. Responses of fresh/ CD25 depleted fresh PBMCs and precultured/ CD25 depleted precultured PBMCs, respectively were compared by an unpaired t test: n.s.; Significantly enhanced IFN- $\gamma$  secretion of CD8 T-cells upon HD preculture of total or CD25 depleted PBMCs relative to fresh or CD25 depleted fresh PBMCs were detected after stimulation with 0.033  $\mu\text{g}/\text{ml}$  (unpaired t test: \*\* P <.005), 0.1  $\mu\text{g}/\text{ml}$  (\* P <.05) and 0.3  $\mu\text{g}/\text{ml}$  (\*\* P <.005) of the PepMix™ CEF standard. Data represent mean  $\pm$  SD for triplicate samples. Experiment was repeated 3 times. ....43

Figure 4.5: **HD preculture prepares T-cells to better respond to antigen, but does not increase the frequency of antigen-specific cells.** Similar frequencies of PP65\_HCMV 495-503-specific T-cells were detected in unstimulated Fresh, HD and LD precultured PBMCs by flow cytometry upon pentamer staining. An HLA-A0201-restricted pentamer was used as a negative control. Gating was performed on viable CD8 T-cells. Experiment was repeated with 2 HLA-A0201 positive healthy donors. ....44

Figure 4.6: **Enhanced sensitivity of human CD8 T-cells to defined viral antigens by HD preculture of PBMCs.** (A) IFN- $\gamma$  responses of CD8 T-cells from fresh or precultured PBMCs from a representative healthy donor were directly compared by ELISPOT assay after stimulation with titrated PepMix™ Influenza A. Unpaired t test: \*\*\* P <.0005; \*\*\*\* P <.0001; (B) Compiled data from 6 healthy donors tested as in Figure 2A. Data represent the mean fold-increase in IFN- $\gamma$  responses of CD8 T-cells from precultured PBMCs relative to CD8 T-cells from fresh PBMCs after stimulation with the PepMix™ Influenza A. Mann-Whitney test: \* P <.05; \*\* P <.01. Data represent median with interquartile range. (C) IFN- $\gamma$  responses of CD8 T-cells from fresh or precultured PBMCs from a CMV-seropositive healthy donor after stimulation with titrated PP65\_HCMV 495-503. (D) Compiled data from 5 donors tested as in Figure 2C. Data presentation as in Figure 2B. Fold increase could not be calculated for the concentrations 0.0001 and 0.001  $\mu\text{g}/\text{ml}$  where no response was detectable in fresh PBMCs. (E) CD8 T-

cell responses in fresh and precultured PBMCs to 2 µg/ml of three different adenovirus-derived peptides. (F) Compiled data from 7 HLA-A01 (HEX\_ADE02 901-910), -A02 (E1A\_ADE02 19-27) or -A24 (HEX\_ADE02 37-45) positive healthy individuals. Data presentation as in Figure 2B.....46

Figure 4.7: **Enhanced recall responses of HD precultured CD8 T-cells to virus-derived peptide pools.** (A) IFN-γ ELISPOT responses of fresh or precultured PBMCs of one representative healthy donor to titrated amounts of the HLA-class I restricted PepMix™ CEF standard. (B) Response of the same donor as shown in Figure 3A to titrated amounts of the negative control pool PepMix™ Human Actin. Unpaired t test: \* P <.05; \*\* P <.005; \*\*\* P <.0005. Data represent mean ± SD for triplicate samples. (C, D) Identification of memory CD8 T-cells as source of for IFN-γ production by intracellular cytokine staining of fresh and precultured PBMCs of one representative donor that is different from Figure 3A, B. Results are shown as percentage of IFN-γ-positive cells among CD8<sup>+</sup>CD45R0<sup>+</sup> cells and CD8<sup>+</sup>CD45R0<sup>-</sup> cells. (E) Compiled data from 22 healthy donors tested as in Figure 2A and presented as in Figure 2B. ....47

Figure 4.8: **Phenotyping of HD precultured PBMCs, LPMCs and TMCs.** Unstimulated mononuclear cells (MCs) from the blood (PBMCs), lamina propria of the small intestine (LPMCs) or tonsils (TMCs) were stained with the given antibodies to determine their frequency of naïve (CD62L<sup>+</sup> CD45R0<sup>-</sup>), effector (CD62L<sup>-</sup> CD45R0<sup>-</sup>), central memory (CD62L<sup>+</sup>CD45R0<sup>+</sup>) and effector memory (CD62L<sup>-</sup>CD45R0<sup>+</sup>) CD4 or CD8 T-cells within living MCs. Results from HD precultured PBMCs and LPMCs originate from the same representative obese patient without type 2 diabetes. Results from TMCs are of another representative tonsil and blood donor. Experiment was repeated ≥ 8 individuals. ....49

Figure 4.9: **IFN-γ release in HD precultured PBMCs and LPMCs in response to TAB08.** (A) Representative IFN-γ ELISPOT assay of fresh or precultured PBMCs as well as LPMCs of one patient with morbid obesity. Cytokine release after stimulation with 1 µg/ml TAB08 (previously: TGN1412) or 1 µg/ml OKT3 was assessed after 16 hours. Unstimulated MCs were used as negative controls. (B) IFN-γ responses to titrated TAB08 were detected by IFN-γ ELISPOT assays, and correlated to the frequencies of CD4 T-cells in MCs from blood or lamina propria as determined by flow cytometry. Statistical comparison of CD4 T-cell responses from LPMCs with those of fresh or HD precultured PBMCs. Unpaired t test: \*\*\*\* P ≤ 0.0001, \*\*\* P ≤ 0.0005, \* P ≤ 0.05. Data represent mean ± SD for triplicate samples of one representative patient out of five. ....50

Figure 4.10: **Loss of T-cell reactivity to TAB08 and SEB in LD cultures of LPMCs.** LPMCs were either kept on ice or dispersed in suspension (1x10<sup>6</sup> cells/ ml) for 2 hours at 37 °C (5 % CO<sub>2</sub>) to simulate tissue exit. IFN-γ responses of T-cells to titrated amounts of TAB08 (previously: TGN1412) and 0.25 µg/ml SEB were analyzed by an IFN-γ secretion assay after stimulation for 16 hours. The IFN-γ secretion assay was combined with surface

staining for (A) CD4 and (B) CD8 T-cells in order to determine the subtype of IFN- $\gamma$  cells. Unpaired t test: \*\*\* P <.0005, \*\* P <.005. Data represent mean  $\pm$  SD for triplicate samples of one representative patient with morbid obesity out of two.....51

Figure 4.11: **Loss of virus-specific CD8 T-cell reactivity in dispersed TMCs.** (A) Tonsillar mononuclear cells (TMCs) were prepared from uninfected fresh human tonsils and were either kept on ice or dispersed in suspension ( $1 \times 10^6$  cells/ ml) for 2 hours at 37 °C (5 % CO<sub>2</sub>) to simulate tissue exit. IFN- $\gamma$  responses to titrated amounts of the HLA-class I restricted PepMix™ CEF standard were analyzed by an IFN- $\gamma$  ELISPOT assay, and the frequency of CD8 memory T-cells in TMC was determined by flow cytometry. Unpaired t test: \* P <.05. (B) Virus-specific IFN- $\gamma$  responses to 0.04 or 0.4  $\mu$ g/ml of the peptide pool were compared between CD8 memory T-cells from TMCs with those of fresh and HD precultured PBMCs of the same individual as presented in Figure 4A. Similar results were obtained after repetition of the experiment. 2way ANOVA \*\*\* P <.0005. Data represent mean  $\pm$  SD for triplicate samples.....53

Figure 4.12: **HD preculture enhances the recall responses of PBMCs to WT1-derived antigens.** (A, B) IFN- $\gamma$  T-cell responses from fresh or precultured PBMCs of one representative HLA-A0201 positive HSCT patient to titrated amounts of the peptide WT1\_HUMAN 126-134 or WT1\_HUMAN 356-364, respectively. Unpaired t test: \*\*\* P <.0005. Data represent mean  $\pm$  SD for triplicate samples. The experiment presented in Figure 5A was repeated for two different patients. (C) Compiled data from Figure 4B from 11 patients. Average time between stem cell transplantation and sampling: 814 days; from 166 to 2372 days. Data are presented as in Figure 2B. (D) Improved monitoring of anti-WT1-directed T-cell responses from an HLA-A0201 positive patient 4 months, 1 year and 5 years after HSCT upon HD preculture of PBMCs. Unpaired t test: \*\* P <.005; \*\*\* P <.0005; \*\*\*\* P <.0001. Data represent mean  $\pm$  SD for triplicate samples. ....54

Figure 4.13: **Specificity controls of the T-cell responses presented in Figure 4.12 (WT1\_HUMAN 126-134/ HLA-A0201, WT1\_HUMAN 356-364/ HLA-A0201).** (A, B) PBMC of HIV sero-negative hematopoietic stem cell transplanted patients that show WT1 dependent IFN- $\gamma$  releases to WT1\_HUMAN 126-134 (Figure 4.12A) or WT1\_HUMAN 356-364 (Figure 4.12B) were also treated in IFN- $\gamma$  ELISPOT assays with titrated amounts of the irrelevant HLA-A0201-restricted peptide HIV-1 pol 476-484. (C) Nonspecific effects of WT1 peptide stimulation were excluded by treating PBMCs of an HLA-A0201 negative healthy donor with titrated WT1\_HUMAN 126-134 or 356-364. No unspecific responses were detected. Unpaired t test: n.s.; The RESTORE effect was demonstrated by TAB08 responses, exclusively in HD precultured PBMCs, but not in fresh PBMCs of all tested patients (A, B) and healthy donors (C). Data represent mean  $\pm$  SD for triplicate samples.....55

Figure 4.14: **The RESTORE effect is independent of cryopreservation.** PBMCs of a representative leukemia patient were frozen, thawed and tested with or without the HD



preculture step. IFN- $\gamma$  secretion of cryoconserved and non-cryoconserved fresh or HD precultured samples were compared by an unpaired t test: n.s.; The RESTORE effect was significantly analyzed by 2way ANOVA. Experiment was repeated  $\geq 3$  times.....56

Figure 4.15: **HD preculture of PBMCs allows generation of CD8 T-cell lines with an improved representation of clones responding to low antigen concentrations.** (A, Left) IFN- $\gamma$  responses of CD8 T-cells from fresh or precultured PBMCs of one HLA-A0201 positive patient to titrated amounts of the peptide WT1\_HUMAN 356-364 before expansion. (Right) Fresh or precultured PBMCs of the same patient were stimulated with 1  $\mu\text{g}/\text{ml}$  of the peptide WT1\_HUMAN 356-364 in a final cell density of  $2 \times 10^6$  cells/ml and were expanded in the presence of IL-2, IL-7 and IL-15 for 2 weeks. After expansion, cells were restimulated with titrated amounts of the peptide WT1\_HUMAN 356-364 or the control pool Human Actin in IFN- $\gamma$  ELISPOT plates for 16 hours. (B, Left) IFN- $\gamma$  responses of CD8 T-cells from fresh or precultured PBMCs of one representative healthy donor to titrated amounts of the HLA-class I restricted PepMix™ CEF standard and the control pool Human Actin before expansion. Fresh or precultured PBMCs of the same donor were stimulated with 0.1  $\mu\text{g}/\text{ml}$  of (middle) the PepMix™ CEF standard or the PepMix™ Human Actin (right) and were expanded under the same conditions as presented in Figure 4.15A. After expansion, virus-specific CD8 T-cells were restimulated with titrated amounts of the PepMix™ CEF standard or the control pool Human Actin in IFN- $\gamma$  ELISPOT plates for 16 hours, respectively. Unpaired t test: \* P <.05; \*\* P <.005; \*\*\* P <.0005; \*\*\*\* P <.0001. Data represent mean  $\pm$  SD for triplicate samples. Experiments were repeated 4 times.....58

Figure 4.16: **CD137 expression on CD8 T-cells from fresh or precultured PBMCs after WT1-specific T-cell expansion.** Fresh or precultured PBMCs of the same HLA-A0201-positive AML patient were simultaneously stimulated with 1  $\mu\text{g}/\text{ml}$  of the peptide WT1\_HUMAN 356-364 in a final cell density of  $2 \times 10^6$  cells/ml and were expanded in the presence of IL-2, IL-7 and IL-15 for 2 weeks. After expansion, cells were restimulated with 10  $\mu\text{g}/\text{ml}$  WT1\_HUMAN 356-364 for 16 hours and stained for CD3, CD8 and CD137. Gating was performed on viable CD8 T-cells. ....59

Figure 4.17: **HD preculture of PBMCs affects TCR signaling of CD8 T-cells.** (A) Total tyrosine phosphorylation patterns were compared by Western blotting between freshly isolated CD8 T-cells and monocytes (1:1, F) and HD precultured co-cultured CD8 T-cells and monocytes (1:1,P) of one representative donor. After cell lysis, proteins were separated under reducing conditions using a 15% polyacrylamide gel. Membranes were probed with 4G10 antibody (anti-pTyr). (B) Phosphorylation of proximal TCR signaling components was compared between CD8 T-cells from fresh and precultured PBMCs. Membranes were probed with antibodies against CD3 $\zeta$  p-Y142, CD3 $\zeta$ , Src p-Y394, Lck, ZAP-70 p-Y319/ Syk p-Y352 and ZAP-70 as indicated. ERK1/2 served as a loading control.

Experiment was repeated  $\geq 3$  times with the exceptions that membranes were probed with antibody against ZAP-70 p-Y319/ Syk p-Y352 only once. ....60

Figure 4.18: **Gene expression analysis of CD8 memory T-cells from fresh and HD precultured PBMCs and tonsils.**

Total RNA was prepared for microarray analysis out of flow cytometry sorted CD8 memory T-cells (CD8<sup>+</sup>CD45R0<sup>+</sup>) from fresh (F) and HD precultured (P) PBMCs of three healthy individuals (1-3) and from CD8 memory T-cells (CD8<sup>+</sup>CD45R0<sup>+</sup>) from fresh PBMCs and TMCs (T) of three children undergoing tonsillectomy (4-6). (A) Agglomerative hierarchical clustering of global gene expression profiles. The cumulated length of vertical lines connecting two samples is indicative for their similarity. (B) Heatmap of differentially expressed genes showing scaled expression values, where dark blue corresponds to the lowest expression and dark red to the highest expression level. ....62

Figure 4.19: **Comparison of the expression profile of CD8 memory T-cells from HD precultured PBMCs and TMCs.**

(A) Radar plot displaying gene set enrichment results from CD8 memory T-cells (CD8<sup>+</sup>CD45R0<sup>+</sup>) from HD precultured PBMCs versus fresh PBMCs (dark grey area) and those from TMCs versus fresh PBMCs (light grey area). Of the 13 functional clusters / pathways shown, each displayed a globally significant (false discovery rate [FDR] <.05) enrichment in at least one comparison. Enrichment FDRs were transformed to  $-\log_{10}(\text{FDR})$  and displayed along the axis for each pathway; FDR <.05 corresponds to  $-\log_{10}(\text{FDR}) > 1.3$ . (B) Heatmap of genes that display concordant expression changes between CD8 memory T-cells (CD8<sup>+</sup>CD45R0<sup>+</sup>) from HD precultured PBMCs and from TMCs relative to fresh PBMCs. ....63

Figure 4.20: **HD preculture of PBMCs affects metabolism of CD8 memory T-cells.**

Differentially expressed glycolysis pathway genes from a comparison of CD8 memory T-cells (CD8<sup>+</sup>CD45R0<sup>+</sup>) from fresh and HD precultured PBMCs are shown (A) in a heatmap of scaled expression values and (B) in a KEGG pathway map with color coded log fold changes. (C) Venn Diagram indicating high concordance of changes in glycolysis-related gene expression changes between CD8 memory T-cells (CD8<sup>+</sup>CD45R0<sup>+</sup>) from fresh PBMCs (presented in 7A and 7B) and pan T-cells from LD precultured PBMCs...64

Figure 4.21: **GLUT1 expression in CD8 memory T-cells from fresh and HD precultured PBMCs.**

Unstimulated fresh (F) and HD precultured (P) PBMCs were stained for the glucose transporter 1 (GLUT1). Expression values are given as  $\Delta\text{MFI}$ : MFI (GLUT1) – MFI (Isotype control). Gating was performed on viable CD8 memory T-cells (CD8<sup>+</sup>CD45R0<sup>+</sup>). (A) HD precultured PBMCs were additionally stimulated with 1  $\mu\text{g}/\text{ml}$  TAB08. (B) PBMCs were additionally precultured at a low cell density (LD).....66

Figure 4.22: **Actin cell adhesion and mobility of CD8 memory T-cells.**

Color-coded log FC of differentially expressed leukocyte transendothelial migration pathway genes from the comparison of CD8 memory T-cells (CD8<sup>+</sup>CD45R0<sup>+</sup>) from fresh and HD precultured PBMCs are shown in a KEGG pathway map. ....67

Figure 4.23: **Integrin expression of CD8 memory T-cells from fresh and precultured PBMCs.**

Unstimulated fresh (F) and HD precultured (P) PBMCs of one representative healthy donor were surface stained to detect the expression of the integrins CD11b, CD18, CD49d, CD29, and CD11a within CD8 memory T-cells (CD8<sup>+</sup>CD45R0<sup>+</sup>). Isotype stainings (Iso) were used as controls. Mean fluorescence intensities (MFI) are given for each staining (left column) and  $\Delta$  MFI were calculated: MFI (Integrin) – MFI (Isotype); (right column). Staining was repeated  $\geq 3$  times with similar results. ....68

Figure 5.1: **Metabolic reprogramming in T-cells controls T-cell functionality.**

Resting T-cells metabolize glucose to pyruvate, which enters the mitochondrial citrate cycle and generates reducing equivalents for fueling ATP production via OXPHOS. Activated T cells engage glycolysis, where pyruvate is fermented to lactate in the cytoplasm even when sufficient oxygen is present to utilize OXPHOS (Warburg effect, aerobic glycolysis). Although both processes generate ATP, glycolysis is less efficient in producing ATP, indicating that it might provide other advantages such as uptake and incorporation of nutrients into the biomass needed for cellular proliferation. Beside T-cell proliferation, aerobic glycolysis regulates cytokine production. The key glycolytic enzyme glyceraldehyde-3-phosphate dehydrogenase (GAPDH) controls effector cytokine production on a translational level. (Chang, Curtis et al. 2013) © Cell Press .....73

Figure 5.2: **Maturation events in blood-derived T-cells and monocytes during HD preculture.**

During HD preculture of PBMCs, monocytes improve their features as accessory cells by an enhanced expression of HLA molecules and the co-stimulatory ligand CD86. T-cells frequently interact with matured monocytes by scanning of MHC molecules that are loaded with self-peptide. Frequent TCR engagement and co-stimulation (CD28-CD86) results in tonic TCR signaling indicated by an enhanced tyrosine phosphorylation of the CD3  $\zeta$  chains and Lck. The primed TCR signaling machinery of “restored” T-cells in combination with increased glycolysis and lactic acid fermentation (referred to as Warburg effect or aerobic glycolysis) which was observed only on the RNA level, but was not on the cellular level until now, lowers the threshold for full T-cell activation. ....75

## List of abbreviations and acronyms

°C	centigrade
µg	microgram
µl	microliter
µm	micrometer
Ab(s)	antibody (ies)
ACTG1	actin, gamma 1
AdV	adenovirus
ALL	acute lymphoblastic leukemia
AML	acute myeloid leukemia
AP-1	activation protein-1
APC	antigen presenting cell
B-cell(s)	bone marrow-derived cell(s)
BCIP	5-bromo-4-chloro-3'-indolyphosphate p-toluidine salt
BCL2	B-cell lymphoma 2
BSA	bovine serum albumin
BSS	buffered salt solution
CD	cluster of differentiation
CDR	complementarity-determining region
CFSE	carboxyfluorescein succinimidyl ester
CO <sub>2</sub>	carbon dioxide
CTL	cytotoxic lymphocytes
DC(s)	dendritic cell(s)
DMSO	dimethyl sulfoxide
DT	diphtheria toxin
DTT	dithiothreitol
<i>e.g.</i>	<i>exempli gratia</i>
EBV	Epstein-Barr virus
ECAR	extracellular acidification rate
EDTA	ethylenediaminetetraacetic acid
ELISPOT	enzyme-linked ImmunoSpot
<i>et al.</i>	<i>et alterii</i>
F	from fresh PBMCs
FACS	fluorescence activated cell sorting
FCS	fetal calf serum
FDR	false discovery rate

---

FTTC	fluorescein-5-isothiocyanat
GAPDH	glyceraldehyde-3-phosphate dehydrogenase
GEO	Gene expression Omnibus
GLUT1	glucose transporter 1
GVL	graft versus leukemia
HCMV	human cytomegalovirus
HD	high density
HIV	human immunodeficiency virus
HLA	human leukocyte antigen
HPLC	high-performance liquid chromatography
HRP	horseradish-peroxidase
HSCT	hematopoietic stem cell transplantation
ICAM-1	intracellular adhesion molecule-1
IFN- $\gamma$	interferon-gamma
Ig	immunoglobulin
IL	interleukin
IQR	interquartile range
ITAM(s)	immunoreceptor-tyrosine-based activation motif(s)
ITGA6	integrin, alpha 6
ITGAM	integrin, alpha M
Itk	IL2-inducible T cell kinase
JAM2	junctional adhesion molecule B
kDa	kilodalton(s)
LAT	linker for the activation of T-cells
Lck	lymphocyte-specific protein tyrosine kinase
LD	low density
LDHA	lactate dehydrogenase A
LFA-1	leukocyte function-associated antigen-1
LIMMA	Linear Models of Microarray Analysis
LN(s)	lymph node(s)
LPMC(s)	lamina propria nuclear cell(s)
LRS-C	leukocoreduction system chamber
mAb(s)	monoclonal antibody (ies)
MB	Microbead
MC(s)	mononuclear cell(s)
MFI	mean fluorescence intensity
mg	milligram
MHC	major histocompatibility complex
ml	milliliter

---

mm	millimeter
MOG	myelin oligodendrocyte glycoprotein
MP1	membrane protein 1
NAD <sup>+</sup>	nicotinamide adenine dinucleotide
NBT	nitro-blue tetrazolium chloride
NFAT	nuclear factor of activated T-cells
NF- $\kappa$ B	nuclear factor $\kappa$ B
NP	nucleocapsid protein
OCR	oxygen consumption rate
OKT3	muromonab-CD3
OVA	ovalbumin
OXPHOS	oxidative phosphorylation
P	from HD precultured PBMCs
PAMP(s)	pathogen-associated molecular pattern(s)
PBMCs	peripheral mononuclear cell(s)
PBS	phosphate buffered saline
PCC	pigeon cytochrome c
PE	phycoerythrin
PFKFB3	6-phosphofructo-2-kinase/fructose-2,6-biphosphatase
pg	picogram
PP1	protein phosphatase 1
PRR(s)	pattern recognition receptor(s)
PVDF	polyvinylidene fluoride
PXN	paxillin
RESTORE	RESetting T-cells to Original REactivity
RNA	ribonucleic acid
rpm	rotations per minute
RT	room temperature
SAMHD1	SAM domain and HD domain-containing protein 1
SDS	sodium dodecyl sulfate
SEA	staphylococcal enterotoxin A
SEB	staphylococcal enterotoxin B
SLP-76	Src homology 2 domain-containing leukocyte phosphoprotein of 76 kDa
SMAC	supra-molecular activation cluster
SOP	standard operation procedure
Streptavidin-AP	streptavidin-alkaline phosphatase
T	from TMCs
TCA	tricarboxylic acid
T-cell(s)	thymus-derived cell(s)

---

TCR	T cell receptor
TMC(s)	tonsillar mononuclear cell(s)
Treg(s)	regulatory T-cell(s)
VCAM-1	vascular cell adhesion protein-1
VCL	vinculin
VLA-4	very late antigen-4
WT1	Wilms tumor gene 1
ZAP-70	$\zeta$ -chain associated protein kinase 70 kDa

## References

Adair, J. R., D. S. Athwal, M. W. Bodmer, S. M. Bright, A. M. Collins, V. L. Pulito, P. E. Rao, R. Reedman, A. L. Rothermel, D. Xu and et al. (1994). "Humanization of the murine anti-human CD3 monoclonal antibody OKT3." Hum Antibodies Hybridomas **5**(1-2): 41-47.

Afonso, G., M. Scotto, A. Renand, J. Arvastsson, D. Vassilieff, C. M. Cilio and R. Mallone (2010). "Critical parameters in blood processing for T-cell assays: validation on ELISpot and tetramer platforms." J Immunol Methods **359**(1-2): 28-36.

Andersen, M. H., I. M. Svane, P. Kvistborg, O. J. Nielsen, E. Balslev, S. Reker, J. C. Becker and P. T. Straten (2005). "Immunogenicity of Bcl-2 in patients with cancer." Blood **105**(2): 728-734.

Bodmer, J. G., S. G. Marsh, E. D. Albert, W. F. Bodmer, B. Dupont, H. A. Erlich, B. Mach, W. R. Mayr, P. Parham and T. Sasazuki (1994). "Nomenclature for factors of the HLA system, 1994." Tissue Antigens **44**(1): 1-18.

Bull, D. M. and M. A. Bookman (1977). "Isolation and functional characterization of human intestinal mucosal lymphoid cells." J Clin Invest **59**(5): 966-974.

Bull, M., D. Lee, J. Stucky, Y. L. Chiu, A. Rubin, H. Horton and M. J. McElrath (2007). "Defining blood processing parameters for optimal detection of cryopreserved antigen-specific responses for HIV vaccine trials." J Immunol Methods **322**(1-2): 57-69.

Cambier, J. C. (1995). "Antigen and Fc receptor signaling. The awesome power of the immunoreceptor tyrosine-based activation motif (ITAM)." J Immunol **155**(7): 3281-3285.

Chakrabarti, R., C. Y. Jung, T. P. Lee, H. Liu and B. K. Mookerjee (1994). "Changes in glucose transport and transporter isoforms during the activation of human peripheral blood lymphocytes by phytohemagglutinin." J Immunol **152**(6): 2660-2668.

Cham, C. M. and T. F. Gajewski (2005). "Glucose availability regulates IFN-gamma production and p70S6 kinase activation in CD8+ effector T cells." J Immunol **174**(8): 4670-4677.

Chang, C. H., J. D. Curtis, L. B. Maggi, Jr., B. Faubert, A. V. Villarino, D. O'Sullivan, S. C. Huang, G. J. van der Windt, J. Blagih, J. Qiu, J. D. Weber, E. J. Pearce, R. G. Jones and E. L. Pearce (2013). "Posttranscriptional control of T cell effector function by aerobic glycolysis." Cell **153**(6): 1239-1251.

Cheng, S. C., J. Quintin, R. A. Cramer, K. M. Shephardson, S. Saeed, V. Kumar, E. J. Giamarellos-Bourboulis, J. H. Martens, N. A. Rao, A. Aghajani-Refah, G. R. Manjeri, Y. Li, D. C. Ifrim, R. J. Arts, B. M. van der Veer, P. M. Deen, C. Logie, L. A. O'Neill, P. Willems, F. L. van de Veerdonk, J. W. van der Meer, A. Ng, L. A. Joosten, C. Wijmenga, H. G. Stunnenberg, R. J. Xavier and M. G. Netea (2014). "mTOR- and HIF-1alpha-mediated aerobic glycolysis as metabolic basis for trained immunity." Science **345**(6204): 1250684.

Conche, C., G. Boulla, A. Trautmann and C. Randriamampita (2009). "T cell adhesion primes antigen receptor-induced calcium responses through a transient rise in adenosine 3',5'-cyclic monophosphate." Immunity **30**(1): 33-43.



- Dana, N., D. M. Fathallah and M. A. Arnaout (1991). "Expression of a soluble and functional form of the human beta 2 integrin CD11b/CD18." Proc Natl Acad Sci U S A **88**(8): 3106-3110.
- Delon, J. and R. N. Germain (2000). "Information transfer at the immunological synapse." Curr Biol **10**(24): R923-933.
- Dennehy, K. M., F. Elias, S. Y. Na, K. D. Fischer, T. Hunig and F. Luhder (2007). "Mitogenic CD28 signals require the exchange factor Vav1 to enhance TCR signaling at the SLP-76-Vav-Itk signalosome." J Immunol **178**(3): 1363-1371.
- Di Bartolo, V., D. Mege, V. Germain, M. Pelosi, E. Dufour, F. Michel, G. Magistrelli, A. Isacchi and O. Acuto (1999). "Tyrosine 319, a newly identified phosphorylation site of ZAP-70, plays a critical role in T cell antigen receptor signaling." J Biol Chem **274**(10): 6285-6294.
- Dietz, A. B., P. A. Bulur, R. L. Emery, J. L. Winters, D. E. Epps, A. C. Zubair and S. Vuk-Pavlovic (2006). "A novel source of viable peripheral blood mononuclear cells from leukoreduction system chambers." Transfusion **46**(12): 2083-2089.
- Duff, G. W. (2006). "EXpert Scientific Group on PHase ONE Clinical Trials Final Report. Norwich, UK: Stationary Office."
- Farber, D. L., N. A. Yudanin and N. P. Restifo (2014). "Human memory T cells: generation, compartmentalization and homeostasis." Nat Rev Immunol **14**(1): 24-35.
- Filbert, H., S. Attig, N. Bidmon, B. Y. Renard, S. Janetzki, U. Sahin, M. J. Welters, C. Ottensmeier, S. H. van der Burg, C. Gouttefangeas and C. M. Britten (2013). "Serum-free freezing media support high cell quality and excellent ELISPOT assay performance across a wide variety of different assay protocols." Cancer Immunol Immunother **62**(4): 615-627.
- Fischer, U. B., E. L. Jacovetty, R. B. Medeiros, B. D. Goudy, T. Zell, J. B. Swanson, E. Lorenz, Y. Shimizu, M. J. Miller, A. Khoruts and E. Ingulli (2007). "MHC class II deprivation impairs CD4 T cell motility and responsiveness to antigen-bearing dendritic cells in vivo." Proc Natl Acad Sci U S A **104**(17): 7181-7186.
- Fox, C. J., P. S. Hammerman and C. B. Thompson (2005). "Fuel feeds function: energy metabolism and the T-cell response." Nat Rev Immunol **5**(11): 844-852.
- Frauwirth, K. A., J. L. Riley, M. H. Harris, R. V. Parry, J. C. Rathmell, D. R. Plas, R. L. Elstrom, C. H. June and C. B. Thompson (2002). "The CD28 signaling pathway regulates glucose metabolism." Immunity **16**(6): 769-777.
- Friedl, P. and B. Weigelin (2008). "Interstitial leukocyte migration and immune function." Nat Immunol **9**(9): 960-969.
- Fuji S., W. J., Kapp M., Baumeister E., Kapp K., Bumm T., Kashiwagi-Fuji H.,Dagvadorj N.,Rammensee H.G., Stevanovic S., Einsele H., Hünig T., Deuretzbacher A., Grigoleit G.U. (2015). "Unexpected high frequency, high avidity, and potent cytotoxic activity of WT1 and Bcl-2-specific CD8+ and CD4+ T cell subsets of healthy donors and alloSCT recipients." in preparation.
- Garbi, N., G. J. Hammerling, H. C. Probst and M. van den Broek (2010). "Tonic T cell signalling and T cell tolerance as opposite effects of self-recognition on dendritic cells." Curr Opin Immunol **22**(5): 601-608.

- Garbi, N. and T. Kreutzberg (2012). "Dendritic cells enhance the antigen sensitivity of T cells." Front Immunol **3**: 389.
- Garcia, K. C., J. J. Adams, D. Feng and L. K. Ely (2009). "The molecular basis of TCR germline bias for MHC is surprisingly simple." Nat Immunol **10**(2): 143-147.
- Germain, R. N. and I. Stefanova (1999). "The dynamics of T cell receptor signaling: complex orchestration and the key roles of tempo and cooperation." Annu Rev Immunol **17**: 467-522.
- Geyeregger, R., C. Freimuller, S. Stevanovic, J. Stemberger, G. Mester, J. Dmytrus, T. Lion, H. G. Rammensee, G. Fischer, B. Eiz-Vesper, A. Lawitschka, S. Matthes and G. Fritsch (2013). "Short-term in-vitro expansion improves monitoring and allows affordable generation of virus-specific T-cells against several viruses for a broad clinical application." PLoS One **8**(4): e59592.
- Grakoui, A., S. K. Bromley, C. Sumen, M. M. Davis, A. S. Shaw, P. M. Allen and M. L. Dustin (1999). "The immunological synapse: a molecular machine controlling T cell activation." Science **285**(5425): 221-227.
- Gubser, P. M., G. R. Bantug, L. Razik, M. Fischer, S. Dimeloe, G. Hoenger, B. Durovic, A. Jauch and C. Hess (2013). "Rapid effector function of memory CD8+ T cells requires an immediate-early glycolytic switch." Nat Immunol **14**(10): 1064-1072.
- Hochweller, K., G. H. Wabnitz, Y. Samstag, J. Suffner, G. J. Hammerling and N. Garbi (2010). "Dendritic cells control T cell tonic signaling required for responsiveness to foreign antigen." Proc Natl Acad Sci U S A **107**(13): 5931-5936.
- Huang, D. W., B. T. Sherman, Q. Tan, J. Kir, D. Liu, D. Bryant, Y. Guo, R. Stephens, M. W. Baseler, H. C. Lane and R. A. Lempicki (2007). "DAVID Bioinformatics Resources: expanded annotation database and novel algorithms to better extract biology from large gene lists." Nucleic Acids Res **35**(Web Server issue): W169-175.
- Huber, W., A. von Heydebreck, H. Sultmann, A. Poustka and M. Vingron (2002). "Variance stabilization applied to microarray data calibration and to the quantification of differential expression." Bioinformatics **18 Suppl 1**: S96-104.
- Hussain, K., C. E. Hargreaves, A. Roghianian, R. J. Oldham, H. T. Chan, C. I. Mockridge, F. Chowdhury, B. Frendeus, K. S. Harper, J. C. Strefford, M. S. Cragg, M. J. Glennie, A. P. Williams and R. R. French (2015). "Upregulation of FcγRIIb on monocytes is necessary to promote the superagonist activity of TGN1412." Blood **125**(1): 102-110.
- Kersh, E. N., A. S. Shaw and P. M. Allen (1998). "Fidelity of T cell activation through multistep T cell receptor zeta phosphorylation." Science **281**(5376): 572-575.
- Koyasu, S., D. J. McConkey, L. K. Clayton, S. Abraham, B. Yandava, T. Katagiri, P. Moingeon, T. Yamamoto and E. L. Reinherz (1992). "Phosphorylation of multiple CD3 zeta tyrosine residues leads to formation of pp21 in vitro and in vivo. Structural changes upon T cell receptor stimulation." J Biol Chem **267**(5): 3375-3381.
- Krawczyk, C. M., T. Holowka, J. Sun, J. Blagih, E. Amiel, R. J. DeBerardinis, J. R. Cross, E. Jung, C. B. Thompson, R. G. Jones and E. J. Pearce (2010). "Toll-like receptor-induced changes in glycolytic metabolism regulate dendritic cell activation." Blood **115**(23): 4742-4749.

- Kumari, S., S. Curado, V. Mayya and M. L. Dustin (2014). "T cell antigen receptor activation and actin cytoskeleton remodeling." *Biochim Biophys Acta* **1838**(2): 546-556.
- Kutscher, S., C. J. Dembek, S. Deckert, C. Russo, N. Korber, J. R. Bogner, F. Geisler, A. Umgelter, M. Neuenhahn, J. Albrecht, A. Cosma, U. Protzer and T. Bauer (2013). "Overnight resting of PBMC changes functional signatures of antigen specific T- cell responses: impact for immune monitoring within clinical trials." *PLoS One* **8**(10): e76215.
- Lee, M., J. N. Mandl, R. N. Germain and A. J. Yates (2012). "The race for the prize: T-cell trafficking strategies for optimal surveillance." *Blood* **120**(7): 1432-1438.
- Li, N., W. Zhang and X. Cao (2000). "Identification of human homologue of mouse IFN-gamma induced protein from human dendritic cells." *Immunol Lett* **74**(3): 221-224.
- Lindenmann, J. (1984). "Origin of the terms 'antibody' and 'antigen'." *Scand J Immunol* **19**(4): 281-285.
- Litman, G. W., J. P. Rast and S. D. Fugmann (2010). "The origins of vertebrate adaptive immunity." *Nat Rev Immunol* **10**(8): 543-553.
- Luhder, F., Y. Huang, K. M. Dennehy, C. Guntermann, I. Muller, E. Winkler, T. Kerkau, S. Ikemizu, S. J. Davis, T. Hanke and T. Hunig (2003). "Topological requirements and signaling properties of T cell-activating, anti-CD28 antibody superagonists." *J Exp Med* **197**(8): 955-966.
- Lunt, S. Y. and M. G. Vander Heiden (2011). "Aerobic glycolysis: meeting the metabolic requirements of cell proliferation." *Annu Rev Cell Dev Biol* **27**: 441-464.
- Lutz, M., A. Worschech, M. Alb, S. Gahn, L. Bernhard, M. Schwab, S. Obermeier, H. Einsele, U. Kammerer, P. Heuschmann, E. Klinker, C. Otto and S. Mielke (2015). "Boost and loss of immune responses against tumor-associated antigens in the course of pregnancy as a model for allogeneic immunotherapy." *Blood* **125**(2): 261-272.
- Maciolek, J. A., J. A. Pasternak and H. L. Wilson (2014). "Metabolism of activated T lymphocytes." *Curr Opin Immunol* **27**: 60-74.
- Mallone, R., S. I. Mannering, B. M. Brooks-Worrell, I. Durinovic-Bello, C. M. Cilio, F. S. Wong, N. C. Schloot and I. o. D. S. T-Cell Workshop Committee (2011). "Isolation and preservation of peripheral blood mononuclear cells for analysis of islet antigen-reactive T cell responses: position statement of the T-Cell Workshop Committee of the Immunology of Diabetes Society." *Clin Exp Immunol* **163**(1): 33-49.
- McMahan, R. H. and J. E. Slansky (2007). "Mobilizing the low-avidity T cell repertoire to kill tumors." *Semin Cancer Biol* **17**(4): 317-329.
- McNeela, E. A. and K. H. Mills (2001). "Manipulating the immune system: humoral versus cell-mediated immunity." *Adv Drug Deliv Rev* **51**(1-3): 43-54.
- Mogensen, T. H. (2009). "Pathogen recognition and inflammatory signaling in innate immune defenses." *Clin Microbiol Rev* **22**(2): 240-273, Table of Contents.
- Molina, T. J., K. Kishihara, D. P. Siderovski, W. van Ewijk, A. Narendran, E. Timms, A. Wakeham, C. J. Paige, K. U. Hartmann, A. Veillette and et al. (1992). "Profound block in thymocyte development in mice lacking p56lck." *Nature* **357**(6374): 161-164.

- Neefjes, J., M. L. Jongsma, P. Paul and O. Bakke (2011). "Towards a systems understanding of MHC class I and MHC class II antigen presentation." *Nat Rev Immunol* **11**(12): 823-836.
- Niedergang, F., A. Hemar, C. R. Hewitt, M. J. Owen, A. Dautry-Varsat and A. Alcover (1995). "The Staphylococcus aureus enterotoxin B superantigen induces specific T cell receptor down-regulation by increasing its internalization." *J Biol Chem* **270**(21): 12839-12845.
- Oka, Y., A. Tsuboi, O. A. Elisseeva, K. Udaka and H. Sugiyama (2002). "WT1 as a novel target antigen for cancer immunotherapy." *Curr Cancer Drug Targets* **2**(1): 45-54.
- Olson, W. C., M. E. Smolkin, E. M. Farris, R. J. Fink, A. R. Czarkowski, J. H. Fink, K. A. Chianese-Bullock and C. L. Slingsluff, Jr. (2011). "Shipping blood to a central laboratory in multicenter clinical trials: effect of ambient temperature on specimen temperature, and effects of temperature on mononuclear cell yield, viability and immunologic function." *J Transl Med* **9**: 26.
- Randriampita, C., G. Boulla, P. Revy, F. Lemaitre and A. Trautmann (2003). "T cell adhesion lowers the threshold for antigen detection." *Eur J Immunol* **33**(5): 1215-1223.
- Revy, P., M. Sospedra, B. Barbour and A. Trautmann (2001). "Functional antigen-independent synapses formed between T cells and dendritic cells." *Nat Immunol* **2**(10): 925-931.
- Rezvani, K., J. M. Brenchley, D. A. Price, Y. Kilical, E. Gostick, A. K. Sewell, J. Li, S. Mielke, D. C. Douek and A. J. Barrett (2005). "T-cell responses directed against multiple HLA-A\*0201-restricted epitopes derived from Wilms' tumor 1 protein in patients with leukemia and healthy donors: identification, quantification, and characterization." *Clin Cancer Res* **11**(24 Pt 1): 8799-8807.
- Rezvani, K., A. S. Yong, B. N. Savani, S. Mielke, K. Keyvanfar, E. Gostick, D. A. Price, D. C. Douek and A. J. Barrett (2007). "Graft-versus-leukemia effects associated with detectable Wilms tumor-1 specific T lymphocytes after allogeneic stem-cell transplantation for acute lymphoblastic leukemia." *Blood* **110**(6): 1924-1932.
- Romer, P. S., S. Berr, E. Avota, S. Y. Na, M. Battaglia, I. ten Berge, H. Einsele and T. Hunig (2011). "Preculture of PBMCs at high cell density increases sensitivity of T-cell responses, revealing cytokine release by CD28 superagonist TGN1412." *Blood* **118**(26): 6772-6782.
- Ronchetti, S., G. Nocentini, M. G. Petrillo and C. Riccardi (2012). "CD8+ T cells: GITR matters." *ScientificWorldJournal* **2012**: 308265.
- Ronchetti, S., O. Zollo, S. Bruscoli, M. Agostini, R. Bianchini, G. Nocentini, E. Ayroldi and C. Riccardi (2004). "GITR, a member of the TNF receptor superfamily, is costimulatory to mouse T lymphocyte subpopulations." *Eur J Immunol* **34**(3): 613-622.
- Sakaguchi, S. (2004). "Naturally arising CD4+ regulatory t cells for immunologic self-tolerance and negative control of immune responses." *Annu Rev Immunol* **22**: 531-562.
- Santos, R., A. Buying, N. Sabri, J. Yu, A. Gringeri, J. Bender, S. Janetzki, C. Pinilla and V. A. Judkowski (2014). "Improvement of IFNg ELISPOT Performance Following Overnight Resting of Frozen PBMC Samples Confirmed Through Rigorous Statistical Analysis." *Cells* **4**(1): 1-18.
- Sathaliyawala, T., M. Kubota, N. Yudanin, D. Turner, P. Camp, J. J. Thome, K. L. Bickham, H. Lerner, M. Goldstein, M. Sykes, T. Kato and D. L. Farber (2013). "Distribution and compartmentalization of human circulating and tissue-resident memory T cell subsets." *Immunity* **38**(1): 187-197.

- Savino, W. and S. D. Silva-Barbosa (1996). "Laminin/VLA-6 interactions and T cell function." Braz J Med Biol Res **29**(9): 1209-1220.
- Schroder-Braunstein, J., V. Pavlov, T. Giese, A. Heidtmann, S. Wentrup, F. Lasitschka, J. Winter, A. Ulrich, A. Engelke, M. Al Saeedi and S. Meuer (2012). "Human mucosal CD4+ T cells but not blood CD4+ T cells respond vigorously towards CD28 engagement." Clin Exp Immunol **168**(1): 87-94.
- Seder, R. A., P. A. Darrah and M. Roederer (2008). "T-cell quality in memory and protection: implications for vaccine design." Nat Rev Immunol **8**(4): 247-258.
- Sharpe, A. H. (2009). "Mechanisms of costimulation." Immunol Rev **229**(1): 5-11.
- Skokos, D., G. Shakhar, R. Varma, J. C. Waite, T. O. Cameron, R. L. Lindquist, T. Schwickert, M. C. Nussenzweig and M. L. Dustin (2007). "Peptide-MHC potency governs dynamic interactions between T cells and dendritic cells in lymph nodes." Nat Immunol **8**(8): 835-844.
- Smith-Garvin, J. E., G. A. Koretzky and M. S. Jordan (2009). "T cell activation." Annu Rev Immunol **27**: 591-619.
- Smith, M. E. and W. L. Ford (1983). "The recirculating lymphocyte pool of the rat: a systematic description of the migratory behaviour of recirculating lymphocytes." Immunology **49**(1): 83-94.
- Starr, T. K., S. C. Jameson and K. A. Hogquist (2003). "Positive and negative selection of T cells." Annu Rev Immunol **21**: 139-176.
- Stebbing, R., L. Findlay, C. Edwards, D. Eastwood, C. Bird, D. North, Y. Mistry, P. Dilger, E. Liefoghe, I. Cludts, B. Fox, G. Tarrant, J. Robinson, T. Meager, C. Dolman, S. J. Thorpe, A. Bristow, M. Wadhwa, R. Thorpe and S. Poole (2007). "Cytokine storm" in the phase I trial of monoclonal antibody TGN1412: better understanding the causes to improve preclinical testing of immunotherapeutics." J Immunol **179**(5): 3325-3331.
- Stefanova, I., J. R. Dorfman and R. N. Germain (2002). "Self-recognition promotes the foreign antigen sensitivity of naive T lymphocytes." Nature **420**(6914): 429-434.
- Straus, D. B. and A. Weiss (1992). "Genetic evidence for the involvement of the lck tyrosine kinase in signal transduction through the T cell antigen receptor." Cell **70**(4): 585-593.
- Suntharalingam, G., M. R. Perry, S. Ward, S. J. Brett, A. Castello-Cortes, M. D. Brunner and N. Panoskaltsis (2006). "Cytokine storm in a phase 1 trial of the anti-CD28 monoclonal antibody TGN1412." N Engl J Med **355**(10): 1018-1028.
- Tabares, P., S. Berr, P. S. Romer, S. Chuvpilo, A. A. Matskevich, D. Tyrsin, Y. Fedotov, H. Einsele, H. P. Tony and T. Hunig (2014). "Human regulatory T cells are selectively activated by low-dose application of the CD28 superagonist TGN1412/TAB08." Eur J Immunol **44**(4): 1225-1236.
- Thomas, N., L. Matejovicova, W. Srikusalanukul, J. Shawe-Taylor and B. Chain (2012). "Directional migration of recirculating lymphocytes through lymph nodes via random walks." PLoS One **7**(9): e45262.
- Tough, M. B. D. F. (2002). "Qualitative differences between naive and memory T cells." Blackwell Sciences Ltd **106**: 127-138.

- Tsuboi, A., Y. Oka, T. Kyo, Y. Katayama, O. A. Elisseeva, M. Kawakami, S. Nishida, S. Morimoto, A. Murao, H. Nakajima, N. Hosen, Y. Oji and H. Sugiyama (2012). "Long-term WT1 peptide vaccination for patients with acute myeloid leukemia with minimal residual disease." Leukemia **26**(6): 1410-1413.
- van Oers, N. S. (1999). "T cell receptor-mediated signs and signals governing T cell development." Semin Immunol **11**(4): 227-237.
- Vander Heiden, M. G., L. C. Cantley and C. B. Thompson (2009). "Understanding the Warburg effect: the metabolic requirements of cell proliferation." Science **324**(5930): 1029-1033.
- Villacres, M. C., S. F. Lacey, C. Auge, J. Longmate, J. M. Leedom and D. J. Diamond (2003). "Relevance of peptide avidity to the T cell receptor for cytomegalovirus-specific ex vivo CD8 T cell cytotoxicity." J Infect Dis **188**(6): 908-918.
- Wahl, D. R., C. A. Byersdorfer, J. L. Ferrara, A. W. Pipari, Jr. and G. D. Glick (2012). "Distinct metabolic programs in activated T cells: opportunities for selective immunomodulation." Immunol Rev **249**(1): 104-115.
- Wang, J., K. Lim, A. Smolyar, M. Teng, J. Liu, A. G. Tse, J. Liu, R. E. Hussey, Y. Chishti, C. T. Thomson, R. M. Sweet, S. G. Nathenson, H. C. Chang, J. C. Sacchettini and E. L. Reinherz (1998). "Atomic structure of an alphabeta T cell receptor (TCR) heterodimer in complex with an anti-TCR fab fragment derived from a mitogenic antibody." EMBO J **17**(1): 10-26.
- Wang, J. H. and E. L. Reinherz (2002). "Structural basis of T cell recognition of peptides bound to MHC molecules." Mol Immunol **38**(14): 1039-1049.
- Wang, T., C. Marquardt and J. Foker (1976). "Aerobic glycolysis during lymphocyte proliferation." Nature **261**(5562): 702-705.
- Warburg, O. (1956). "On the origin of cancer cells." Science **123**(3191): 309-314.
- Watanabe, M. Y. a. T. (2012). "New Paradigm of T cell Signaling: Learning from Malignancies." J Clin Cell Immunol **S12:007**: 2155-9899.
- Wegner, J., S. Hackenberg, C. J. Scholz, S. Chuvpilo, D. Tyrsin, A. A. Matskevich, G. U. Grigoleit, S. Stevanovic and T. Hunig (2015). "High-density preculture of PBMC restores defective sensitivity of circulating CD8 T-cells to virus- and tumor-derived antigens." Blood.
- Wolf, K., R. Muller, S. Borgmann, E. B. Brocker and P. Friedl (2003). "Amoeboid shape change and contact guidance: T-lymphocyte crawling through fibrillar collagen is independent of matrix remodeling by MMPs and other proteases." Blood **102**(9): 3262-3269.
- Wu, L. C., D. S. Tuot, D. S. Lyons, K. C. Garcia and M. M. Davis (2002). "Two-step binding mechanism for T-cell receptor recognition of peptide MHC." Nature **418**(6897): 552-556.
- Ziegler, W. H., R. C. Liddington and D. R. Critchley (2006). "The structure and regulation of vinculin." Trends Cell Biol **16**(9): 453-460.

## Curriculum vitae









